

5-1-2012

Burial and Exhumation History of Mississippian Strata in East-Central Nevada

Yuki Yunika Agulia

University of Nevada, Las Vegas, aguliay@unlv.nevada.edu

Follow this and additional works at: <https://digitalscholarship.unlv.edu/thesesdissertations>



Part of the [Geology Commons](#), and the [Stratigraphy Commons](#)

Repository Citation

Agulia, Yuki Yunika, "Burial and Exhumation History of Mississippian Strata in East-Central Nevada" (2012). *UNLV Theses, Dissertations, Professional Papers, and Capstones*. 1529.
<https://digitalscholarship.unlv.edu/thesesdissertations/1529>

This Thesis is protected by copyright and/or related rights. It has been brought to you by Digital Scholarship@UNLV with permission from the rights-holder(s). You are free to use this Thesis in any way that is permitted by the copyright and related rights legislation that applies to your use. For other uses you need to obtain permission from the rights-holder(s) directly, unless additional rights are indicated by a Creative Commons license in the record and/or on the work itself.

This Thesis has been accepted for inclusion in UNLV Theses, Dissertations, Professional Papers, and Capstones by an authorized administrator of Digital Scholarship@UNLV. For more information, please contact digitalscholarship@unlv.edu.

BURIAL AND EXHUMATION HISTORY OF MISSISSIPPIAN
STRATA IN EAST-CENTRAL NEVADA

By

Yuki Yunika Agulia

Bachelor of Science
Gadjah Mada University, Indonesia
2007

A thesis submitted in partial fulfillment
of the requirements for the

Master of Science Degree in Geoscience

Department of Geoscience
College of Science
The Graduate College

University of Nevada, Las Vegas
May 2012

Copyright by Yuki Yunika Agulia Graduate Student 2012
All Rights Reserved



THE GRADUATE COLLEGE

We recommend the thesis prepared under our supervision by

Yuki Yunika Agulia

entitled

Burial and Exhumation History of Mississippian Strata in East-Central Nevada

be accepted in partial fulfillment of the requirements for the degree of

Masters of Science in Geoscience

Department of Geoscience

Andrew D.Hanson, Ph.D., Committee Chair

Terry L. Spell, Ph.D., Committee Member

Rodney V. Metcalf, Ph.D., Committee Member

Vernon F. Hodge, Ph.D., Graduate College Representative

Ronald Smith, Ph. D., Vice President for Research and Graduate Studies
and Dean of the Graduate College

May 2012

ABSTRACT

Burial and Exhumation History of Mississippian Strata in East-Central Nevada

by

Yuki Yunika Agulia

Dr. Andrew Hanson, Examination Committee Chair
Associate Professor of Geology
University of Nevada, Las Vegas

Zircon (U-Th)/He analyses and vitrinite reflectance (Ro) analyses were performed on a suite of Mississippian sedimentary rocks collected in east-central Nevada in order to test Permian exhumation described in a previous study.

The zircon analyses produced three clusters of ages: 1) older than, 2) similar to, and 3) younger than depositional age. The majority of zircons shows ages that are older than the sandstone deposition age. Young ages were recorded in three localities that may indicate reset ages/residence within the (U-Th)/He partial retention zone (HePRZ). Moderate-high ratios of Th/U may indicate a magmatic source. Vitrinite reflectance (Ro) analyses show values between 0.54% - 1.56% which indicate early mature - postmature stage with respect to potential hydrocarbon maturation. The hypothesized regional Permian exhumation was not documented in this study, and the Ro values in all locations are too low to have caused thermal resetting of the (U-Th)/He system.

ACKNOWLEDGEMENTS

I would love to give my special gratitude to my advisor, Dr. Andrew Hanson for his supervision, critics, motivation, understanding, and patient in guiding me through this project until the finishing touch of my thesis. I would also want to deliver my appreciation for my thesis committee Dr. Terry Spell, Dr. Rod Metcalf, and Dr. Vernon Hodge for being very supportive and for their constructive inputs in my thesis.

Special thanks for Tom Muntean who was so kindly guided me through the laboratory process, field assistance, and discussion, also Nick Downs for his help during my zircon separation process.

The (U-Th)/He laboratory staff at University of Kansas was very helpful providing me with assistantship during my analysis. Thank you especially to Danny Stockli, Roman, Sarah, and Joe for the explanations and discussions about the data.

I would love to say thank you for ExxonMobil Indonesia, for the material and non-material support in the development of my education for my future career. I feel really happy to be part of UNLV Geoscience Department that has been giving me a great opportunity to increase my knowledge about geology, and meet with great professors and colleagues.

My buddies Nick, LaOde, Carl, and Leon, thank you very much for sharing a nice memory winning the IBA competition. Bobby and James, Josh and Aubrey, Andy and Rachel, thank you for giving me fun experiences outside the academic territory. My other friends Swapan, Mike, Jon Carter, Inessa, Laura, Mai, and all, thank you for each of you for being a very good friend of mine. Thank you for Maria, Liz, Katherine, Rainee, Joy, and Amber for your help in the department office every time I need one.

To my family, my husband, and my Indonesian friends in Vegas, thank you with extra-extra love for all the support and faiths you have given me. I would never be success without you all.

I started my study in the fall of 2009. The first time I came, I had a very little knowledge about living in the United States. I remember the first day I got into school; I met with new friends and new teachers, including my advisor, Dr. Andrew Hanson. I remember my classes in my first semester, and how I started making friends. I followed several interesting classes with amazing teachers. I loved my geological fieldtrips and I feel very fortunate to experiencing a wonderful fieldwork I did for my thesis. I experienced my first snow during my fieldwork, and I still remember how my advisor convinced me that my tent would not be blown away by wind as long I stay inside, even though I apologize for driving him crazy with my pointless questions including the question about the color of the blue mountain bird. I saw lots of beautiful places and wildlife in the desert. Tom taught me a special skill of identifying animals from their poops. All those memories make two years seem like yesterday, and the time passed very fast. The funny thing is even now, there are still a lot of my friends who cannot believe that there is a school in Las Vegas.

TABLE OF CONTENT

ABSTRACT.....iii

ACKNOWLEDGEMENTS.....iv

CHAPTER 1 INTRODUCTION.....1

CHAPTER 2 GEOLOGICAL FRAMEWORK.....5

 Previous Study.....10

CHAPTER 3 METHODS.....13

 Rock Sample Collection.....13

 (U-Th)/He Zircon Analyses.....15

 Vitrinite Reflectance Analyses.....17

CHAPTER 4 RESULTS.....18

 4.1 Antelope Valley (U-Th)/He Zircon and Ro Analyses18

 4.2 Burnt Mtn. (U-Th)/He Zircon and Ro Analyses 19

 4.3 Buck Mtn. (U-Th)/He Zircon and Ro Analyses..... 19

 4.4 Cherry Creek (U-Th)/He Zircon and Ro Analyses 20

 4.5 Cave Lake (U-Th)/He Zircon and Ro Analyses 20

 4.6 Diamond Peak (U-Th)/He Zircon and Ro Analyses 20

 4.7 Duckwater (U-Th)/He Zircon and Ro Analyses 21

 4.8 Ely (U-Th)/He Zircon and Ro Analyses 21

 4.9 Gap Mtn. (U-Th)/He Zircon and Ro Analyses 21

 4.10 Grant Range (U-Th)/He Zircon and Ro Analyses 22

 4.11 Hot Creek (U-Th)/He Zircon and Ro Analyses 22

 4.12 Illipah (U-Th)/He Zircon and Ro Analyses 23

 4.13 Southern Snake Range (U-Th)/He Zircon and Ro Analyses 23

 4.14 Northern Pancake Range (U-Th)/He Zircon and Ro Analyses..... 23

 4.15 Pancake Range (U-Th)/He Zircon and Ro Analyses 24

 4.16 Sixmile Spring (U-Th)/He Zircon and Ro Analyses..... 24

 4.17 Northern Snake Range (U-Th)/He Zircon and Ro Analyses 25

 4.18 Northern Egan Range Ro Analysis..... 25

CHAPTER 5 DISCUSSION.....26

CHAPTER 6 INTERPRETATION.....30

 Antelope Valley 31

 Diamond Peak.....31

 Cherry Creek.....33

 Magmatic versus Metamorphic Zircons34

CHAPTER 7 CONCLUSION.....	36
APPENDIX A.....	38
APPENDIX B.....	99
REFERENCES.....	106
VITA.....	114

CHAPTER 1

INTRODUCTION

East-central Nevada is known, in part, for its petroleum resources. The main location of these resources is Railroad Valley (RRV) which is located in Nye County, 60 miles southwest of Ely and approximately 250 miles north of Las Vegas (Figure 1). Bound by the Pancake Range on the west and the Grant Range and White Pine Range on the east, the Grant Canyon field has produced the largest volume of oil in RRV. It has produced approximately 20 million barrels of oil since the 1980s (Anna et al., 2007).

Previous studies in this area indicated that several formations potentially contribute to the oil and gas in RRV. However, the Mississippian Chainman Shale is known as the most important source rock because of its great thickness, organic richness, and wide lateral distribution from eastern Nevada to western Utah (Meissner, 1995; Anna et al., 2007).

Although the Mississippian Chainman Shale is an important source rock, few studies have been conducted to constrain the burial history of these Mississippian strata. One previous (U-Th)/He zircon study by Druschke (2009) indicated that there was significant burial (>6 km) of the Mississippian strata followed by exhumation in the Permian, which resulted in major erosion of Pennsylvanian to Permian strata in the Egan Range (the next range to the east of RRV). I hypothesized that significant post-Mississippian deposition occurred (>6 km) which was followed by exhumation in the Late Permian in east-central Nevada. I tested this hypothesis by collecting and analyzing a suite of rock samples taken from ranges that surround RRV. Outcrop samples were

collected from both the Chainman Shale and Scotty Wash Sandstone, which is a clastic member of the Chainman Shale, in widespread areas with good spatial distribution.

The (U-Th)/He zircon analysis method is well established in geochronology and thermochronology studies for understanding the thermal history of a variety of rock types (e.g. Farley, 2002; Reiners et al., 2004; Reiners, 2005). This analysis involves age determination from the retention of alpha particles (^4He nuclei), as a function of temperature, within a mineral during the radioactive decay of ^{238}U , ^{235}U , ^{232}Th , and ^{147}Sm (e.g. Wolf et al., 1996; Reiners, 2005). Closure temperatures represent the quantitative retention of helium retained within the crystal. Reiners and Farley (2000) proposed a minimum closure temperature of about 180°C for helium diffusion from zircon. However, Reiners et al. (2002), Tagami et al. (2003), Stockli (2005), and Wolfe and Stockli (2010) showed that helium is partially retained within zircon between $140 - 200^\circ\text{C}$, a phenomenon known as helium partial retention, which occurs within the helium partial retention zone (zircon HePRZ). If a geothermal gradient of $30^\circ\text{C}/\text{km}$ is assumed then a zircon closure temperature of $\sim 180^\circ\text{C}$ corresponds to the depth of 6 km in the crust.

Nasdala et al. (2004), Reiners (2005), and Shuster et al. (2006) studied the relationship of effective uranium concentration (calculated as $[\text{U}]_e = [\text{U}] + [\text{Th}]0.235 + [\text{Sm}]0.005$), as a proxy for radiation damage, and a decrease in helium retentivity. Alpha particles are more likely to be lost from the crystal when $[\text{U}]_e$ is high, thus resulting in the calculation of anomalously young ages. A negative correlation between $[\text{U}]_e$ and zircon helium age is useful for documenting slow cooling and residence of zircons within the HePRZ (Stockli et al., 2010).

The standard alpha-ejection (F_T) correction performed in this analysis assumes a homogenous parent isotope distribution to calculate the amount of ^4He daughter product lost due to alpha-ejection in the outer 20 μm of the mineral (e.g. Farley et al., 1996). However, heterogeneous distribution of parent isotopes within zircon is a common feature and may be responsible for inaccuracies in He ages. Hourigan et al. (2005) studied the effects of U-Th zonation on zircons with a wide variety of crystal morphologies. He concluded that zircons with U-Th enriched cores produce significantly anomalously old ages. Enriched rim zircons, however, shown significantly anomalously young age inaccuracies. Geologically meaningless ages due to zonation may be detected by examining the dispersion of helium ages from multiple single zircon analyses for a single sample. If multiple single zircon helium ages shown good agreement, zonation is probably not affecting the helium ages (Reiners, 2005). Another way to detect U-Th zonation in single zircons is by using depth-profile techniques developed by Hourigan et al. (2005). This method helps to build models to see patterns and customized alpha-ejection corrections specific to each zircon.

(U-Th)/He analyses were performed on zircons separated from the Scotty Wash Sandstone. Ages younger than the depositional age may be the result of 1) regional exhumation after subjection to deep burial, 2) residence within the HePRZ, or 3) younger thermal overprint.

Vitrinite refers to a group of organic particles that originate from terrigenous plants that are commonly preserved as detrital pieces in certain sedimentary rocks. Vitrinite reflectance analysis (R_o) is conducted using a petrographic microscope in order to rank the thermal maturity of a rock as a function of both time and temperature.

Samples are analyzed using light reflected from polished vitrinite particles present in the rocks (Rowan, 2006). Vitrinite is an important constituent of Devonian and younger sedimentary rocks because land-plants had evolved prior to this time.

Vitrinite reflectance (R_o) analyses were completed on Chainman Shale samples collected in close stratigraphic proximity to Scotty Wash Sandstone samples in order to determine the thermal maturity and burial history of the Chainman Shale. The vitrinite analyses constrain the rank of shale samples using optical properties that change with maturation. The R_o values constrain the maximum time/temperature conditions to which the rock has been subjected. The data generated from these analyses were combined with the data from previous studies to constrain the burial and exhumation story of much of east-central Nevada, including RRV.

This study significantly contributes to our understanding of the thermal maturation of the Chainman Shale in RRV and adjacent areas. It also provides an understanding of the source rock and its overburden story for the petroleum system in east-central Nevada.

CHAPTER 2

GEOLOGICAL FRAMEWORK

The study area in east-central Nevada (Figure 1) is a part of the Great Basin Province. This province extends throughout Nevada, western Utah, southeastern Oregon, and northwestern Arizona. Today, this area is characterized by north-south trending mountain ranges bound by normal faults and separated by valleys with Tertiary and Quaternary strata (Eaton, 1979).

Stratigraphy in the Great Basin consists of a wide variety of rocks that reflect a wide range of depositional environments (Figure 2) (Anna et al., 2007). In the lower to middle Paleozoic, the area was a passive margin carbonate platform. The tectonic setting changed in the late Paleozoic, which resulted in marine clastic and carbonate deposition. Deposition continued with continental lacustrine and volcanic rocks in the Mesozoic and Cenozoic. The study area underwent multiple tectonic events that resulted in the geology seen today. Late Precambrian rifting was followed by several major tectonic events including the Antler orogeny, Sonoma orogeny, development of the Central Nevada Thrust, Sevier contraction, and Basin and Range extension. All of these tectonic events created complex structural and stratigraphic patterns in this area (Anna et al., 2007).

The Antler orogeny began in the late Devonian to Early Mississippian and is represented by Roberts Mountain thrust as the principal structural feature (Carpenter et al., 1994) (Figure 3). This tectonic event transported the Roberts Mountains allochthon, which consisted of lower Paleozoic deep marine sedimentary rocks, cherts, dark shales, and volcanic rocks, onto the carbonate shelf of the western North America continent and

created flexural loading lead to the development of the Antler foreland basin to the east of the thrust fault (Wilson and Laule, 1979; Speed and Sleep, 1982; Dickinson et al., 1983).

According to Goebel (1991), Giles and Dickinson (1995), and Giles (1996) the Antler foreland succession consists of the Devonian Pilot-Joana Limestone and the Mississippian Chainman Shale. The paleocurrents and petrographic data from the central Diamond Mountains of eastern Nevada indicate that the sediment was derived from the Antler orogenic belt and that transport was from the west to the east (Poole and Sandberg, 1991). Trexler and Cashman (1991) proposed a revision of the Mississippian stratigraphy in Nevada based on unconformities that they identified in the Diamond Mountains (Figure 4). They concluded that the Antler foreland-basin strata were deformed, exhumed, and eroded in the middle Mississippian. This event created what they called the C2 boundary. A late Mississippian successor basin was then established and persisted into the Pennsylvanian (~318 - 330 Ma). The successor basin is bound on the west by the relict Antler highland, and on the east by a siliciclastic shelf and the craton margin. Strata that overlay the C2 boundary range from nonmarine, siliciclastic, deltaic rocks in the west, to shallow-marine carbonates, conglomerates, litharenites, and lagoonal shales in central Nevada, and to shelf and lagoonal carbonaceous shales and quartzites in eastern Nevada. They interpreted that the heterolithic siliciclastic sediments of this age as the recycled products of the Antler orogen and foreland-basin strata (Trexler and Cashman, 1991, 1997; Perry, 1994, 1995). In contrast, the quartz arenitic Scotty Wash Sandstone was deposited as lowstand shelf deposits derived from the craton which was to the east

and southeast (Trexler and Cashman, 1991). These strata are unconformably overlain by Pennsylvanian limestone throughout the Great Basin.

Renewed compressional tectonics resulted in the emplacement of the Golconda allochthon above the Antler highland in the Permian - Triassic (Gabrielse et al., 1983). This event is known as the Sonoma orogeny. The allochthon consists of deepwater sedimentary rocks (chert-argillite-limestone-greenstone). However, this event did not have a major impact on the burial or exhumation history of the study area (Anna et al., 2007).

Thrusting that caused the Central Nevada Thrust Belt (CNTB) was the next tectonic event and its age is constrained to Triassic to middle Cretaceous. The CNTB is a set of north-south trending, dominantly east-vergent thrust faults and folds which are located in the hinterland of the Sevier orogeny (Figure 5). This belt has been segmented by Basin and Range extension in the Neogene. Today the evidence of this thrust system is only observed in the ranges of the Basin and Range Province (Taylor, 2001). According to Cameron and Chamberlain (1987), these structures can be delineated as far north as the northern Diamond Range and as far south as northwestern Clark County. The Newark Canyon Formation was deposited in the early Cretaceous in association with CNTB thrust faulting and folding (Cameron and Chamberlain, 1987).

The Cordilleran thrust system developed during the Cretaceous to early Tertiary Sevier orogeny. This tectonic event occurred because of convergence between the Farallon Plate and the North American continent. The Sevier fold and thrust belt and its foreland basin are located to the east in Utah and adjacent areas. The Sevier thrusts caused thin-skinned deformation that generally propagated from west to east. This event

created repetition of sedimentary sequences above the basement, folding of associated strata in the foredeep basin, and deposited thick sediments as much as several thousand meters thick (Anna et al., 2007).

In the Tertiary, extension caused numerous normal faults that led to the formation of the Basin and Range Province in western North America (Armstrong, 1972). The extension is temporally linked with the cessation of plate convergence and the initiation of lateral slip of the Pacific plate past the North American plate (Eaton, 1979). Dickinson (2002) proposed that the extension was driven by gravitational collapse due to unstable over-thickened crust. This tectonic event extended the Basin and Range by up to 200% since the late Oligocene (Hamilton, 1978; Wernicke et al., 1988). Metamorphic basement is visible at some localities in the Basin and Range as metamorphic core complexes (MCC) that were brought to the surface as a result of the crustal extension (Spencer, 1984; Wernicke, 1981; Coney and Harms, 1984). The timing and magnitude of the extension varied in many places. Salyards and Shoemaker (1987) suggested that the extension initially began in the southern Basin and Range and propagated north over time. This tectonic event was accompanied by volcanism and the peak of eruptions occurred in the late Oligocene – early Miocene (Christiansen and Yeats, 1992).

The Mississippian Chinaman Shale is the main focus of this study and it is the main petroleum source rock for RRV (Sadlick, 1965; Poole and Claypool, 1984; Meissner, 1995). The thickness of this formation in eastern Nevada is between 600 and 1,800 m, and it dominantly contains type II kerogen that is oil prone, with a minor amount of gas prone type III kerogen (Sadlick, 1965; Poole and Claypool, 1984). According to French (1983), total organic carbon for this formation ranges from 1.0% to

3.5% and the thermal maturity is in the mature - overmature stage. As described by Trexler et al, (2003), the Chainman Shale overlies the C2 boundary (Figure 4). In central and eastern Nevada, this formation was deposited in a lagoonal to shelf environment with a source that appears to be recycled Antler foreland-basin strata (Trexler and Cashman, 1991). The Chainman Shale has been divided into at least six members (Sadlick, 1965), the most prominent member is the Scotty Wash Sandstone (Trexler et al., 1995). The thickness of this member ranges from 120 - 250 m (Trexler et al., 1995). This member consists of super-mature, well-bedded, quartz arenite sandstone, which characteristically has amalgamated, meter-scale, cross laminated beds (Trexler et al., 1995). The detritus for the Scotty Wash Sandstone was derived from the craton to the east (Trexler and Cashman, 1991). According to Cashman and Trexler (1994), in the northern and western part of east-central Nevada, the Scotty Wash Sandstone is equivalent to the Diamond Peak Fm. To the south, it is equivalent to the Eleana Fm.

According to a study by Wilson and Laule (1979), the Diamond Peak Formation is thickest near the Antler belt and thins rapidly eastward. Their study indicated that the formation is composed mainly of coarse sands and gravels conglomerate and limestone and that clast size increases toward to the Antler belt to the west.

Petrography and stratigraphic studies in southern Nevada (Cashman and Trexler, 1991) separated the Mississippian Eleana Formation into two units. The first unit consists of sedimentary rocks from the western Eleana Range that were interpreted as submarine fan deposits; they contain significant amounts of chert, feldspar, and both volcanic and sedimentary lithic grains. They correlated this unit with the Dale Canyon - Chainman Shale - Diamond Peak section near Eureka. The source of these sediments was the Antler

allochthon and foreland basin. The second unit consists of quartz arenites with rare chert and detrital heavy minerals from the eastern Eleana Range. They tentatively interpreted these strata to be a shallow shelf deposit, with sediments derived from the continent to the east. They considered them to be equivalent to the Scotty Wash - Chainman section of eastern Nevada. One sample of the Eleana Formation was collected at the Hot Creek locality for this study, which is located to the west of Eleana Range. Therefore, this sample is considered to be equivalent with rocks in the western Eleana Range, e.g. the Diamond Peak Formation and thus is considered to be laterally equivalent to the Scotty Wash Sandstone (Figure 2).

Previous Studies

Because Railroad Valley (Figure 6) is the main oil producer in the state of Nevada, numerous studies have been conducted specifically to understand its petroleum system (e.g. Anna et al., 2007; Walker et al., 1992; Montgomery et al., 1999; French, 1983; Pekarek, 2005). The Chainman Shale is known as the most important source rock, and thermal maturity studies of this formation have been conducted by several researchers.

Harris et al. (1980) reported that in the western, northern, and far north eastern areas of Nevada, the Mississippian through Triassic rocks have high to very high conodont alteration index (CAI) value from 4.0 to 8.0. However, in southern and eastern Nevada, the value are uniformly low (CAI value ranging from 1.0 to 2.0 which indicate immature to mature rocks with respect to oil generation) with a few exceptions likely due to high heat flow from nearby igneous or hydrothermal sources.

Poole and Claypool's (1984) data indicate that submature and marginally mature Mississippian source rocks are present in west-central Utah and east-central Nevada. However, the Diamond Mountains (Eureka mining district) reached a super-mature stage of maturation. Rowan et al. (1992) used Landsat Thematic Mapper Images to map thermal maturity in the Chainman Shale and found high values, which correspond to the high maturity in the Chainman, are also present in the Diamond Mountains. On the other hand, low to moderate values that correspond to low maturity are found in the northwestern Pancake Range. In addition, Ahdyar (2011) conducted several analyses on the Eocene Sheep Pass Formation and Chainman Shale samples in the southern Egan Range. His vitrinite reflectance data indicate that the Sheep Pass Formation has low maturity (0.46% Ro and Tmax 436-347 °C); in contrast his Chainman Shale samples exhibit moderate - high maturity (0.68 - 1.01% Ro and Tmax 442 - 455 °C).

Anna et al. (2007) suggested that there are several potential sources that may have contributed to the heating of source rocks in the eastern Great Basin. These include heat flow from mantle and crustal sources, and hydrothermal fluids associated with gold deposits, geothermal systems, and volcanic activity. They noted that in the Battle Mountain High (BMH), northern part of the Great Basin province, along with several hot spots along the western and northeast province margins indicate high heat flow.

Druschke (2009) produced (U-Th)/He detrital zircon ages from the Mississippian Scotty Wash Sandstone in the Egan Range, east of RRV, that are Late Permian (265 Ma). He interpreted this age as being indicative of deep burial followed by later Permian exhumation and cooling (Figure 7.A and 7.B). If this interpretation is correct and occurs

throughout the region, it would significantly alter our understanding of Late Permian burial and exhumation.

CHAPTER 3

METHODS

The methods for this project consisted of fieldwork and laboratory analyses. Fieldwork was conducted in order to collect rock samples for subsequent laboratory analyses. The laboratory methods included rock sample preparation for vitrinite reflectance (Ro) and analysis using (U-Th)/He methods.

Rock Sample Collection

Field activity was done to collect samples in Mississippian strata in east - central Nevada. Two Mississippian formations were targeted: the Chainman Shale and the Scotty Wash Sandstone (Figure 8), or their lateral age-equivalent units (i.e. the Eleana Formation and the Diamond Peak Formation). Published geologic maps of Northern Nye County (Kleinhampl and Ziony, 1985), Eureka County (Roberts et al., 1967), White Pine County (Hose et al., 1976), and Lincoln County (Tschanz and Pampeyan, 1970) were used to identify the field localities. I collected samples in targeted areas that provide relatively equal distribution of samples throughout the study area (Figure 9). All sample collection locations were recorded by hand-held GPS (Table 1 and Table 2).

Eighteen Mississippian sandstone samples were collected in several different locations. The localities include Antelope Valley (z10AV35), Burnt Mountain (z10BM04), Buck Mountain (z10BU26), Cherry Creek (z10CC34), Cave Lake (z10CL29), Diamond Peak (z10DP21), Duckwater (z10DW17), Ely (z10EL41), Gap Mountain (z10GM01), Grant Range (z10GR07), Hot Creek (z10HC10), Illipah

(z10IL27), southern Snake Range (z10MW37), northern Pancake Range (z10NP19), Pancake Range (z10PR13 and z10PR16), Sixmile Spring (z10SP32), and northern Snake Range (z10SR39) (Figure 9).

Twenty two samples from the Chainman Shale were collected from different areas. The sample localities include Gap Mountain (10GM02, 10GM03), Burnt Mountain (10BM05, 10BM06), Grant Range (10GR08, 10GR09), Hot Creek (10HC11, 10HC12), Pancake Range (10PR14), Duckwater (10DW18), northern Pancake Range (10NP20), Diamond Peak (10DP22, 10DP23), Buck Mountain (10BU24, 10BU25), Illipah (10IL28), Cave Lake (10CL30), Sixmile Spring (10SP31), northern Egan Range (10SE33), Antelope Valley (10AV36), southern Snake Range (10MW38), and Ely (10EL40) (Figure 9).

All samples were collected from outcrops. Targeted outcrops were fresh, not weathered, and free of alteration that was suggestive of hydrothermal activity. The Chainman Shale was recognized in the field based on its black/dark grey color and its stratigraphic position. Because of the nature of shale, outcrops were sometimes covered by soil at the surface. Therefore, fresh samples were collected by creating a pit by digging into the soil using a shovel/hammer. I sampled shales that were black, fresh, platy, unaltered, and free of recent organic material. The Scotty Wash Sandstone in the field is yellow-red to purplish, clean quartz sandstone or pebbly conglomerate. Weathered rinds of Scotty Wash samples were removed in the field to get the freshest possible sample and to protect them from contamination.

All samples were labeled sequentially using a consistent method. The first two numbers for each sample indicate the year when the sample was collected. The following

two letters indicate the location, and the last two numbers indicate the samples' number. For example, 10DP21 indicates the sample was taken in the year 2010, at a location near Diamond Peak, and was the twenty first sample collected. In addition, a lower case "z" was added to the front of the sample number for each sample that underwent (U-Th)/He zircon analyses (a laboratory requirement).

(U-Th)/He Zircon Analyses

Before zircons could be sent out for analyses, detrital zircons had to be extracted from the sandstone samples. The samples were first crushed and zircons were removed using standard heavy liquid and magnetic separation techniques at the Rock Preparation Laboratory of the University of Nevada Las Vegas. The method used was similar to the one used described by Forrester (2009).

Once zircons were separated in the laboratory, the individual zircons were handpicked, photographed, and measured under a microscope (dimensions are listed for all zircons on Figures 10A-R) for α -ejection correction. The zircons were then analyzed following the procedures from the (U-Th)/He laboratory, University of Kansas (<http://www.geo.ku.edu/programs/tectonics/helab.shtml>) described by Wolfe and Stockli (2010). This analysis involved a single-zircon technique where the daughter and parent products were measured for each zircon. Preferred zircons are euhedral to subhedral with morphology as close as possible to the ideal geometry. Analyzed zircons had a/b axes that were at least 70 μ m. All zircons had c axis lengths between 80-200 μ m. Grains ideally have no visible fractures and minimal inclusions. However, the zircons from the Scotty Wash Sandstone were typically subrounded.

Each zircon was individually imaged and measured to complete the alpha-ejection (F_T) correction (e.g. Farley, 2002). The zircons were then wrapped in Pt foil (1×1 mm) and degassed by laser heating at ~1300°C for 10 minutes and subsequently reheated until completely degassed (>99% of He had been extracted). Helium abundances were measured using ^3He isotope dilution and quadrupole mass spectrometry was used to measure the ratios of $^3\text{He}/^4\text{He}$. Each zircon was then unwrapped and dissolved using HF-HNO₃ and HCl pressure vessel digestion procedures for a total of 4 days. U-Th parent concentrations were then measured by inductively coupled plasma-mass spectrometry (ICP-MS). All of the zircons have been corrected for alpha-ejection using techniques described by Farley (2002). Analytical uncertainties quoted from internal laboratory standards are 8% (2 σ).

Data collected from these analyses were entered into a relative probability plot using the Isoplot3.70 program created by Ludwig (2008) to show the distribution of ages. The age distribution is shown in cumulative-probability/histogram plots. The input data were the values and their errors. These plots show the cumulative probability distribution obtained by summing the probability distributions of a suite of data with normally-distributed errors. The input data were comprised of 2 columns which are the age values and their errors. The program processed the selected data and presented them in graphic form for the each location. The x-axis shows the age distribution and the y-axis shows the number of samples that plot in each bin. The curve shows the age relative probability. The Age Pick program of Gehrels (2009) was then used to generate ages that would represent the cumulative probability ages derived from a minimum of three (3) data points that are close to each other.

Vitrinite Reflectance Analyses

Twenty two (22) samples from the Chainman Shale were collected from different areas and sent to the Egsploration Company for analysis (<http://egsploration.com>). In the laboratory, all samples were prepared and analyzed by using the methods from ISO 7404-2, ISO 7404-3, and ISO 7404-5 with some modifications. Vitrinite reflectance determination was performed in a dark-room using a Zeiss Standard Universal research microscope-photometer system (MPM01K) equipped with a tungsten-halogen lamp (12V, 100W). The stage of maturation was defined by a quantitative measurement of the light reflected by vitrinite from a vertical beam of 546 nm incident light. The reflected light is measured from the surface of a polished sample submerged under the standard oil (Zeiss immersion oil with n_e 1.517 at 23°C).

Source rock maturation stages were defined by Peters and Cassa (1994). Based on their classification, vitrinite reflectance (R_o) values less than 0.60% correspond to the immature stage, R_o values between 0.60% - 0.90% correspond to the mature stage, and R_o values greater than 1.20% correspond to post-mature stage.

CHAPTER 4

RESULTS

From the sandstone samples, a total of 164 zircons were separated and analyzed using the zircon (U-Th)/He technique (Figure 10.A to 10.R). The helium ages results are presented in Table 3.

The vitrinite reflectance laboratory reported that the vitrinite reflectance analyses for the Chainman Shale samples revealed low to high abundance of organic matter. The lowest organic matter abundance was found in sample 10NP20 (northern Pancake Range), and the highest organic matter abundance was found in sample 10BM05 (Buck Mountain) and 10GR09 (Grant Range). Organic matter identified as vitrinite material was plentiful in many samples, as well as inertinite and liptinite materials. Pyrite also occurred in many shale samples. Vitrinite images were photographed under the microscope and are shown in Figure 11.

Figures 12.A to 12.R are geologic maps that show where the Scotty Wash Sandstone and Chainman Shale samples were collected at every location.

The (U-Th)/He ages and Ro results for every location will be explained in the following paragraphs.

4.1. Antelope Valley (U-Th)/He zircon and Ro Analyses

The Scotty Wash sample collected at Antelope Valley produced twelve zircons that were analyzed for (U-Th)/He ages. Three of the zircons (z10AV35- 1, 2, and 3) did not produce helium ages due to laboratory procedural error during laser heating process (these ages are not included in calculations and interpretations). Three zircons, z10AV35-

4, 7, and 11, yielded zircon ages (430.4 ± 34.4 Ma, 391.4 ± 31.3 Ma, and 1078.4 ± 86.3 Ma respectively) that are older than the Mississippian age. One zircon (z10AV35-9) yielded an age (319.3 ± 25.5 Ma) that is similar to the depositional age. Five other zircons (z10AV-5, 6, 8, 10, 12) show ages (250.5 ± 20.0 Ma, 245.6 ± 19.6 Ma, 289.7 ± 23.2 Ma, 267.5 ± 21.4 Ma, and 232.9 ± 18.6 Ma) younger than the depositional age. The Chainman Shale sample from this location (10AV36) has an Ro value of 0.57%.

4.2. Burnt Mountain (U-Th)/He zircon and Ro Analyses

The Scotty Wash Sandstone sample collected at Burnt Mtn. yielded eight zircons that were analyzed using the zircon (U-Th)/He technique. One zircon (zBM04-1) did not record any He concentration (0 age) due to laboratory procedural error during the laser heating process. Therefore, this sample was not used for further calculations. The other 6 zircons (zBM04- 2, 3, 4, 5, 6, and 7) yielded ages of 337.0 ± 27.0 Ma, 419.5 ± 33.6 Ma, 523.8 ± 41.9 Ma, 561.3 ± 44.9 Ma, 358.9 ± 28.7 Ma, and 812.9 ± 65.0 Ma respectively. A single zircon (z10BM04-8) yielded an age (132.2 ± 10.6 Ma) that is younger than Permian. Two Chainman Shale samples that were sent for Ro analyses (10BM05 and 10BM06) show results of 0.83% and 0.82% respectively.

4.3. Buck Mountain (U-Th)/He zircon and Ro Analyses

All nine zircons that were analyzed from the Scotty Wash Sandstone sample at Buck Mountain yielded helium ages that are older than the Mississippian. The ages range from 452.1 ± 36.2 Ma (z10BU26-1) to as old as 1580.0 ± 126.4 Ma (z10BU26-7). Two Chainman samples (10BU24 and 10BU25) collected from this locality show Ro value of 0.86% and 0.87% respectively.

4.4. Cherry Creek (U-Th)/He zircon and Ro Analyses

The Scotty Wash Sandstone sample collected at Cherry Creek produced ten zircons that were analyzed for (U-Th)/He ages. All of them yielded ages that are younger than the sandstone depositional time. The helium ages recorded in the sample range from 83.9 ± 6.7 Ma (z10CC34-4) to 217.2 ± 17.4 Ma (z10CC34-5). The Chainman Shale sample was not found at this location. Therefore, vitrinite reflectance analysis was not performed.

4.5. Cave Lake (U-Th)/He zircon and Ro Analyses

There were a total of nine zircons collected from Scotty Wash Sandstone at this location. There are two zircons that have ages that are younger than the sandstone depositional age. Those zircons are z10CL29-4 and z10CL29-5 and they have ages of 250 ± 20.1 Ma and 255.4 ± 20.4 Ma respectively. The z10CL29-3 zircon has an age value (298.2 ± 23.9 Ma) that is similar to the sandstone depositional age. The other 6 zircons produced older ages that range between 347.3 ± 27.8 Ma (z10CL29-7) to as old as 1170.0 ± 93.6 Ma (z10CL29-1). One Chainman Shale sample collected from this location (10CL30) produced a result of 0.89% Ro.

4.6. Diamond Peak (U-Th)/He zircon and Ro Analyses

A total of 10 zircons from the Diamond Peak locality were measured for (U-Th)/He analyses. All 10 of the zircons produced ages that are younger than the Mississippian. One zircon, z10DP21-10, recorded a very young age of 15.0 ± 1.2 Ma. The rest of the zircons within the sample recorded ages that are no older than 232.2 ± 18.6 Ma. The two Chainman samples that were collected from this area show the highest Ro values compared to the rest of the samples in this study. 10DP22 produced an Ro

value of 1.56%, and 10DP23 collected from the upper stratigraphy yielded an Ro value of 1.50%.

4.7. Duckwater (U-Th)/He zircon and Ro Analyses

The majority of the zircons collected at the Duckwater locality yielded ages that are older than the Mississippian. Two of the 10 zircons, z10DW17-3 and z10DW17-8 show ages that are younger than the sandstone depositional age (176.5 ± 14.1 Ma and 186.3 ± 14.9 Ma respectively). The remaining 8 zircons yielded ages that range from 507.4 ± 40.6 Ma (z10DW17-2) to 1424.4 ± 114.0 Ma (zDW17-10). Zircons z10DW17-3 and z10DW17-8 have U concentration of 485.3 ppm and 441.7 ppm respectively, which are higher than the rest of the zircons within this sample (Table 3). One Chainman Shale sample was sent for vitrinite reflectance analysis. The sample had an Ro result of 0.84%.

4.8. Ely (U-Th)/He zircon and Ro Analyses

For the 6 zircons collected from the Scotty Wash Sandstone near Ely, most of their ages lay within the range of the sandstone depositional age (z10EL41- 1, 2, 3, 4, and 6 yielded helium ages of 339.6 ± 27.2 Ma, 324.0 ± 25.9 Ma, 305.0 ± 24.4 Ma, 299.3 ± 23.9 Ma, and 332.5 ± 26.6 Ma respectively). One zircon (zEL41-5, with an age of 283.5 ± 22.7 Ma) is slightly younger than the majority of the zircons within the sample. The Chainman Shale sample collected from this locality has an Ro value of 1.0%.

4.9. Gap Mountain (U-Th)/He zircon and Ro Analyses

Of the 10 zircons that were analyzed using the (U-Th)/He technique, two of them show ages that are older than the sandstone deposition. These older ages are shown by zircons z10GM01-3 and z10GM01-8. Their helium ages are 374.0 ± 29.9 Ma and 392.4 ± 31.4 Ma respectively. Meanwhile, 7 other zircons (z10GM01- 1, 2, 4, 5, 7, 9, and 10)

produced ages similar to the Scotty Wash Sandstone depositional age (327.2 ± 26.2 Ma, 299.8 ± 24.0 Ma, 350.0 ± 28.1 Ma, 306.3 ± 24.5 Ma, 448.4 ± 35.9 Ma, 342.5 ± 27.4 Ma, and 315.1 ± 25.2 Ma respectively). Meanwhile, z10GM01-6 shows a minor age of 283.9 ± 22.7 Ma. Two Chainman Shale samples were collected at this area. Sample 10GM02 has an Ro value of 0.62%. Sample 10GM03, which is stratigraphically located below 10GM02, shows an Ro value of 0.63%.

4.10. Grant Range (U-Th)/He zircon and Ro Analyses

Out of 10 zircons that were measured using (U-Th)/He technique, half of them produced ages that are similar to the Scotty Wash Sandstone depositional age. z10GR07-1, 3, 5, 6, and 10 show helium ages of 313.9 ± 25.1 Ma, 327.4 ± 26.2 Ma, 348.7 ± 27.9 Ma, 331.5 ± 26.5 Ma, and 350.4 ± 28.0 Ma. The other half of the samples show ages that are older than the sandstone deposition. z10GR07-2, 4, 7, 8, and 9 produced helium ages that range between 388.0 ± 31.0 Ma and 460.9 ± 36.9 Ma. Two Chainman samples were collected from this mountain range. 10GR08 and 10GR09 have Ro results of 0.76% and 0.70% respectively.

4.11. Hot Creek (U-Th)/He zircon and Ro Analyses

The Eleana Sandstone sample from Hot Creek locality produced 8 zircons that were processed for (U-Th)/He analyses. The majority of the zircons within the sample produced ages that are older than the Mississippian, and they range from 380.1 ± 30.4 Ma to 1000.2 ± 80.0 Ma. One zircon (z10HC10-2) has an age that is younger than the Permian (217.2 ± 17.4 Ma). The two Chainman samples collected from the Hot Creek Range (10HC11 and 10HC12) were sampled at locations that were separated by a normal fault. Sample 10HC11 has an Ro value 0.85%, and 10HC12 has an Ro value 0.92%.

4.12. Illipah (U-Th)/He zircon and Ro Analyses

Only 3 zircons were collected from this location, and they were measured using (U-Th)/He technique. One zircon (z10IL27-3) produced a late Permian age (288.0 ± 23.0 Ma), and the other two zircons (z10IL27- 1 and 2) produced ages that are older than the Mississippian (429.5 ± 34.4 Ma and 360.7 ± 28.9 Ma). One Chainman Shale sample collected from the Illipah locality has an Ro value of 0.65% Ro.

4.13. Southern Snake Range (U-Th)/He and Ro Analyses

From the Scotty Wash Sandstone collected at this location, 13 zircons (labeled z10MW37- 1 to 13) produced (U-Th)/He ages. All of the zircon ages (362.3 ± 29.0 Ma to 686.7 ± 54.9 Ma) are older than the Mississippian. The Chainman Shale taken from this locality has an Ro value of 1.02%.

4.14. Northern Pancake Range (U-Th)/He and Ro Analyses

A Scotty Wash Sandstone sample collected in the northern Pancake Range produced a total of ten zircons. The zircons were measured using the (U-Th)/He technique. The majority of them show ages that are older than the Mississippian. The older ages are from 8 zircons labeled z10NP19- 1, 2, 3, 4, 7, 8, 9, and 10, and they yielded ages that range from 706.0 ± 56.5 Ma to 1579.7 ± 126.4 Ma. In addition to these results, there are two other zircons that represent younger ages. Zircon z10NP19-5 shows an age of 307.6 ± 24.6 Ma, and z10NP19-6 shows 171.5 ± 13.7 Ma. These last two zircons also show higher U concentration than the rest of the zircons within the sample with 482.5 ppm and 943.3 ppm respectively. One sample that was analyzed for vitrinite reflectance analysis did not yield any results due to insufficient organic matter content.

4.15. Pancake Range (U-Th)/He and Ro Analyses

There were two Scotty Wash Sandstone samples collected at different locations in the Pancake Range, they are z10PR13 and z10PR16. From sample z10PR13, 9 zircons were measured for (U-Th)/He analyses. Of the 9 zircons, the majority of them show ages that are older than Mississippian (514.4 ± 41.2 Ma - 1246.3 ± 99.7 Ma). One zircon from z10PR13-9 produced a younger age of 167.3 ± 13.4 Ma. One Chainman Shale sample collected from this location has an Ro value of 0.76%. Ten zircons from the z10PR16 sample were measured using the (U-Th)/He technique. Four of the zircons (z10PR16- 1, 4, 6, 7, and 10) show ages that ranged from 364.7 ± 29.2 Ma to 776.8 ± 62.1 Ma, which are older than the sandstone depositional age. The other four zircons (z10PR16- 2, 3, 5, and 8) have upper Mississippian ages (305.5 ± 24.4 Ma, 323.9 ± 25.9 Ma, 355.1 ± 28.4 Ma, and 348.0 ± 27.8 Ma) that overlap with the sandstone depositional age. Meanwhile, two zircons from z10PR16-2 and z10PR16-9 produced ages that are younger than the Mississippian (305.5 ± 24.4 Ma and 226.2 ± 18.1 Ma respectively). The last two zircons also show higher U concentrations than the rest of the zircons within the same sample (374.4 ppm for z10PR16-2 and 496.8 ppm for z10PR16-9).

4.16. Sixmile Spring (U-Th)/He zircon and Ro Analyses

Ten zircons from Sixmile Spring were measured for (U-Th)/He helium ages. Eight zircons yielded ages that are older than the Mississippian (519.0 ± 41.5 Ma to 1194.9 ± 96.6 Ma). However, two zircons produced ages that are younger than the Mississippian. Sample z10SP32-7 produced an age of 255.9 ± 20.5 Ma, and another zircon (z10SP32-9) produced an age of 18.4 ± 1.5 Ma. The z10SP32-7 and z10SP32-9 zircons also show higher U concentrations than the remaining zircons within the sample

(374.4 ppm and 322.8 ppm respectively). One Chainman Shale sample was sent for Ro analysis. It has an Ro value of 0.54%. This value is the lowest Ro value compared to other samples throughout the study area.

4.17. Northern Snake Range (U-Th)/He zircon and Ro Analyses

One Scotty Wash Sandstone sample was collected in the northern Snake Range. Of the 7 zircons analyzed, four zircons from this sample produced ages that are similar to the sandstone depositional age. Zircons z10SR39- 2, 4, 6, and 7 show ages of 302.6 ± 24.2 Ma, 340.9 ± 27.3 Ma, 321.0 ± 25.7 Ma, and 345.0 ± 27.6 Ma. Two of the zircons (z10SR39-5 and z10SR39-8) show older ages of 412.6 ± 33.0 Ma and 602.1 ± 48.2 Ma respectively. One zircon (z10SR39-1) shows an anomalously old age of 2988.7 ± 239.1 Ma.

4.18. Northern Egan Range Ro Analysis

One Chainman Shale sample (10SE33) was collected at this locality. It has an Ro value of 0.92%. No Scotty Wash Sandstone samples were found at this locality.

CHAPTER 5

DISCUSSION

Generally, zircon age results from (U-Th)/He analyses in this study can be clustered into three groups: 1) older than the Scotty Wash Sandstone depositional age, 2) similar to the sandstone depositional age (~318 – 330 Ma), and 3) younger than the sandstone depositional age. Zircon ages in the third group are generally younger than Permian.

Based on these data, there is little evidence for Permian cooling as previously hypothesized. Out of the total 163 samples, only 3 zircons from separate locations produced Permian ages. These include one zircon from Antelope Valley (z10AV35-10) that shows 267.0 ± 21.4 Ma, one zircon from Cave Lake (z10CL29-5) that shows 255.4 ± 20.4 Ma, and one zircon from the Illipah (z10IL27-3) that shows 288.0 ± 23.0 Ma.

Throughout the study area, the (U-Th)/He zircon results are shown to be dominated by ages that are older than the Mississippian Scotty Wash Sandstone depositional age. This result is seen in many locations including Burnt Mountain, Buck Mountain, Cave Lake, Duckwater, Hot Creek, Illipah, southern Snake Range, northern Pancake Range, Pancake Range (z10PR13), and Sixmile Spring. Samples from the Grant Range and the Pancake Range (z10PR16) contain zircons with ages that are older than the sandstone depositional age as well as zircons that are within the depositional age range of the Scotty Wash Sandstone. Zircons from Scotty Wash Sandstone sample taken from Ely, Gap Mtn., and northern Snake Range localities show He age results that are mainly dominated by ages within the range of the sandstone depositional time. Zircons

that are dominated by younger ages are mainly found in samples from Antelope Valley, Diamond Peak, and Cherry Creek.

Several zircon ages are considered to be discrepancies from analytical errors, and therefore they are excluded from probability age calculations. Samples z10BM04-8, z10CL29-4, z10CL29-5, z10DP21-10, z10DW17-3, z10DW17-8, zEL41-5, z10GM01-6, z10HC10-2, z10IL27-3, z10PR13-9, z10PR16- 2 and z10PR16-9 produced younger ages than the majority of ages within their samples. These anomalously young ages may occur because of parent zonation due to high U concentration within the crystal rim, irregular morphologies, inclusions, or unidentified cracks that lead to helium loss. On the other hand, z10SR9-1 produced anomalously old age. The most likely explanation for this age is due to low U concentration within the rim of the crystal, or a crystal rim being broken during unpacking from the Pt foil. Inaccuracies due to parent isotope zonation within the zircon crystals can be addressed using LA-ICPMS prior to the (U-Th)/He analysis as described by Hourigan et al. (2005). Unfortunately, this method was not performed in this study.

Probability plots for helium ages in every sample are shown in Figure 13.A to 13.R. The (U-Th)/He detrital zircon dating produced peak ages of 250 Ma (Antelope Valley), 1044 Ma and 1321 Ma (Buck Mountain), 148 Ma (Cherry Creek), 357 Ma (Cave Lake), 50 Ma (Diamond Peak), 1009 Ma and 1319 Ma (Duckwater), 318 Ma (Ely), 322 (Gap Mountain), 338 Ma (Grant Range), 397 Ma and 468 Ma (Hot Creek), 338 Ma (southern Snake Range) , 353 Ma and 1155 Ma (two samples at Pancake Range), 1131 Ma (Sixmile Spring), 327 Ma (northern Snake Range). Meanwhile, the probability age calculations for samples from Burnt Mountain., Illipah, and northern Pancake did not

produce any age peaks because of large age differences among the zircons in those samples. The probability ages for all samples in each location are presented in Figure 14.

Both Antelope Valley and Cherry Creek are located in the northern part of the study area, whereas Diamond Peak is located on the western edge of the study area. According to the data presented in Table 3, negative correlations between effective uranium concentration [U]e and zircon helium ages are found within the sandstone samples collected at Antelope Valley and Diamond Peak (Figure 15.A and 15.B). This may be best explained by residence within a paleo-zircon HePRZ. A negative correlation between [U]e and zircon helium ages is not seen for the Cherry Creek sample, therefore I interpret the helium ages from Cherry Creek to represent a resetting event.

Paired vitrinite reflectance and zircon ages from each location provide the ideal data needed in order to constrain the burial history of the Mississippian strata in this study (Figure 16). Unfortunately, there was no vitrinite reflectance sample collected from Cherry Creek. The majority of vitrinite reflectance values in the area around RRV were in the range of 0.70% - 0.90%. Based on source rock classification from Peters and Cassa (1994) (Figure 17), these values indicate mature source rock with respect to oil and gas generation. The lowest (0.54% Ro) value was found in Sixmile Spring and in Antelope Valley (0.57% Ro). These numbers indicate that the rocks have reached a very late immature stage of source rock or a very early maturity where the source rock has just started to generate oil (Peters and Cassa, 1994). On the other hand, two samples taken from farther west at the Diamond Peak location recorded the highest Ro value (1.56% and 1.50%), which indicate postmature source rock (Peters and Cassa, 1994). Based on these data, vitrinite reflectance values in the study area show that the Chainman Shale

generally reached the oil generation stage. Figure 18 shows that the lowest Ro value in this study (0.54%) is roughly equivalent to paleotemperature of ~55°C, and the highest Ro value from the Diamond Peak is roughly equivalent to an ~150°C paleotemperature (Hunt, 1996). Figure 19 shows Ro value contour lines throughout the study area.

CHAPTER 6

INTERPRETATION

The majority of the vitrinite reflectance samples are between 0.70% - 0.90% R_o , which indicates they reached the oil window. These results are in good agreement with previous studies regarding the thermal maturity of the Chainman Shale in east-central Nevada (Poole and Claypool, 1984; Rowan et al., 1992).

The majority of zircons collected from this study show ages older than the Scotty Wash Sandstone depositional age. These zircons mostly have sub-rounded shapes indicative of abrasion during transportation. I interpret these as detrital zircons that were eroded from either older rocks of the exhumed Antler orogen and Antler foreland or the North American craton which were then transported and were re-deposited in the Antler successor basin.

The zircon ages that are similar to the sandstone depositional age could be attributed to two different possibilities. One possibility is that they resulted from deep burial and rapid exhumation, erosion, transportation, and deposition of the sediments from the Antler highland in the west to the Antler successor basin during this period of time. A second plausible explanation is that these zircons came from volcanic eruptions from a postulated island arc farther to the west of the Antler highland, or from the North American craton, and that they were transported by wind to the Antler successor basin. One possible source for volcanic zircons is from the northern Sierra Nevada, e.g. Upper Paleozoic volcanic rocks studied by Hannah and Mores (1986) that may have contributed to the provenance of the zircons within the Scotty Wash Sandstone.

Several ages younger than Permian were recorded in zircons collected from Diamond Peak, Cherry Creek, and Antelope Valley locations. Each location will be individually explained in the following paragraphs.

Antelope Valley

The relative probability plot from Antelope Valley shows one peak age (250 Ma) younger than the Permian (Figure 13.A), and the negative correlation between the effective uranium concentration and zircon ages may indicate that the sample resided in the HePRZ (Stockli et al., 2010). On the other hand, the corresponding Chainman Shale sample has a very low vitrinite reflectance value (0.57% Ro). This phenomenon may have occurred because of a local thermal source that occurred near the location of the sandstone sample, but was far enough away from the Chainman Shale to not influence its thermal maturity. If this scenario is true, the area that is closer to the thermal source would have reached higher temperatures. This could explain how the zircon was heated and was reset or partially reset but left the Chainman Shale exposed to lower temperatures (low Ro). Evidence of hydrothermal veins was found near the area where the rock samples were collected. However, this explanation is problematic because both samples were separated by only a short distance (~100 m) in the field, so the Chainman Shale sample should have also recorded high heat flow.

Diamond Peak

The Diamond Peak location has the highest Ro values (1.50% and 1.56%) and the youngest zircon peak age at 50 Ma (Figure 13.F). These results may have arisen from three possible scenarios. The first scenario is that the young zircon ages and high Ro

values are the result of deep burial in the Antler successor basin that occurred as the result of the emplacement of the Roberts Mountain allochthon. According to Trexler et al. (1995) the Roberts Mountain Thrust (RMT) is located directly west of the Diamond Peak Range, which means that the thickest sections in the Antler foreland basin occur to the east of the thrust. Another similar scenario that may have contributed to this phenomenon is the presence of the Triassic - Middle Cretaceous Central Nevada Thrust Belt (CNTB), which occurred east of the Diamond Peak Range. The third scenario involves younger thermal overprinting that resulted in increased thermal maturation of the shale. Anna et al. (2007) pointed out that areas in northern and western Nevada have high thermal gradients that may be associated with geothermal systems linked to mineralization. This phenomenon might have affected the Diamond Peak area, causing the high maturity of the Chainman and causing a partial resetting of ages for the zircons in the Scotty Wash Sandstone. According to Hose et al. (1976), the Diamond Peak location is located close to the Newark mining district (about ~3 km from the sample location). Tertiary volcanic rocks (map unit = Tov) consisting of rhyodacite, quartz latite, andesite, and tuff are mapped adjacent to the mountain range and may have contributed to this mineralization (Figure 12.F). Schmauder et al. (2005) found that hydrothermal activity that produced mineralization at Bald Mountain (Ruby Range), 80 km northeast of Eureka may have taken place in the Eocene and became significantly more intense during the Miocene.

The negative correlation between zircon helium age and effective uranium concentration in this sample may indicate residence within a paleo-zircon HePRZ setting

(e.g. Shuster et al., 2006). The high Ro values from this location also support this interpretation because they roughly correspond to a ~150°C paleotemperature.

Cherry Creek

Located farther to the north in the study area, the Cherry Creek location zircons also yielded ages younger than the depositional age of the Scotty Wash Sandstone. The majority of zircons in this location have early Cretaceous ages, and the peak age is 148 Ma (Figure 13.D). Unfortunately, no Chainman Shale sample was collected from this locality.

One interpretation is that this location was subjected to a younger thermal overprint that produced thermal resetting of the zircons. Another interpretation for this young cooling age is that it resulted from the resetting of the zircons as a result of differential loading and exhumation that locally occurred in this area. However, no major geological structures that could account for this scenario are known.

Overall, the (U-Th)/He results shows little evidence for the hypothesized Permian cooling reported in the previous study in the Egan Range (Druschke, 2009). In addition, no Ro samples in this study have values higher than 1.56%. Based on Hunt's (1996) classification, the maximum vitrinite reflectance values determined in this study represent paleotemperatures of approximately 150°C for Mississippian rocks in the study area which is not adequate to cause complete resetting of the (U-Th)/He system. The Ro results in this study are in good agreement with other studies, e.g. from Ahdyar (2011) and Rowan et al. (1992), regarding the thermal maturity of the Chainman Shale.

I conclude that burial of the Chainman Shale and the Scotty Wash Sandstone was not sufficient to produce temperatures high enough to reset the (U-Th)/He system in east-

central Nevada. I infer that the Permian "cooling ages" reported by Druschke (2009) are not the result of deep burial followed by exhumation in the Permian. The zircons in that study were possibly metamict or there were flaws in the data set. The data may have been misinterpreted if the author failed to recognize potential residence within a (U-Th)/He partial retention zone (HePRZ).

Magmatic versus metamorphic zircons

Although it was not central to this project, recent research has shown that the Th/U ratio of zircons can be used for provenance interpretations. Williams et al. (1996) suggested that magmatic zircon could be distinguished from metamorphic zircon by looking at the ratio of Th/U. According to their study, metamorphic zircons have lower Th/U (<0.1) concentration compared to zircons from magmatic crystallization.

Table 3 shows that the zircons in this study have moderate to high ratios with the exception of two zircons that show low values of 0.09 in z10NP19-6 and z10PR16-10. This finding leads to the interpretation that zircons from the study area are most likely magmatic and may support the scenario of an island arc provenance for the zircons that have Mississippian (U-Th)/He ages, or other igneous provenance from the exhumed and eroded Antler highland, or magmatism from eastern North America.

However, Moller et al. (2002) suggested that metamorphic zircons in their study were not always easily distinguished by low Th/U concentration as previously suggested by Williams et al. (1996). Furthermore, Moller et al. (2003) prefer identification of metamorphic and magmatic zircon based on morphology and internal structure using cathodoluminescence. Crystals with oscillatory zoning can be interpreted as magmatic growth that reflects slow growth from a fluid-rich boundary layer. In contrast,

metamorphic zircons often have recrystallized rims on existing crystals that show little or no internal zoning and have shapes unrelated to existing features. Moreover, geochemical characterization of zircon based on trace elements like Hf and Y could also be used to support the interpretation (Moller et al., 2003).

CHAPTER 7

CONCLUSION

(U-Th)/He data from zircons in the Scotty Wash Sandstone indicate cooling ages dominated by Mississippian and older ages in most locations (Burnt Mtn., Buck Mtn., Cave Lake, Duckwater, Hot Creek, Illipah, southern Snake Range, northern Pancake Range, Pancake Range, and Sixmile Spring). These older ages are interpreted as detrital zircons that were eroded from older sources which were deposited in the Antler successor basin. Zircons from Ely, Gap Mtn., and northern Snake Range localities are dominated by ages that are similar to the depositional age of the Scotty Wash Sandstone, and may represent rapid burial and exhumation of the Antler orogen or from volcanic input, e.g., the northern Sierra Nevada. Zircons from Grant Range and Pancake Range localities show ages that fall within the span of the deposition time of the Scotty Wash Sandstone and older.

Zircons from Diamond Peak, Antelope Valley, and Cherry Creek produced ages that are younger than the Permian. I interpret that Antelope Valley and Diamond Peak results to represent partially reset ages, and Cherry Creek's zircon ages are reset. These phenomena are probably related to burial and/or younger thermal overprints.

In addition to these data, most zircons show moderate to high Th/U and may indicate a magmatic source.

The majority of vitrinite reflectance (R_o) values in the study area are in the range of 0.70% to 0.90%. These values indicate paleo-temperatures that roughly correspond to ~55 to ~150°C. The lowest R_o values were recorded in sample 10SP31 (Sixmile Spring)

and 10AV36 (Antelope Valley), with R_o values of 0.54% and 0.57% respectively. The highest value recorded was taken from Diamond Peak (10DP22) with R_o value of 1.56%.

Based on the vitrinite reflectance analyses, the maximum burial of Mississippian strata occurred in the western part (Diamond Range) of the study area, but the depth of burial did not exceed 5 km.

Overall, this study does not support the hypothesized regional Permian cooling documented in Egan Range.

APPENDIX A

FIGURES

W 117° 30'

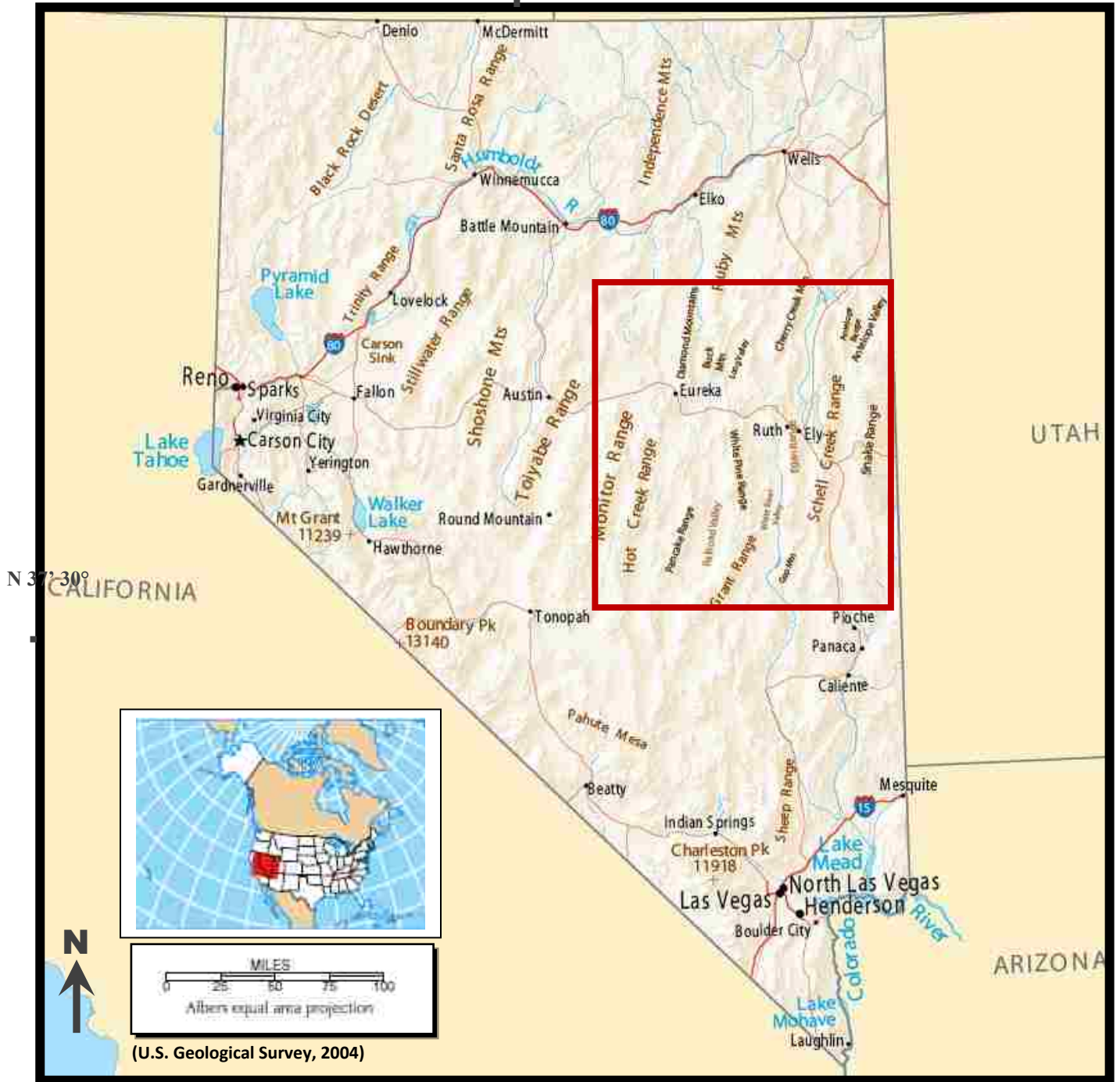


Figure 1. Map shows the state of Nevada. The study area in east-central Nevada occupies the area inside the red box.

East - Central Nevada

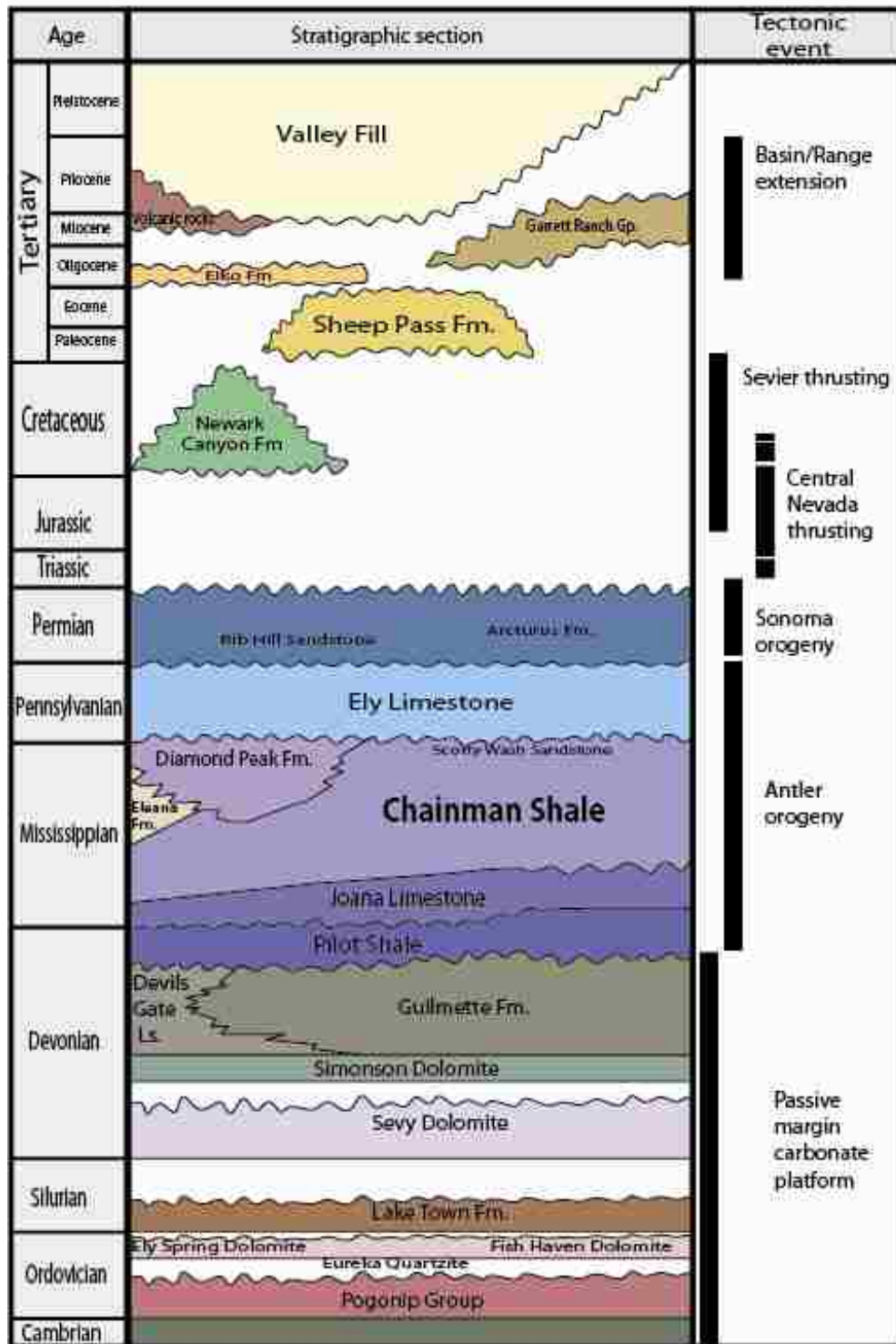


Figure 2. Regional stratigraphy and major tectonic events history for east-central Nevada region (modified from Anna et al., 2007).

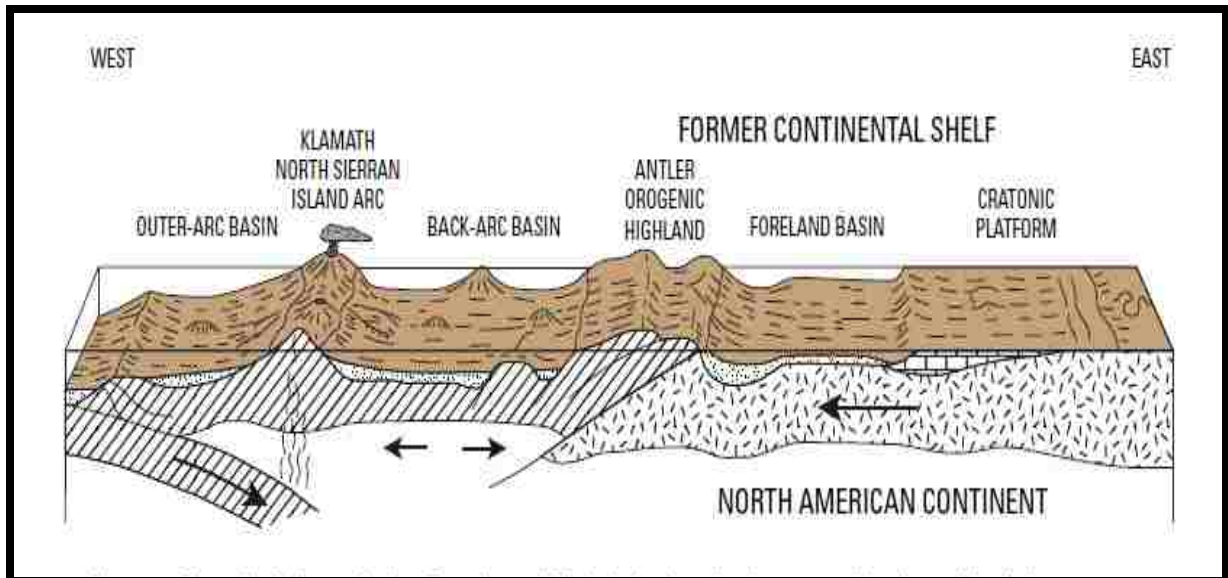


Figure 3. Hypothetical tectonic configuration of western North America during Late Devonian – early Mississippian time. East vergent thrusting resulted in uplift of the Antler Orogenic Highlands, and flexural loading of the craton edge created an eastward-migrating foredeep which is shown here as the site of the foreland basin (Cook, 1988; Anna et al., 2007).

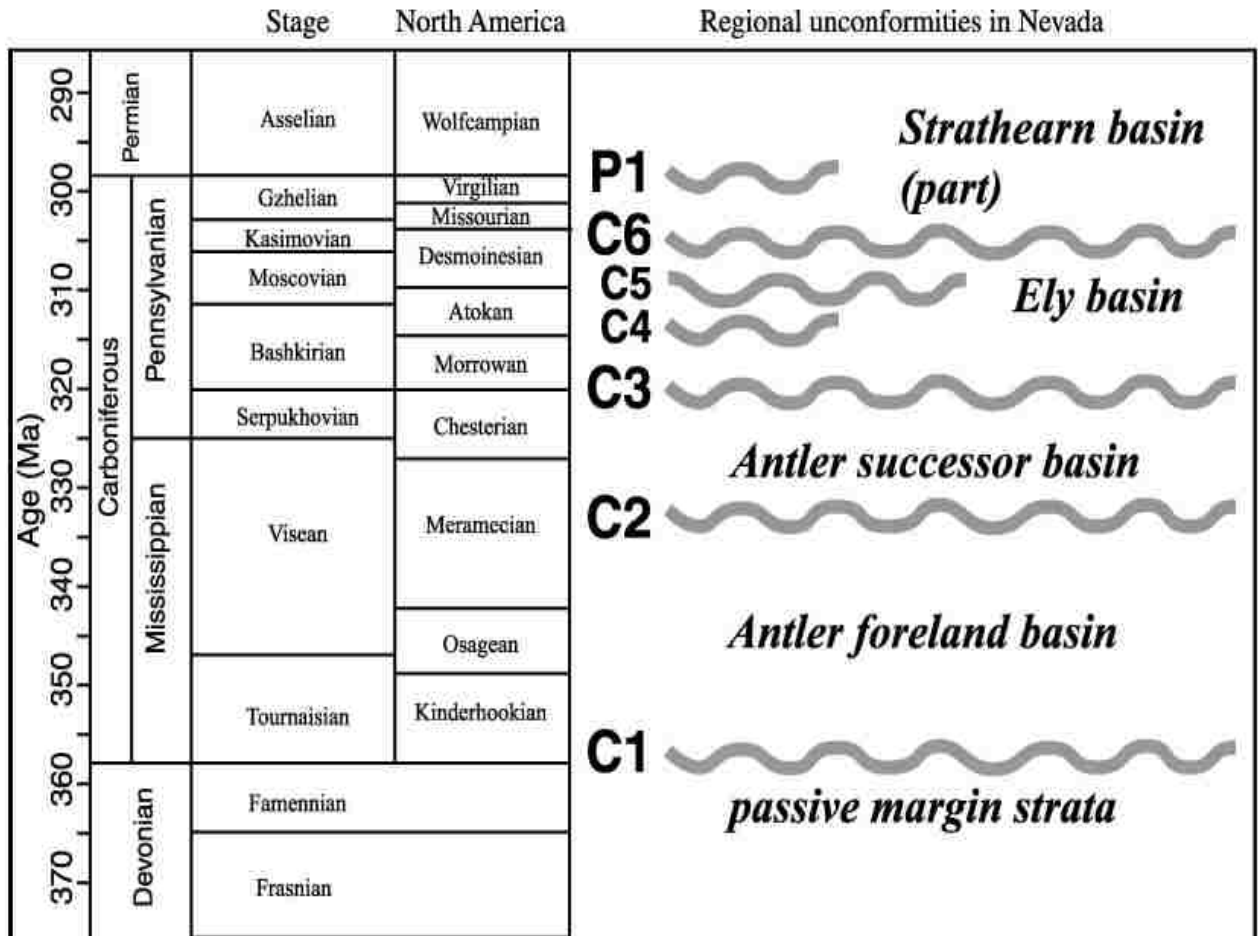


Figure 4. Regional unconformities of the Carboniferous in the Great Basin, western North America (Snyder and Trexler, 2000; Snyder et al., 2000; Trexler et al., 2004). The Mississippian Chainman Shale and Scotty Wash Sandstone were deposited within the Antler successor basin (Trexler et al., 2003).

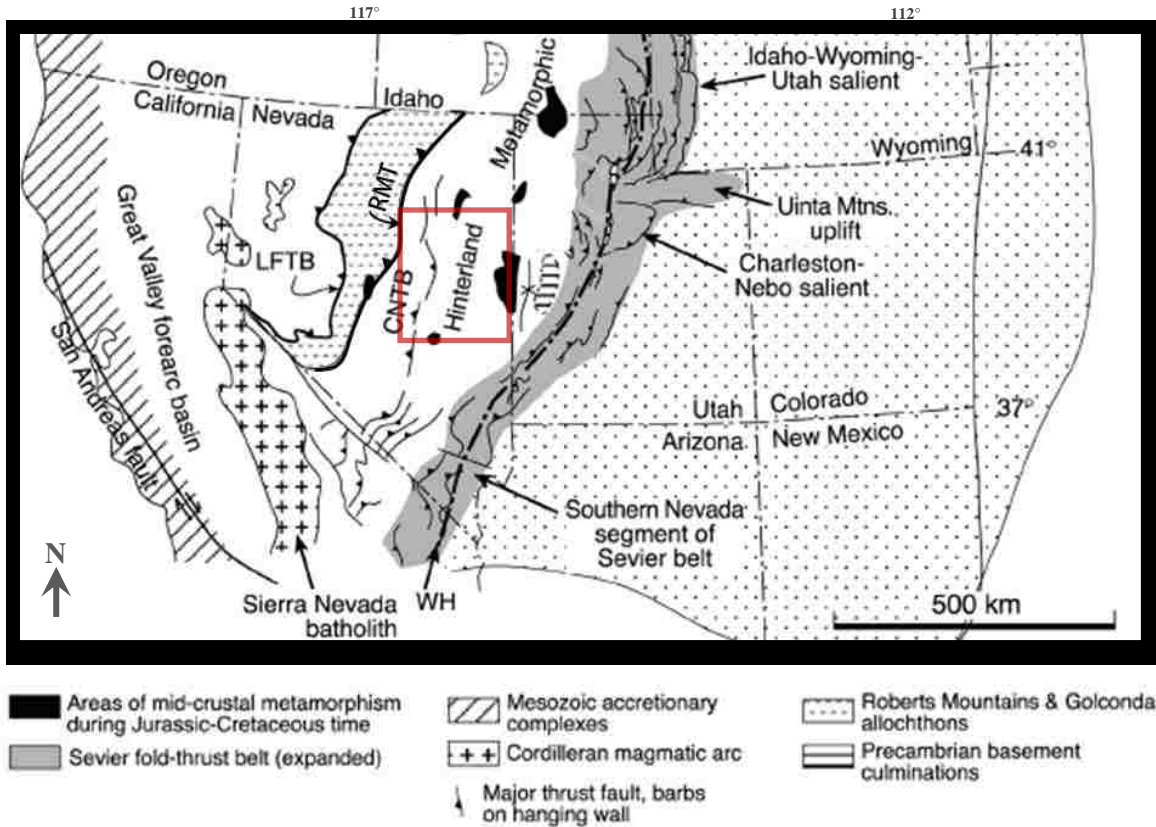


Figure 5. Simplified map showing the major tectonic features of the U.S. Cordillera. The map shows the location of the Lunning-Fencemaker thrust belt (LFTB), Central Nevada Thrust Belt (CNTB), and Roberts Mountain Thrust (RMT) in east-central Nevada relative to the study area (shown by the red square). The stippled region represents the Western Interior Basin (modified from DeCelles, 2004).

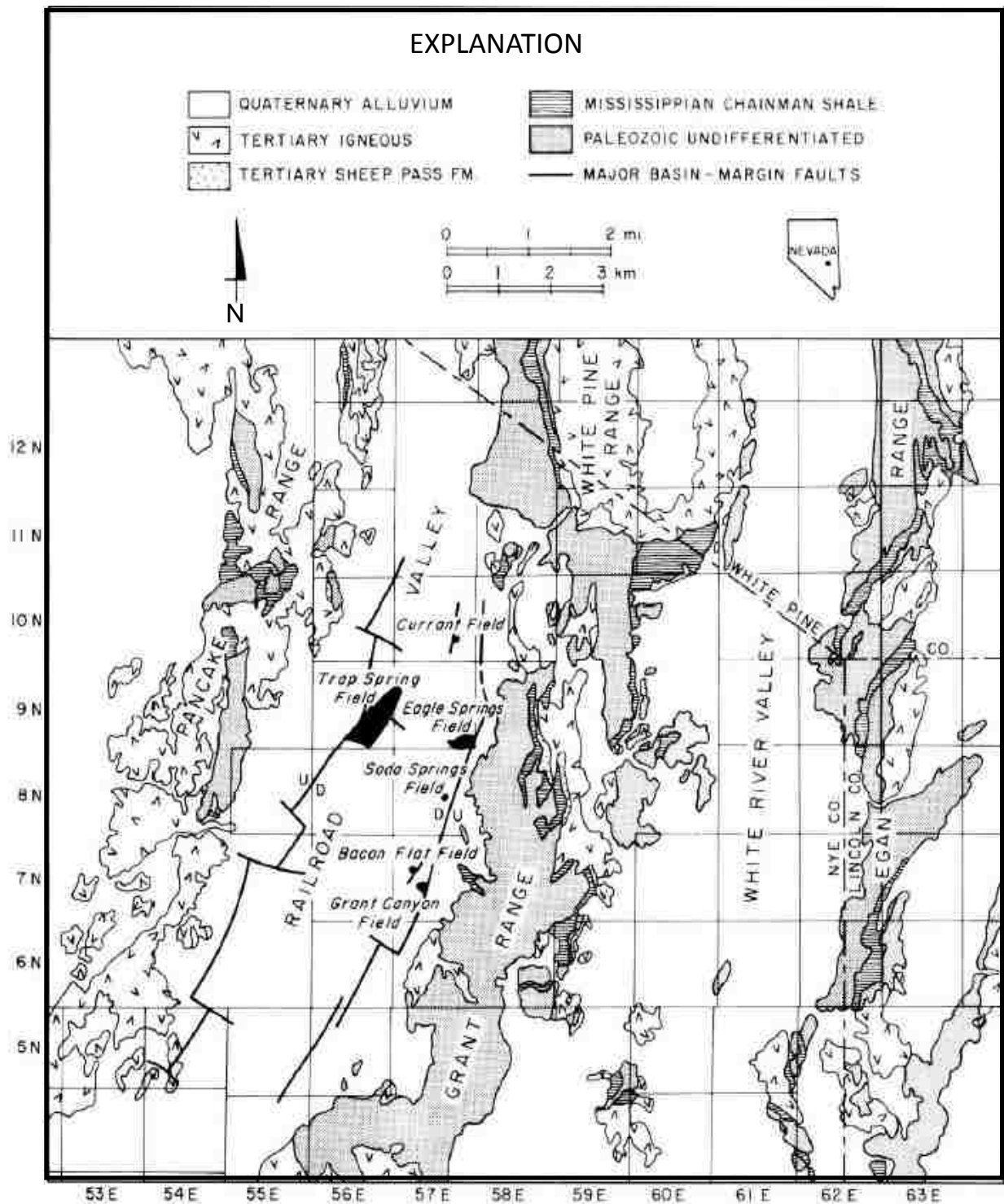


Figure 6. Generalized geologic map of Railroad Valley (RRV) in Nevada. RRV oil fields are located along the faults at the western and eastern boundaries of the valley (Hughes and Carlson, 1987).

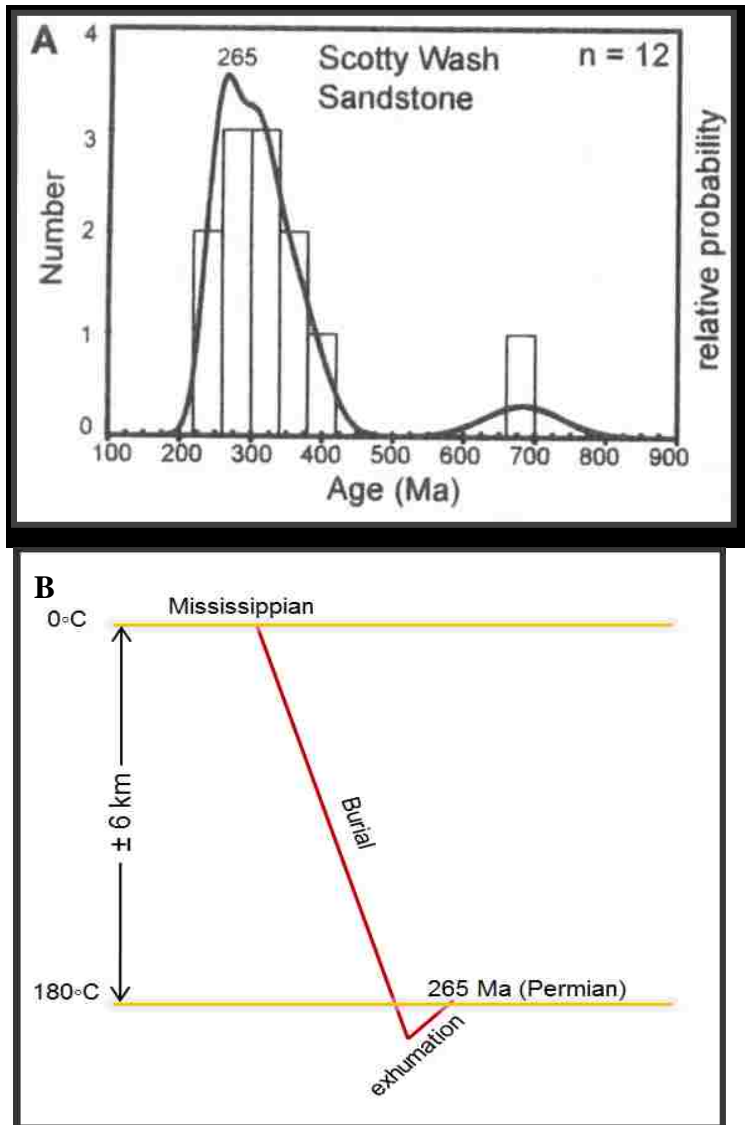


Figure 7. A) (U-Th)/He results published by Druschke (2009) based on detrital zircons from the Scotty Wash Sandstone in the Egan Range, Nevada; and B) one interpretation of the results. In this interpretation the Permian age is assumed to be the result of resetting of the (U-Th)/He system. This interpretation assumes a 30°C/km geothermal gradient and a burial depth of more than 6 km, followed by exhumation and cooling to temperatures less than ~180°C. In this model, the Permian age is interpreted as an exhumation age.

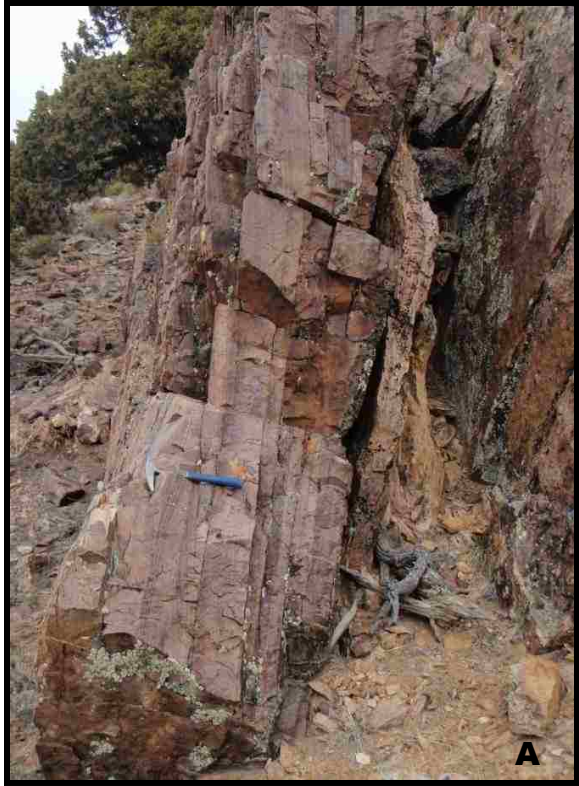


Figure 8. Outcrop photo of A) Scotty Wash Sandstone, and B) Chainman Shale.

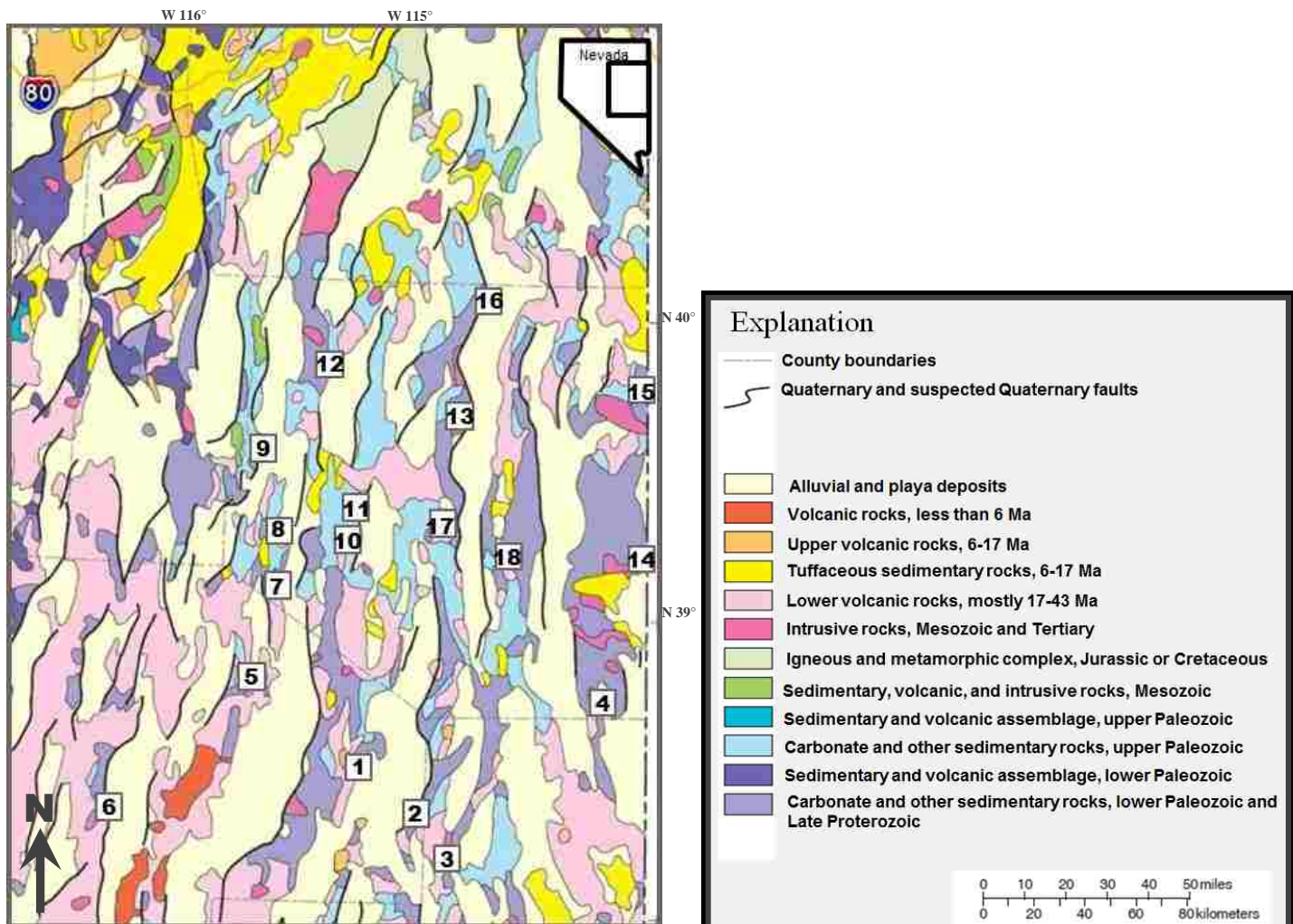


Figure 9. Generalized geologic map of the study area. Numbers represent the sample location, 1) Grant Range, 2) Gap Mtn., 3) Burnt Mtn., 4) southern Snake Range, 5) Pancake Range, 6) Hot Creek, 7) Duckwater, 8) northern Pancake Range, 9) Diamond Peak, 10) Sixmile Spring, 11) Illipah, 12) Buck Mtn., 13) northern Egan Range, 14) northern Snake Range, 15) Antelope Valley, 16) Cherry Creek, 17) Ely, 18) Cave Lake (modified from Nevada Bureau of Mines and Geology Map 57).

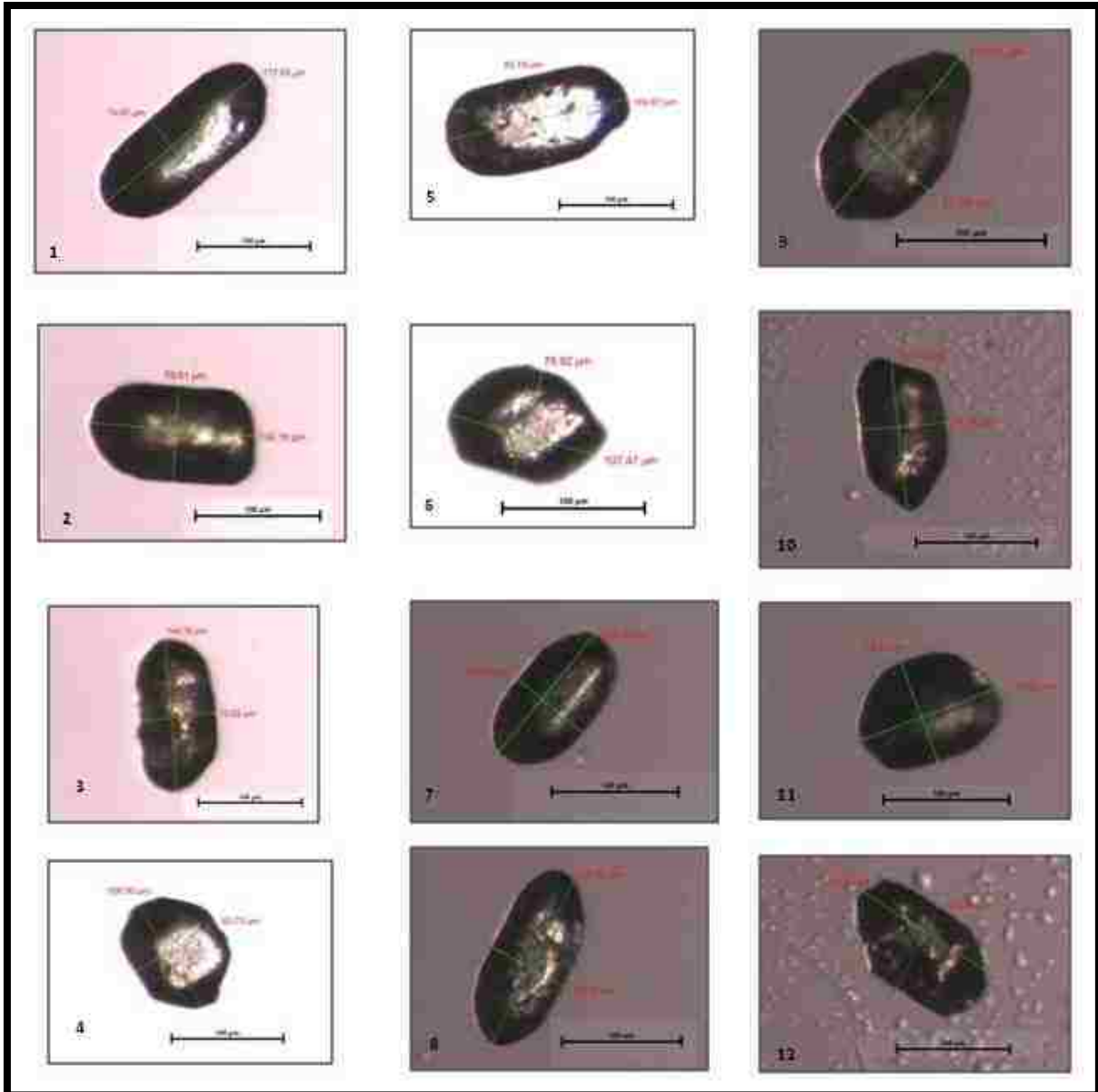


Figure 10.A. Photographs of zircon grains collected from Antelope Valley that were used for (U-Th)/He analyses. All zircons are shown under reflected light. The scale bar shown in each photograph is constant and is 100 μm long.

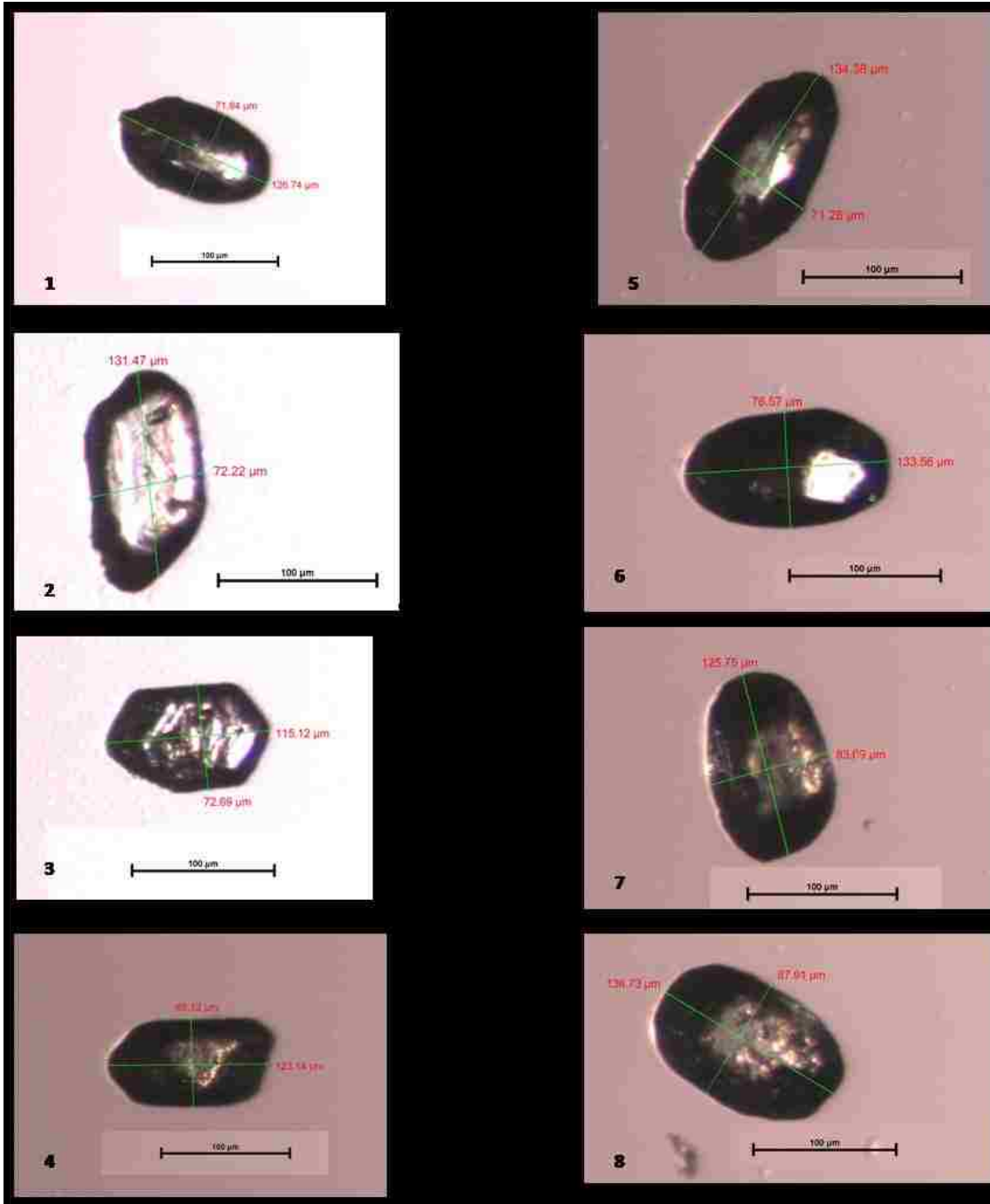


Figure 10.B. Photographs of zircon grains collected from Burnt Mtn. that were used for (U-Th)/He analyses. All zircons are shown under reflected light. The scale bar shown in each photograph is constant and is 100 μm long.

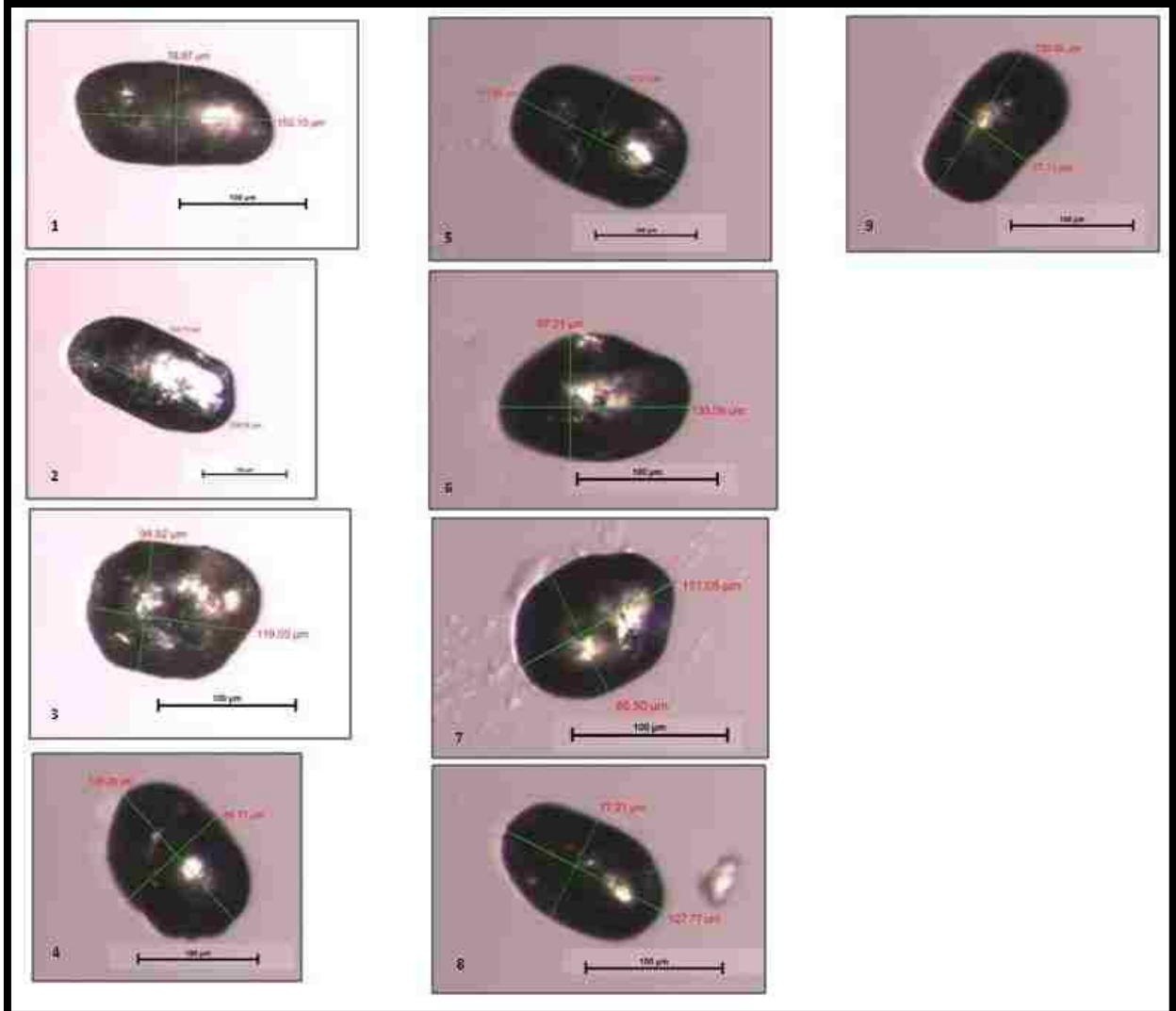


Figure 10.C. Photographs of zircon grains collected from Buck Mtn. that were used for (U-Th)/He analyses. All zircons are shown under reflected light. The scale bar shown in each photograph is constant and is 100 μm long.



Figure 10.D. Photographs of zircon grains collected from Cherry Creek that were used for (U-Th)/He analyses. All zircons are shown under reflected light. The scale bar shown in each photograph is constant and is 100 µm long.

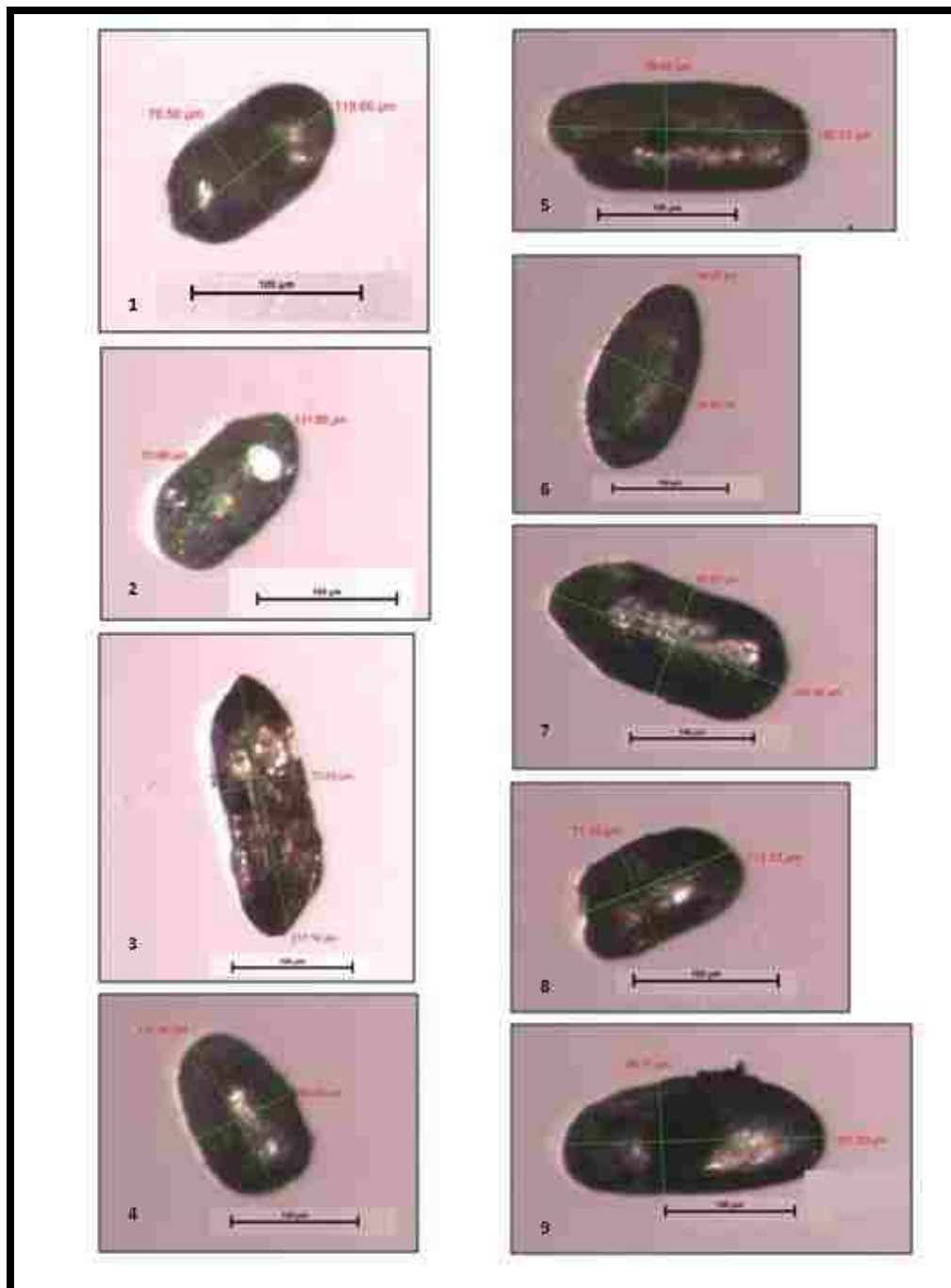


Figure 10.E. Photographs of zircon grains collected from Cave Lake that were used for (U-Th)/He analyses. All zircons are shown under reflected light. The scale bar shown in each photograph is constant and is 100 µm long.

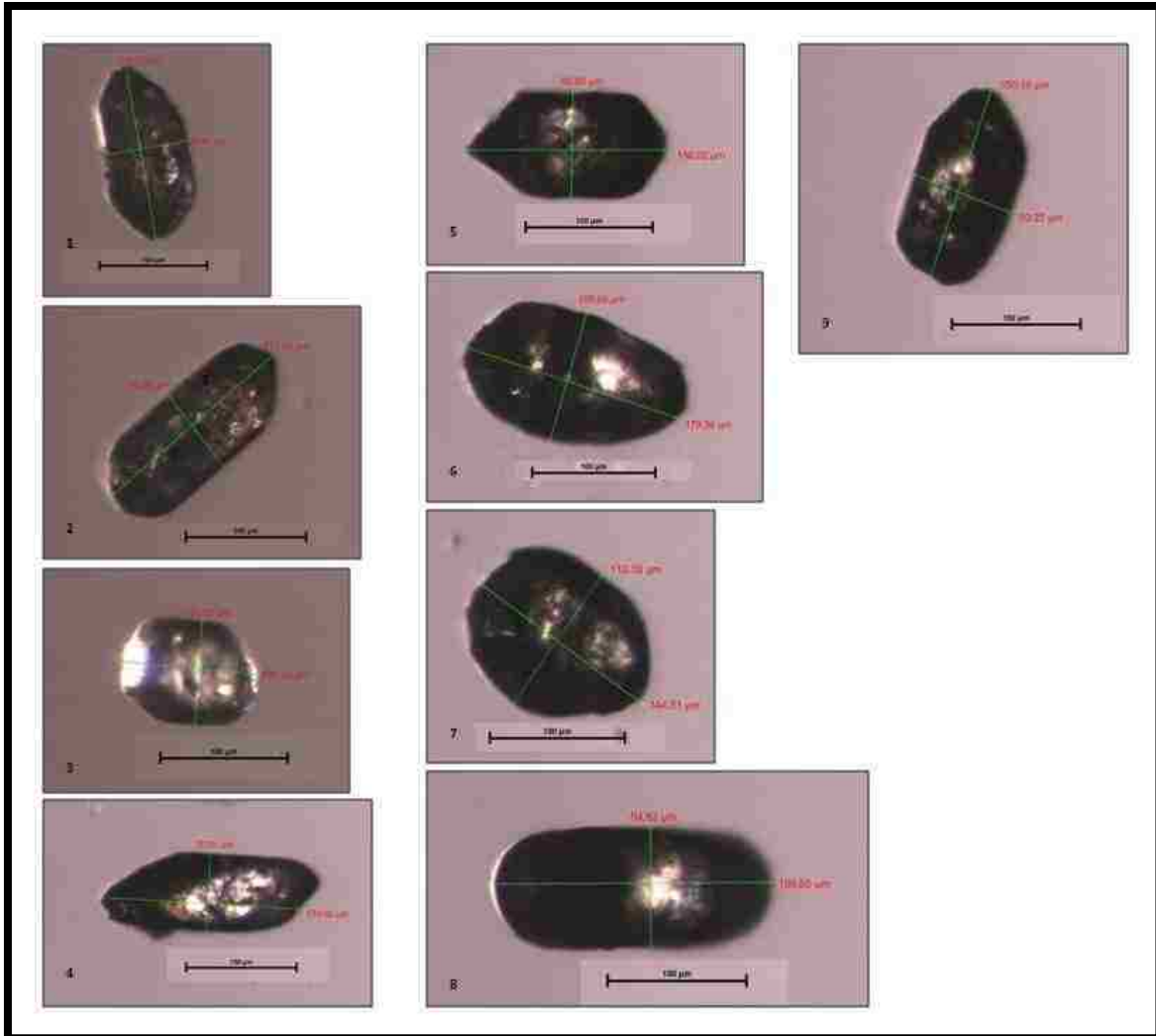


Figure 10.F. Photographs of zircon grains collected from Diamond Peak that were used for (U-Th)/He analyses. All zircons are shown under reflected light. The scale bar shown in each photograph is constant and is 100 μm long.

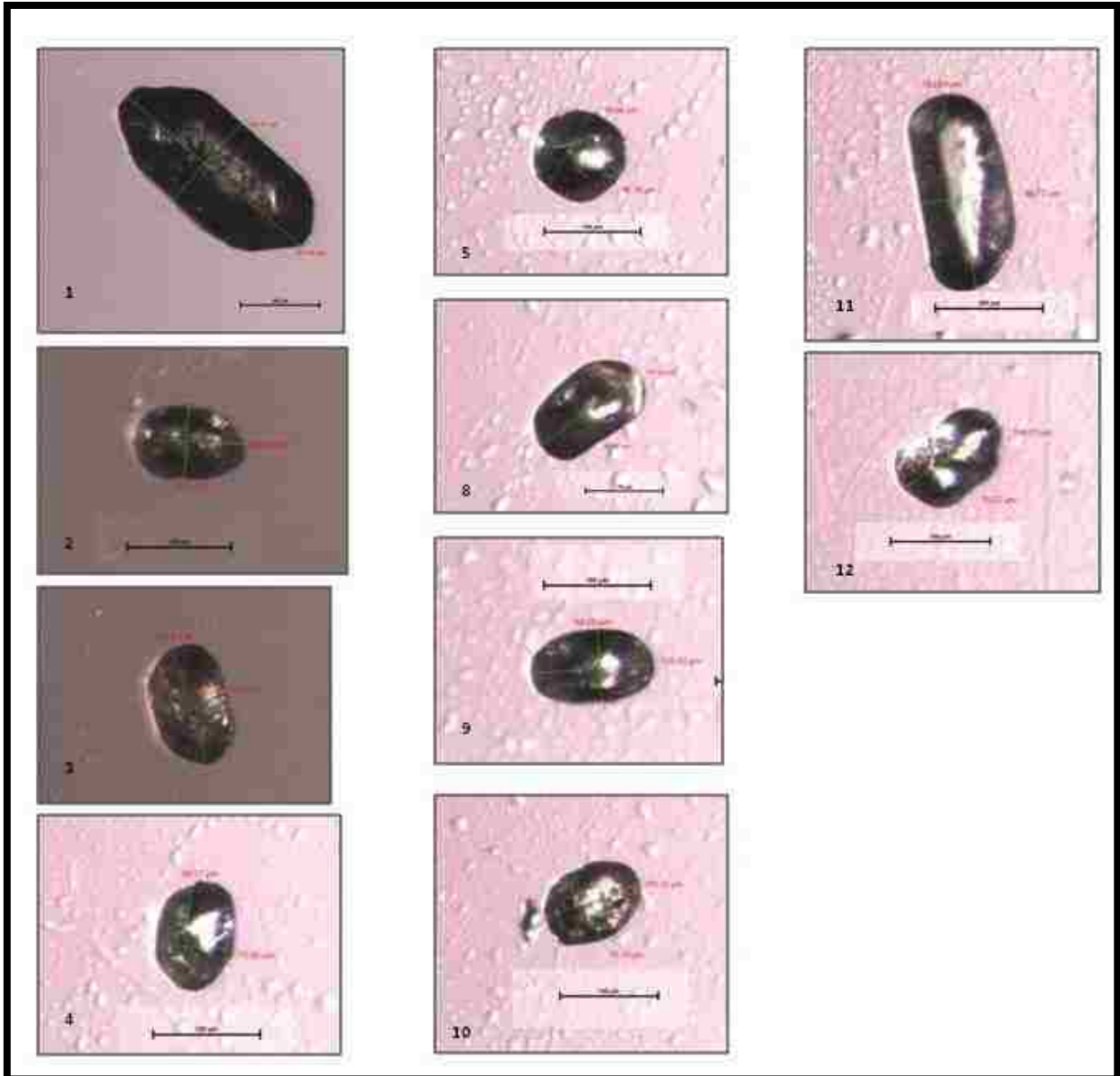


Figure 10.G. Photographs of zircon grains collected from Duckwater that were used for (U-Th)/He analyses. All zircons are shown under reflected light. The scale bar shown in each photograph is constant and is 100 µm long.

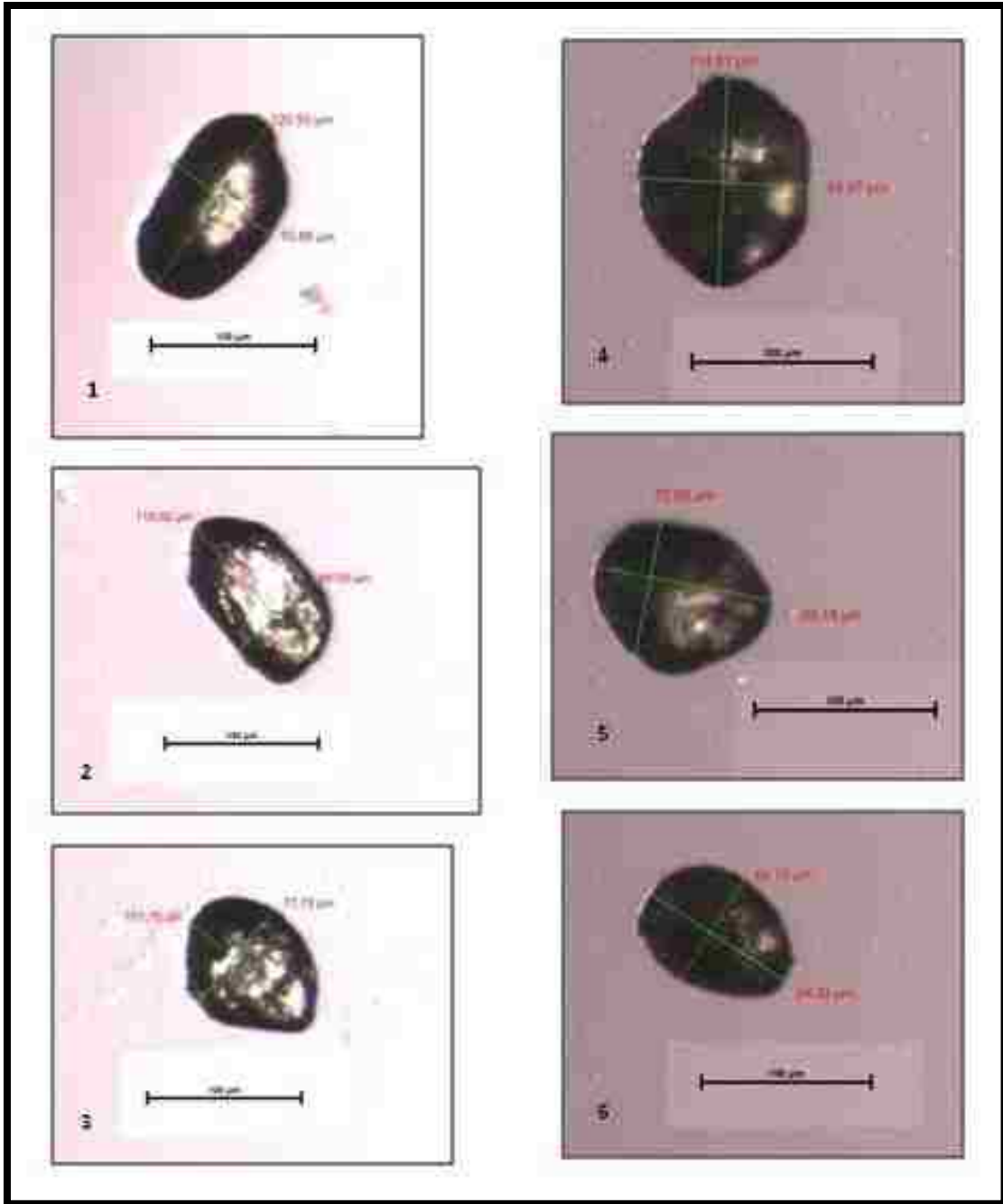


Figure 10.H. Photographs of zircon grains collected from Ely that were used for (U-Th)/He analyses. All zircons are shown under reflected light. The scale bar shown in each photograph is constant and is 100 μm long.

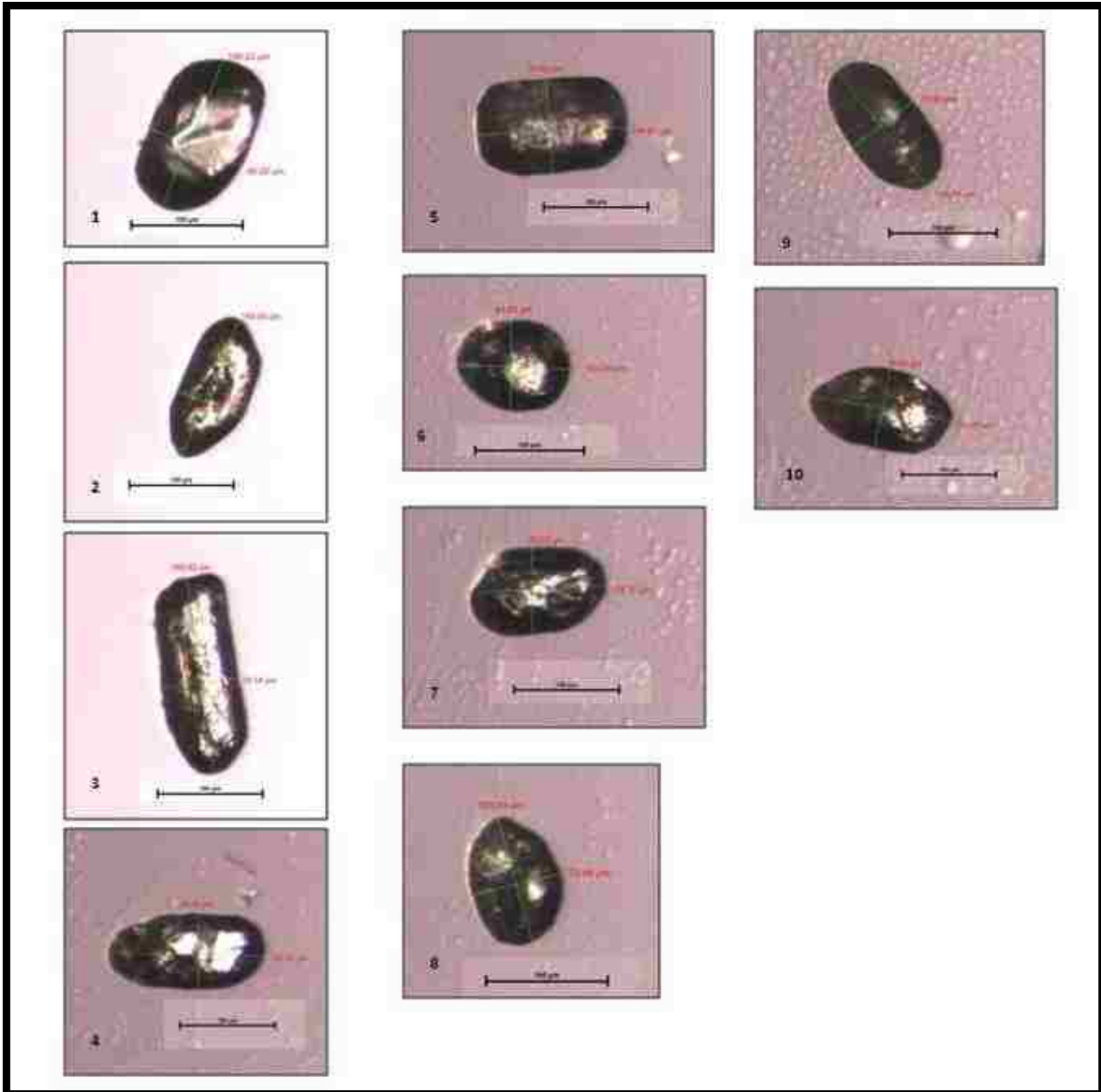


Figure 10.I. Photographs of zircon grains collected from Gap Mtn. that were used for (U-Th)/He analyses. All zircons are shown under reflected light. The scale bar shown in each photograph is constant and is 100 μm long.

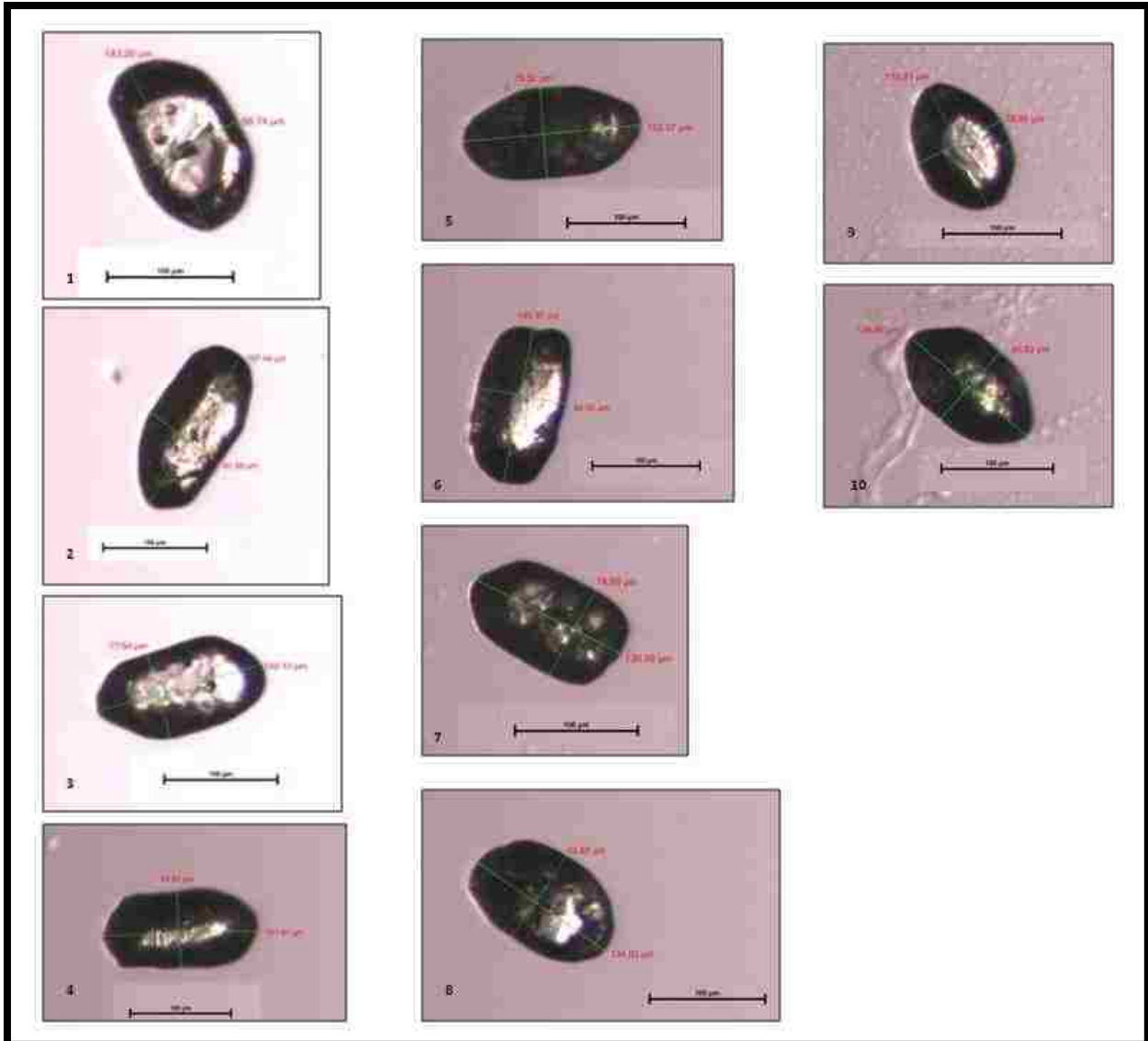


Figure 10.J. Photographs of zircon grains collected from Grant Range that were used for (U-Th)/He analyses. All zircons are shown under reflected light. The scale bar shown in each photograph is constant and is 100 μm long.

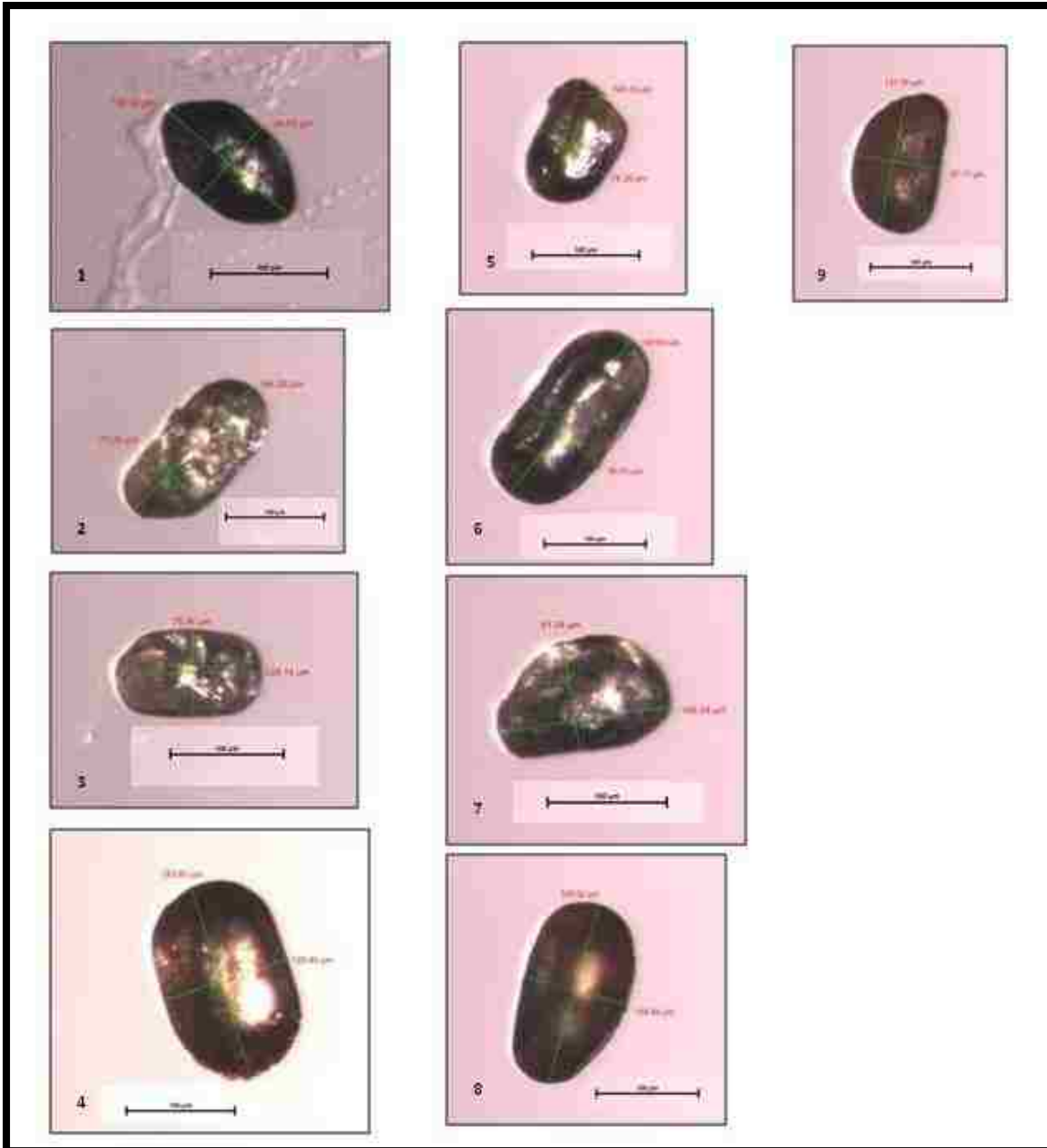


Figure 10.K. Photographs of zircon grains collected from Hot Creek that were used for (U-Th)/He analyses. All zircons are shown under reflected light. The scale bar shown in each photograph is constant and is 100 μm long.

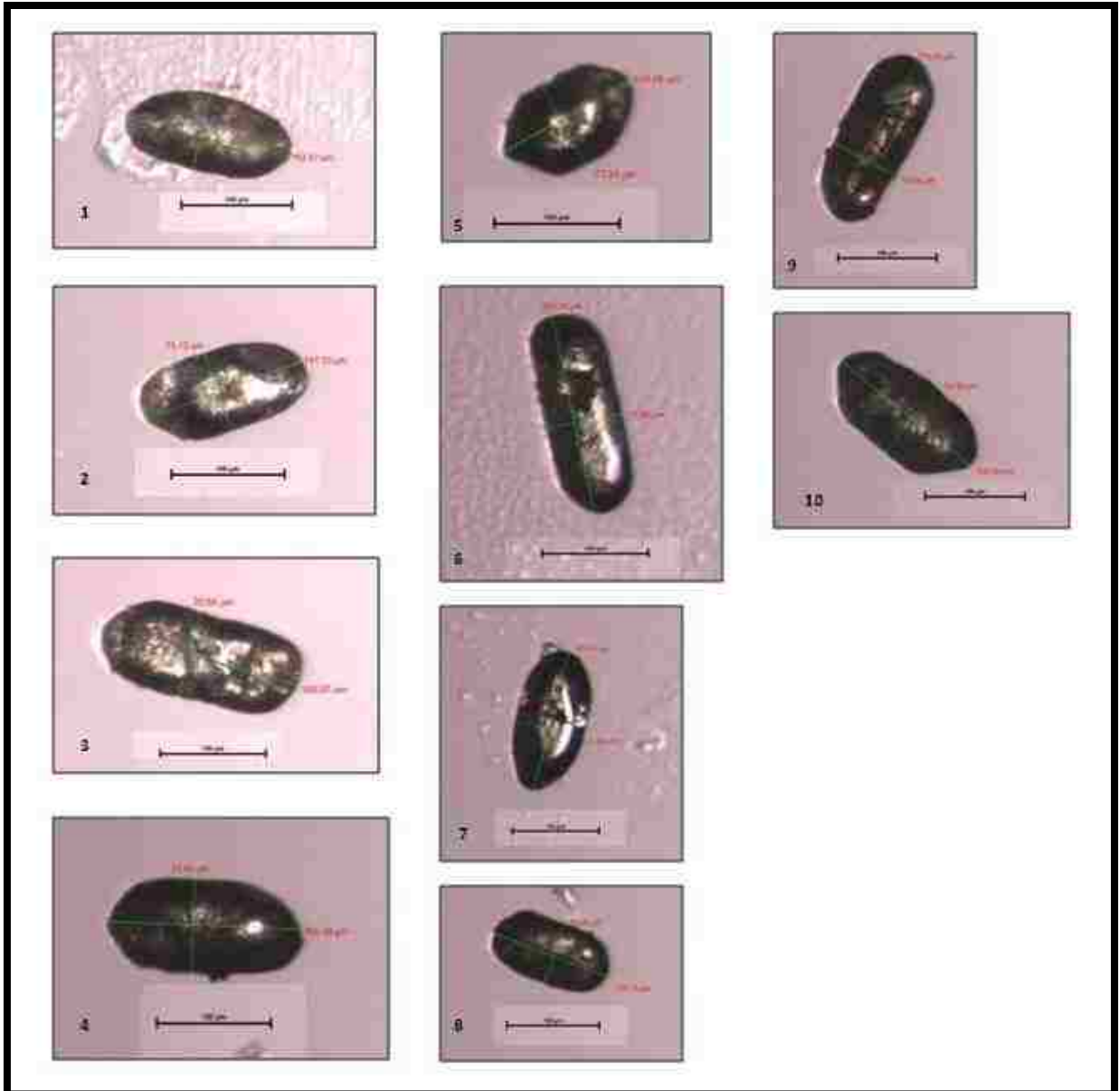


Figure 10.L. Photographs of zircon grains collected from Illipah that were used for (U-Th)/He analyses. All zircons are shown under reflected light. The scale bar shown in each photograph is constant and is 100 μm long.

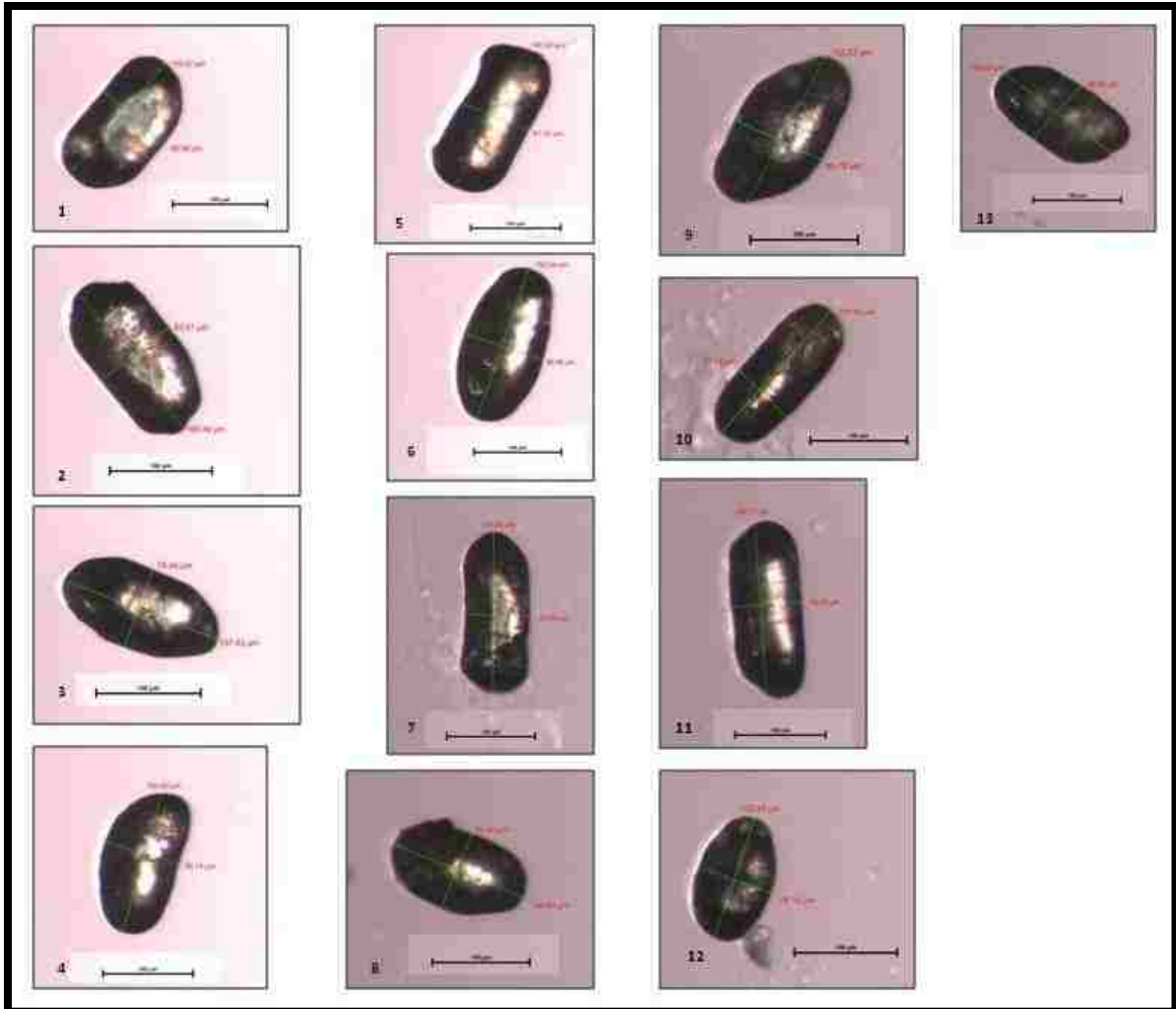


Figure 10.M. Photographs of zircon grains collected from southern Snake Range that were used for (U-Th)/He analyses. All zircons are shown under reflected light. The scale bar shown in each photograph is constant and is 100 μm long.

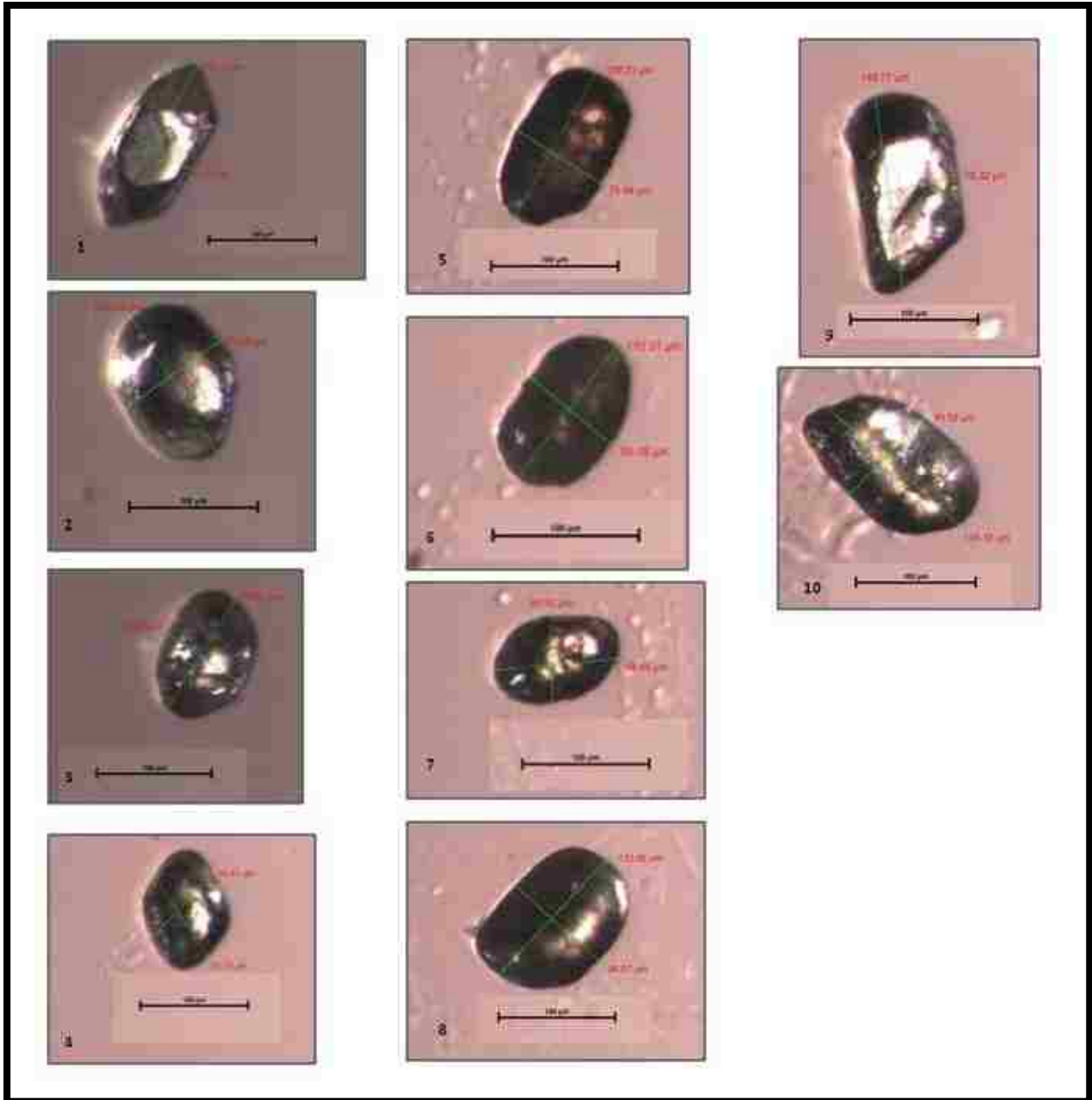


Figure 10.N. Photographs of zircon grains collected from northern Pancake Range that were used for (U-Th)/He analyses. All zircons are shown under reflected light. The scale bar shown in each photograph is constant and is 100 μm long.



Figure 10.O. Photographs of zircon grains collected from Pancake Range (z10PR13) that were used for (U-Th)/He analyses. All zircons are shown under reflected light. The scale bar shown in each photograph is constant and is 100 μm long.

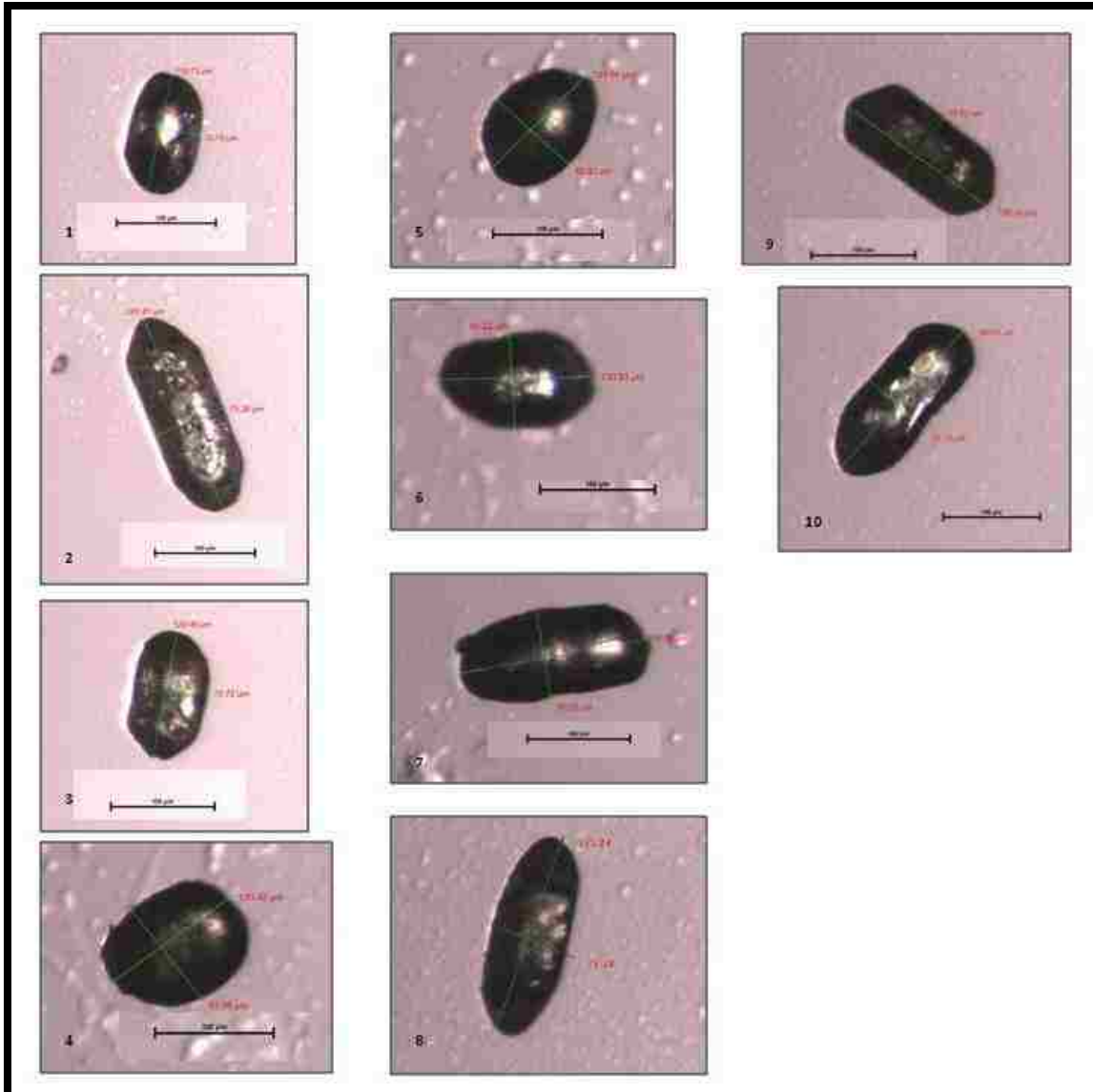


Figure 10.P. Photographs of zircon grains collected from Pancake Range (z10PR16) that were used for (U-Th)/He analyses. All zircons are shown under reflected light. The scale bar shown in each photograph is constant and is 100 µm long.

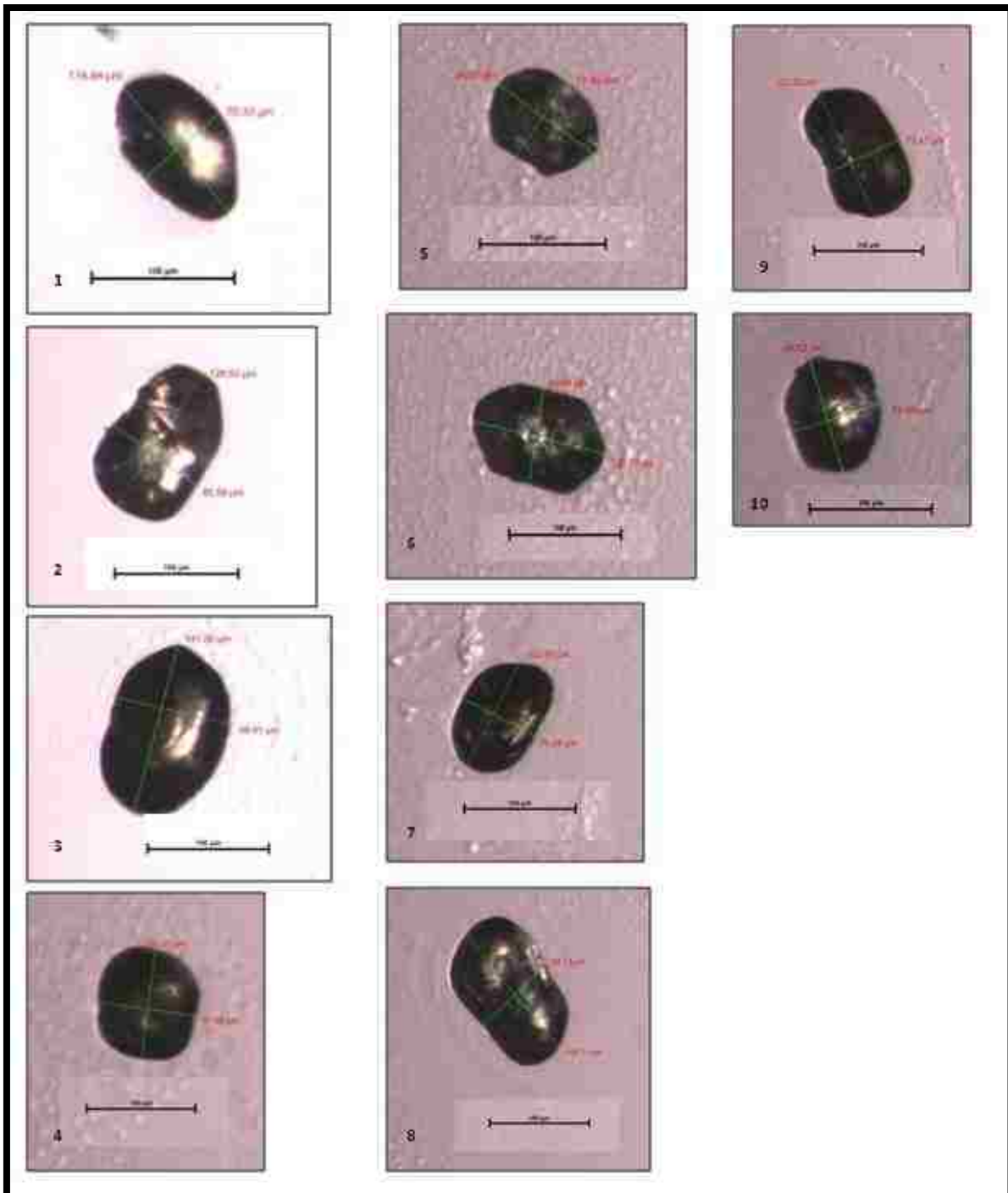


Figure 10.Q. Photographs of zircon grains collected from Sixmile Spring that were used for (U-Th)/He analyses. All zircons are shown under reflected light. The scale bar shown in each photograph is constant and is 100 μm long.

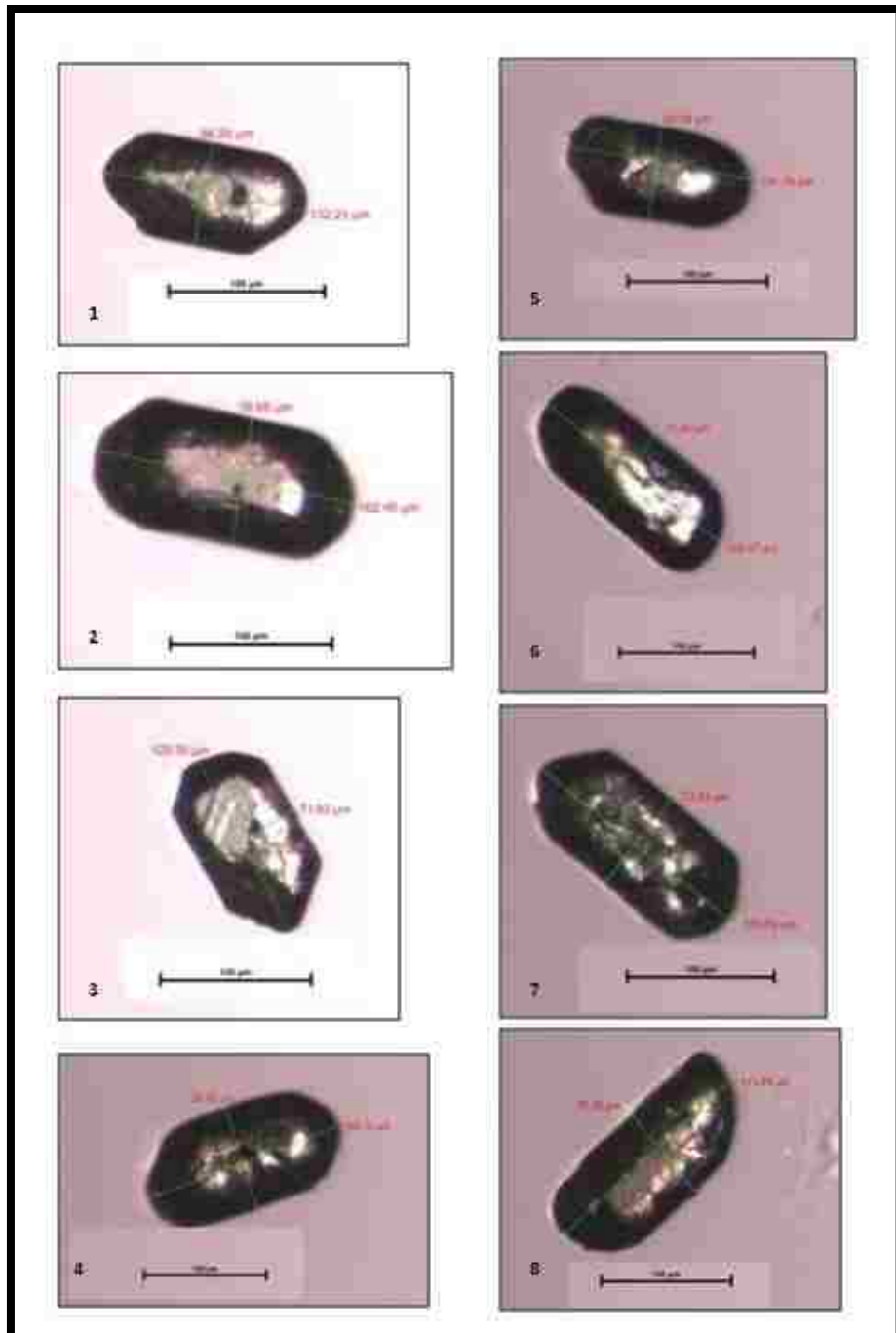


Figure 10.R. Photographs of zircon grains collected from southern Snake Range that were used for (U-Th)/He analyses. All zircons are shown under reflected light. The scale bar shown in each photograph is constant and is 100 μm long.

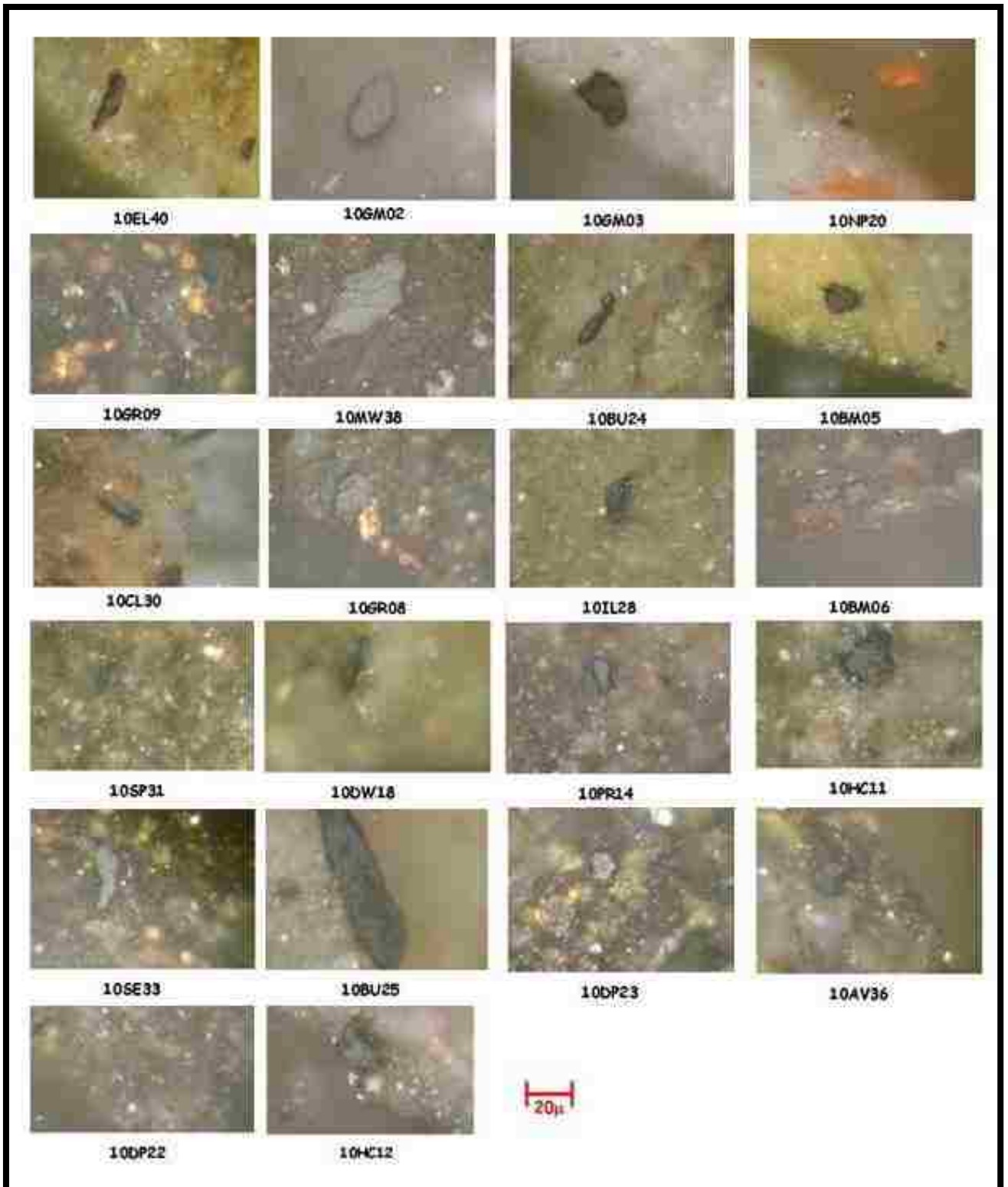


Figure 11. Selected images from each sample that underwent petrographic vitrinite reflectance analyses.

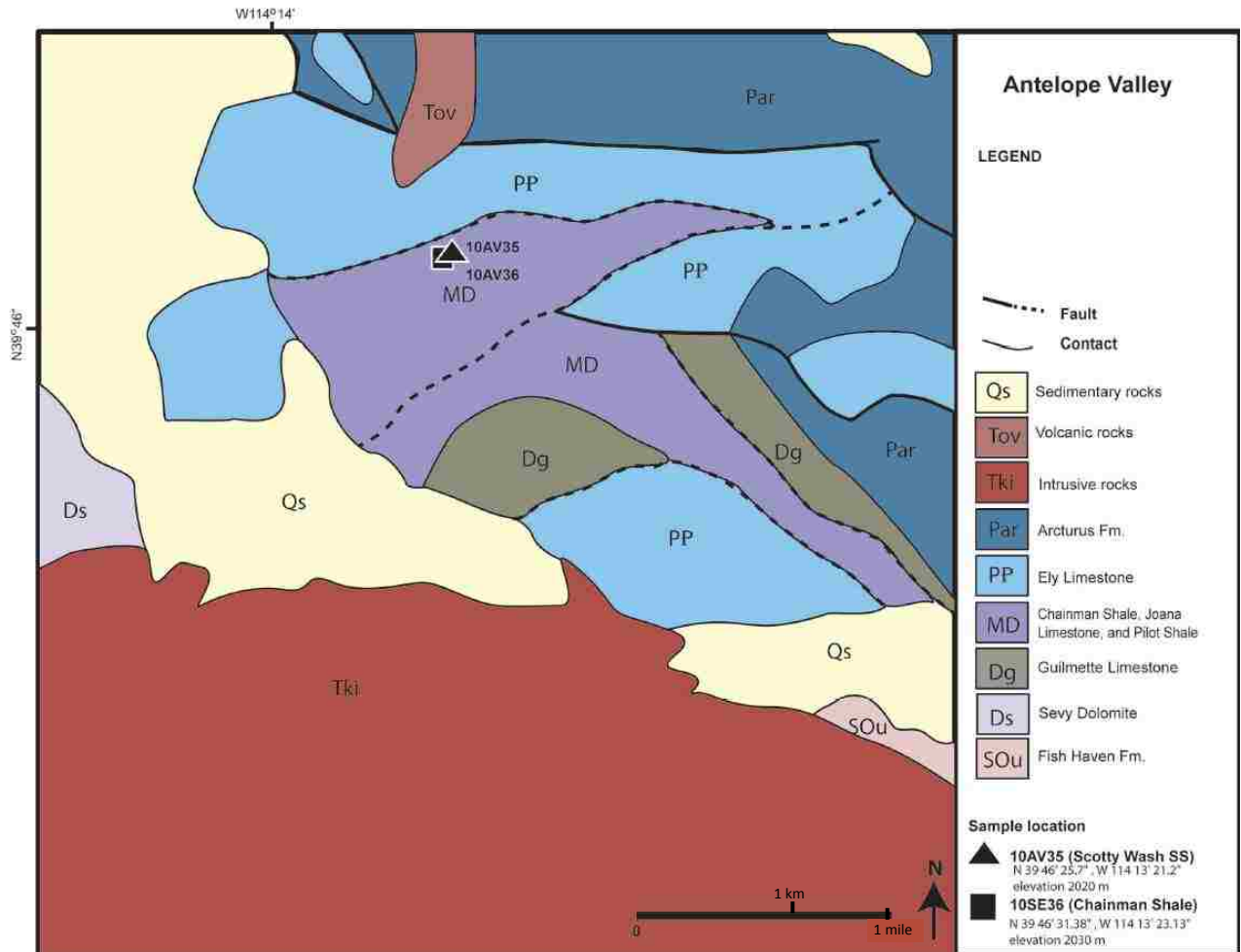


Figure 12.A. Geologic map showing the sample locations at Antelope Valley (modified from Kleinhampl and Ziony, 1985).

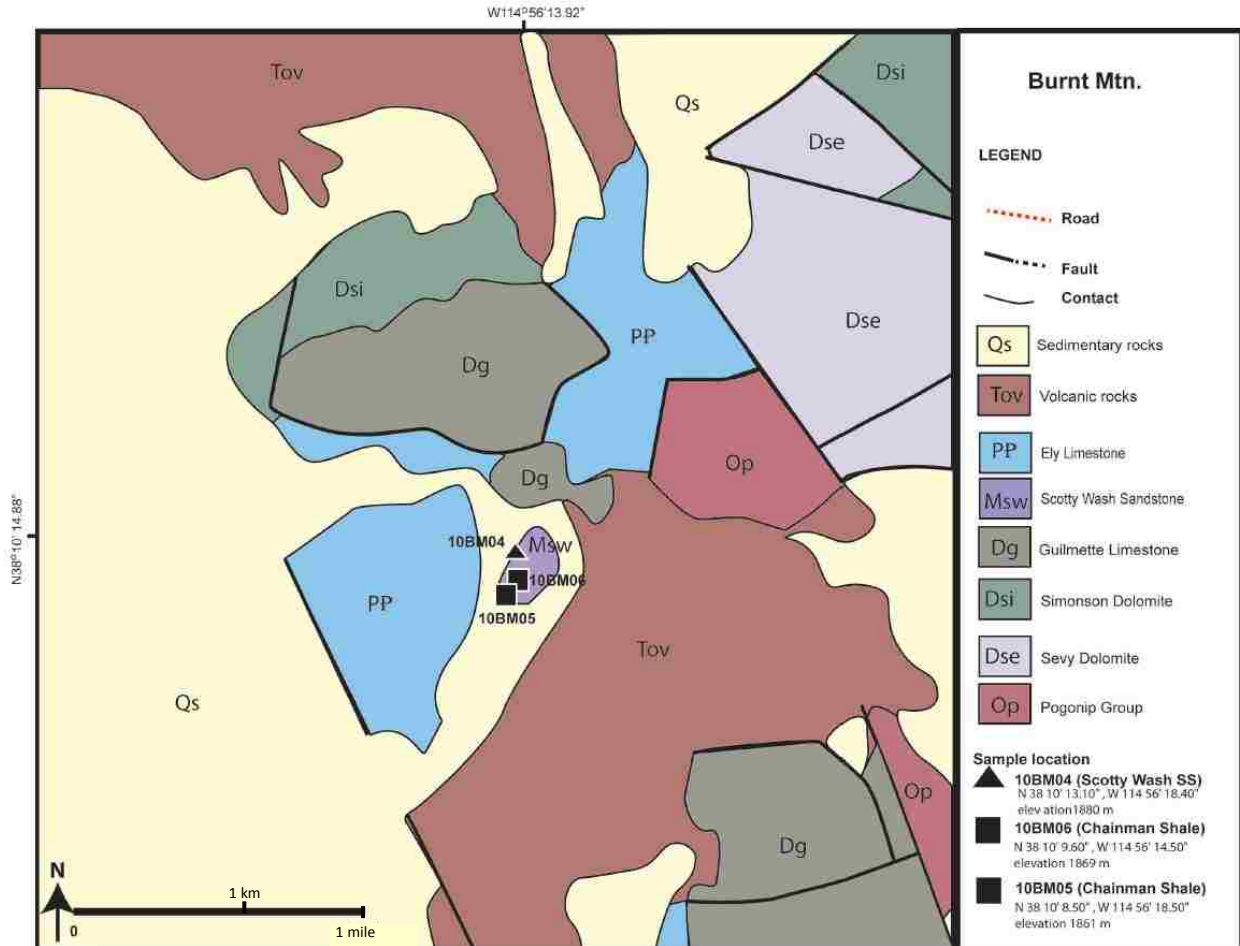


Figure 12.B. Geologic map showing the sample locations at Burnt Mountain (modified from Tschanz and Pampeyan, 1970).

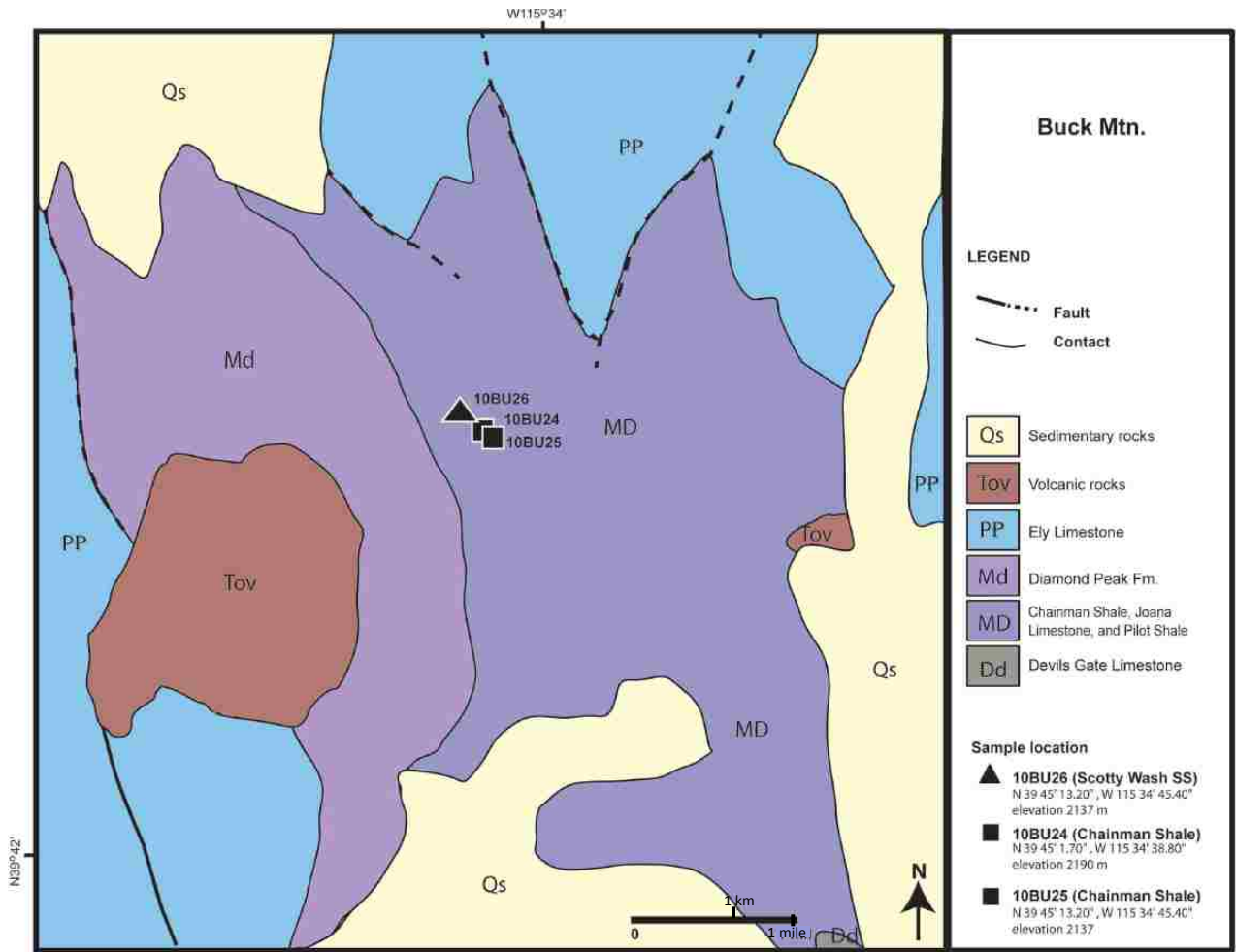


Figure 12.C. Geologic map showing the sample locations at Buck Mountain (modified from Hose and Blake, 1976).

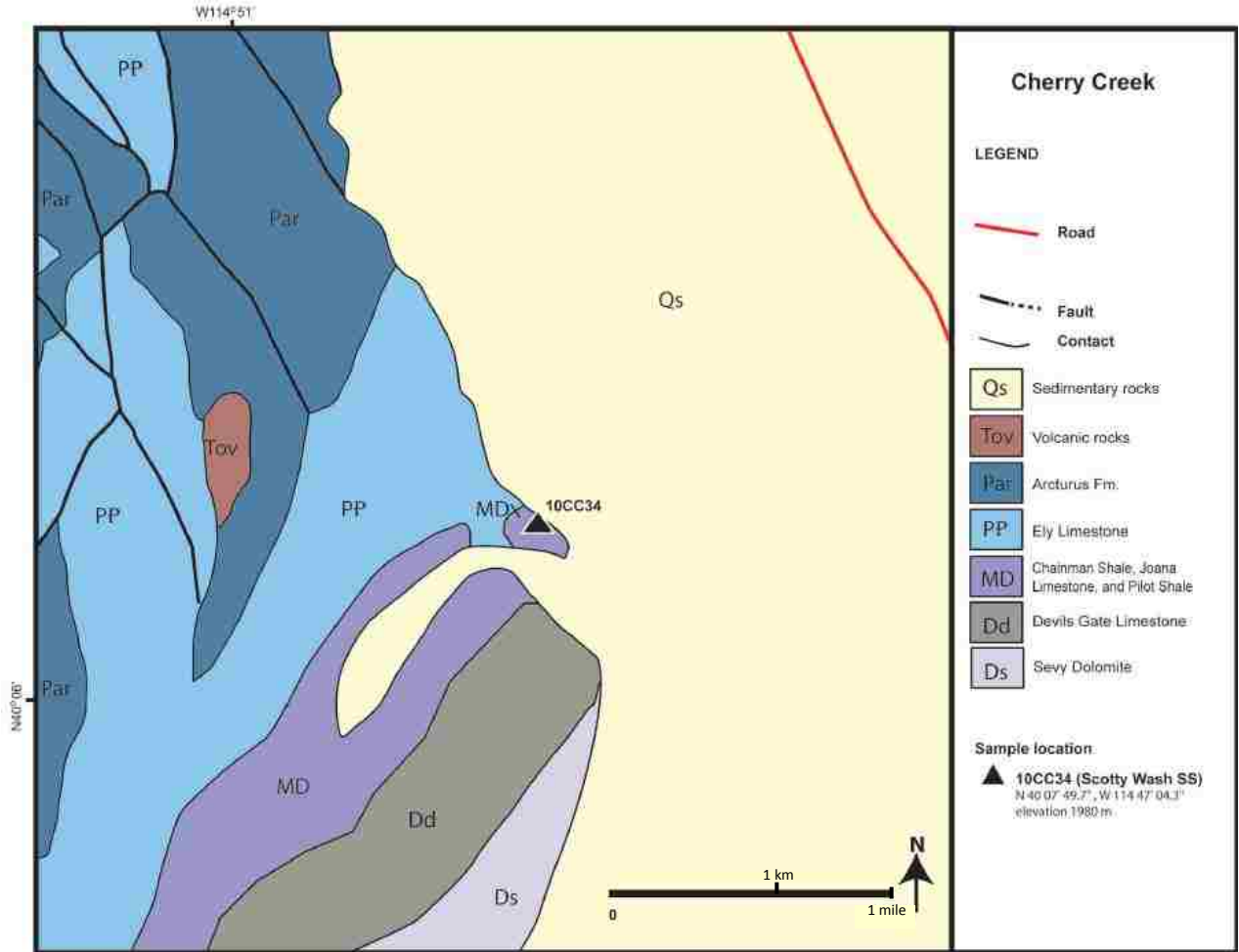


Figure 12.D. Geologic map showing the sample location at Cherry Creek (modified from Hose and Blake, 1976).

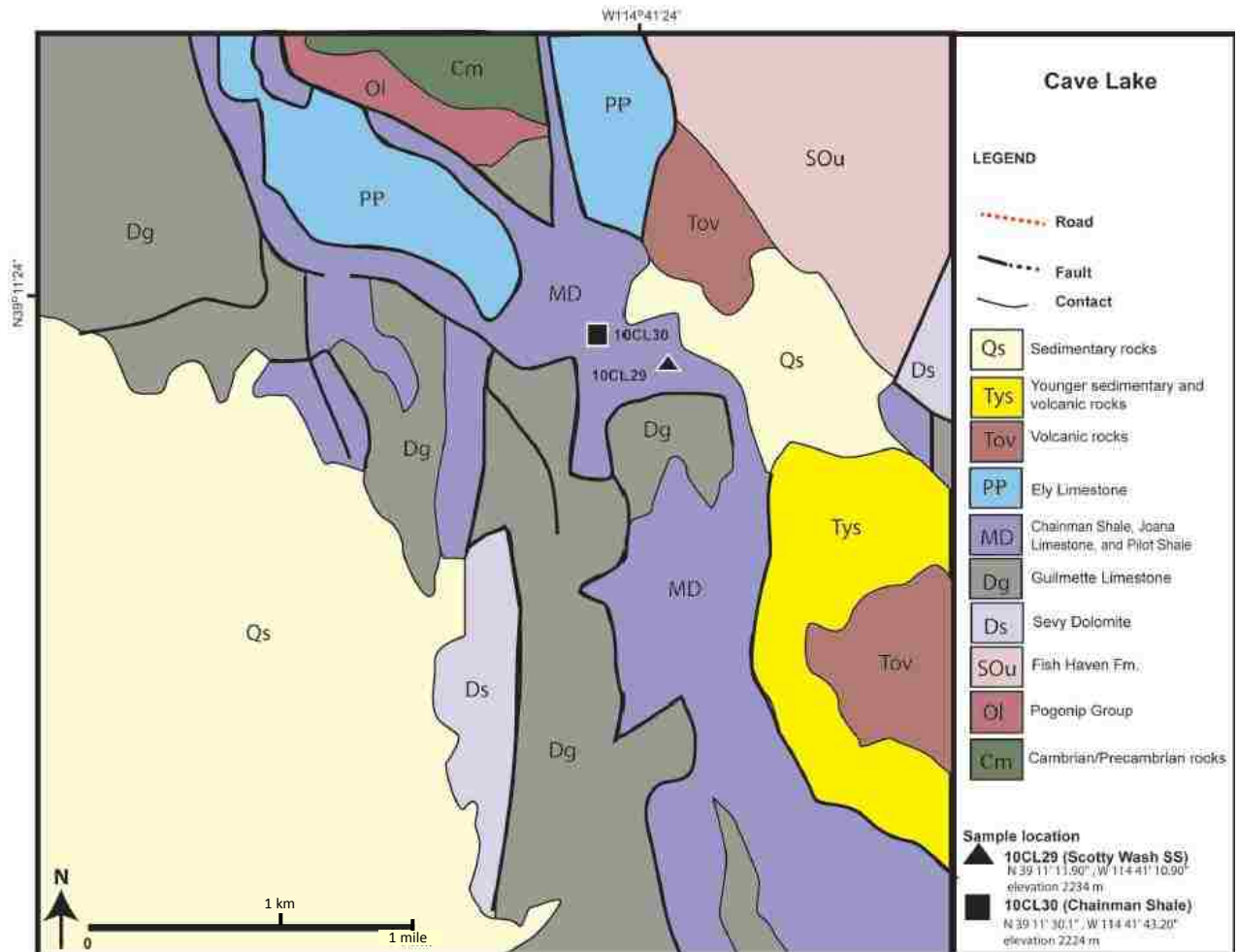


Figure 12.E. Geologic map showing the sample locations at Cave Lake (modified from Hose and Blake, 1976).

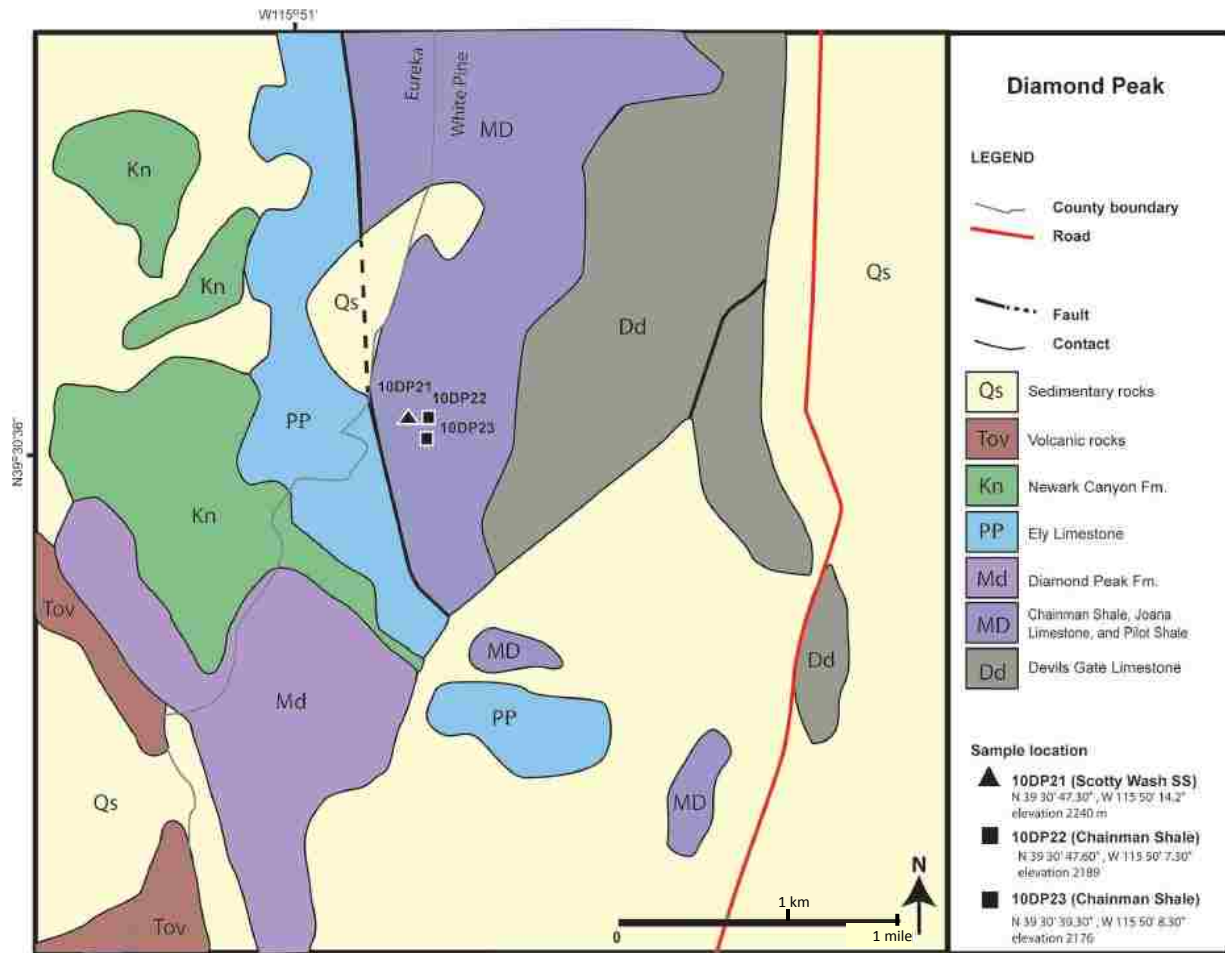


Figure 12.F. Geologic map showing the sample locations at Diamond Peak (modified from Hose and Blake, 1976).

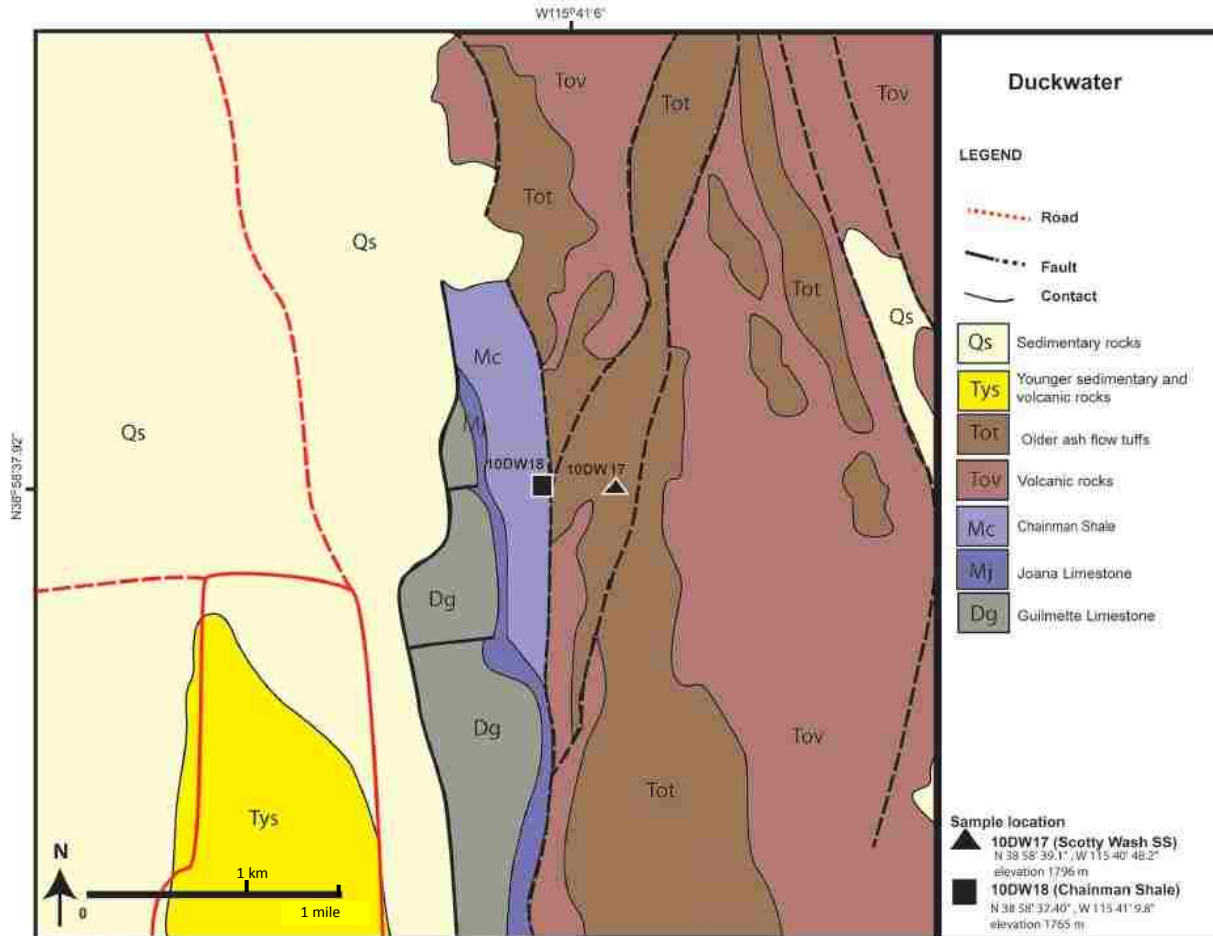


Figure 12.G. Geologic map showing the sample locations at Duckwater (modified from Hose and Blake, 1976). The Scotty Wash Sandstone sample was found in a very small outcrop surrounded by Tov which cannot be shown on the geologic map.

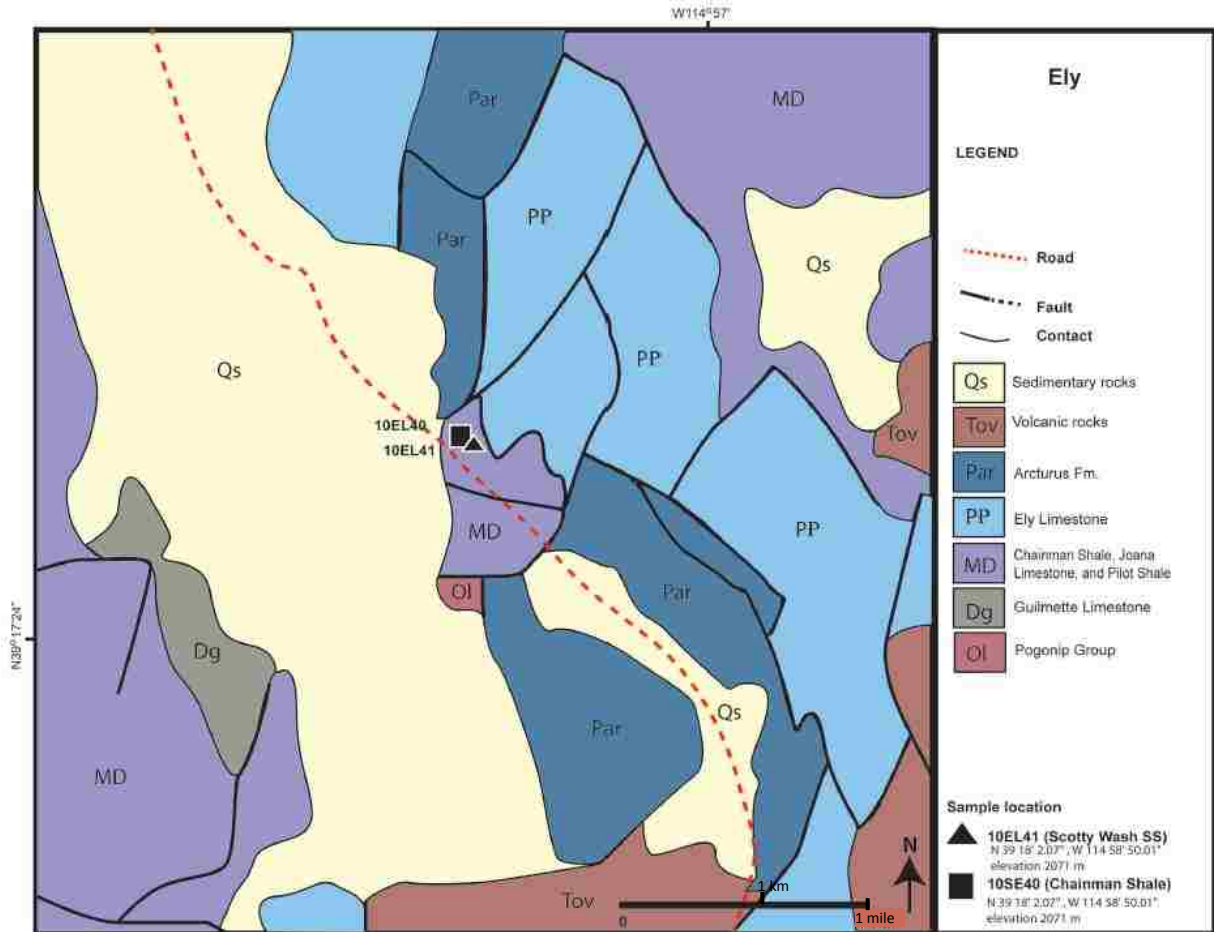


Figure 12.H. Geologic map showing the sample locations near Ely (modified from Hose and Blake, 1976).

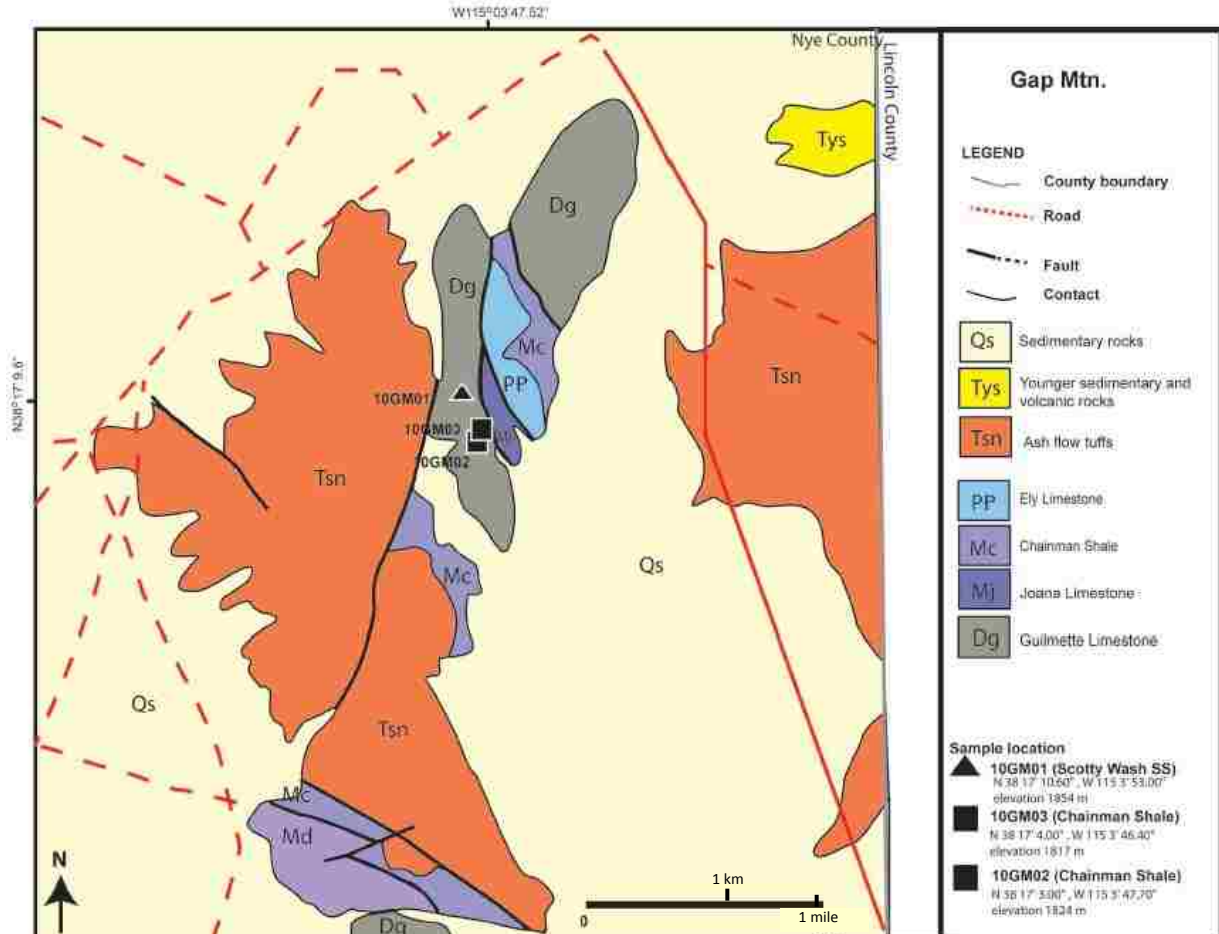


Figure 12.I. Geologic map showing the sample locations at Gap Mountain (modified from Kleinhampl and Ziony, 1985).

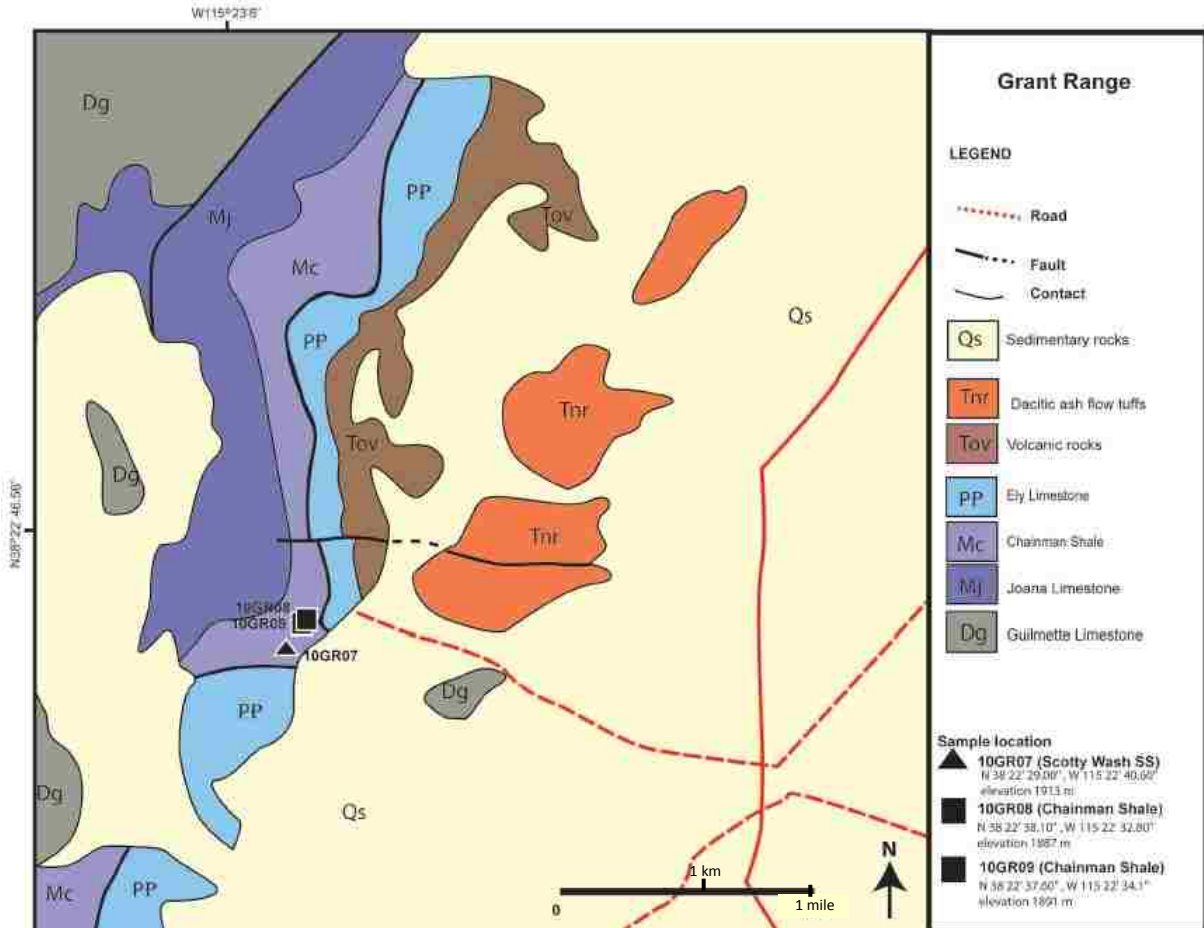


Figure 12.J. Geologic map showing the sample locations in the Grant Range (modified from Kleinhampl and Ziony, 1985).

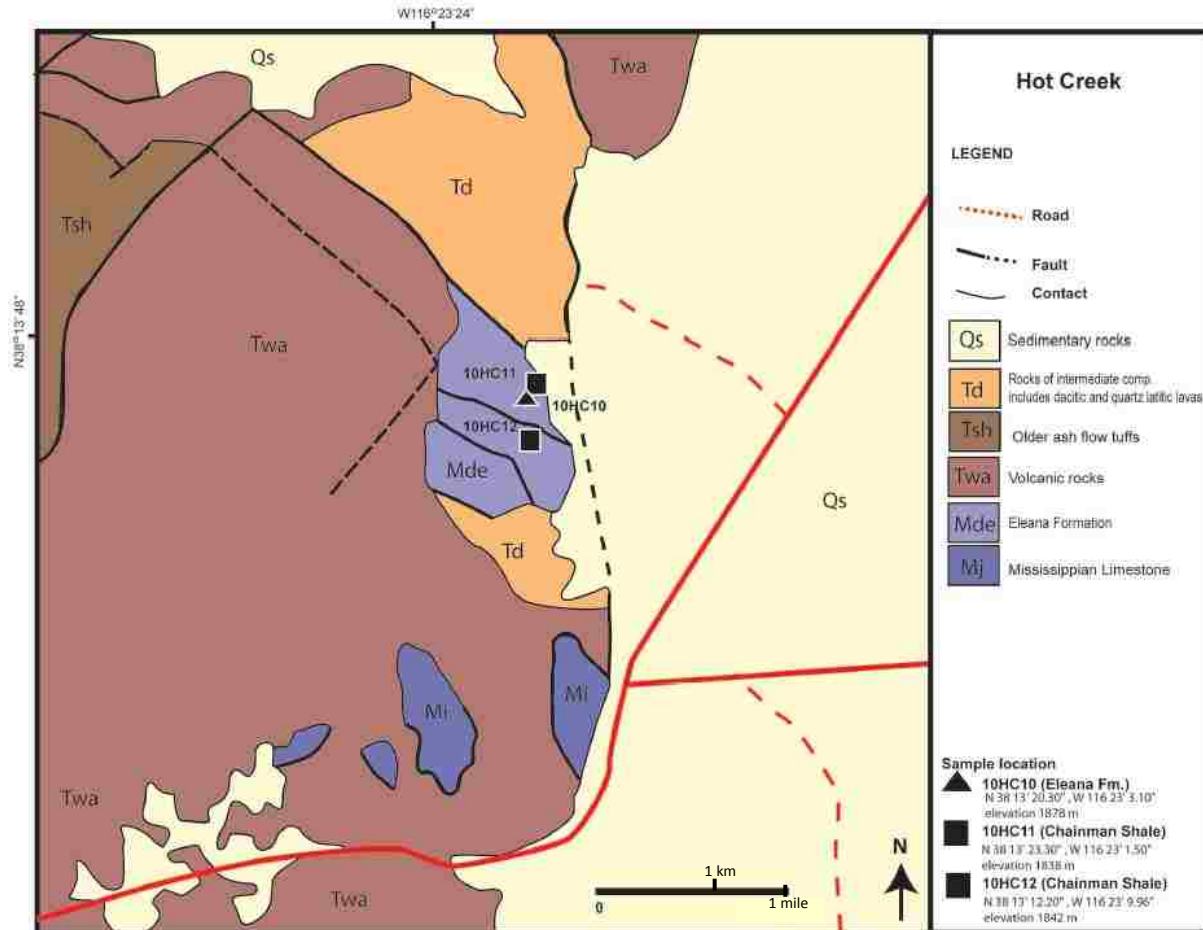


Figure 12.K. Geologic map showing the sample locations at Hot Creek (modified from Kleinhampl and Ziony, 1985).

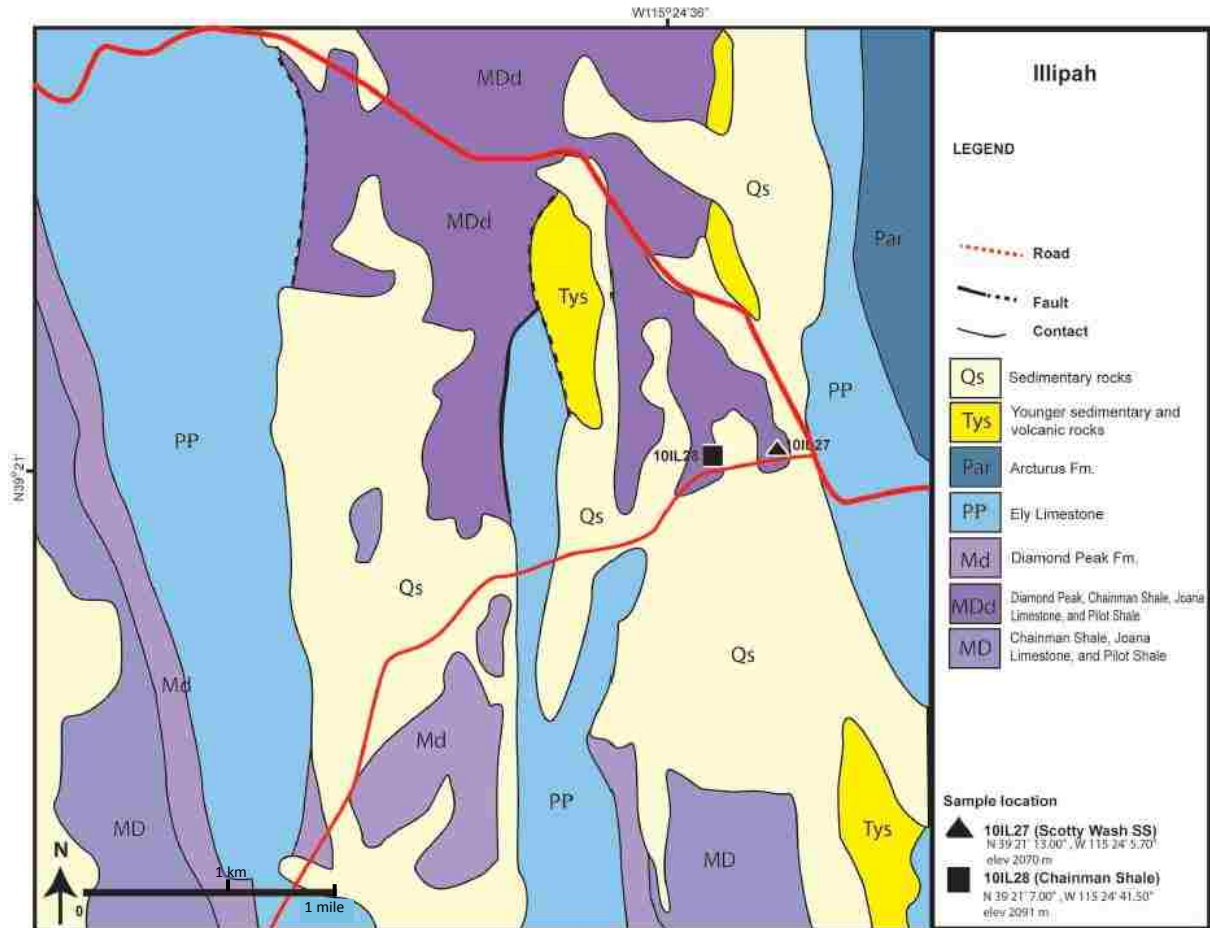


Figure 12.L. Geologic map showing the sample locations at Illipah (modified from Hose and Blake, 1976).

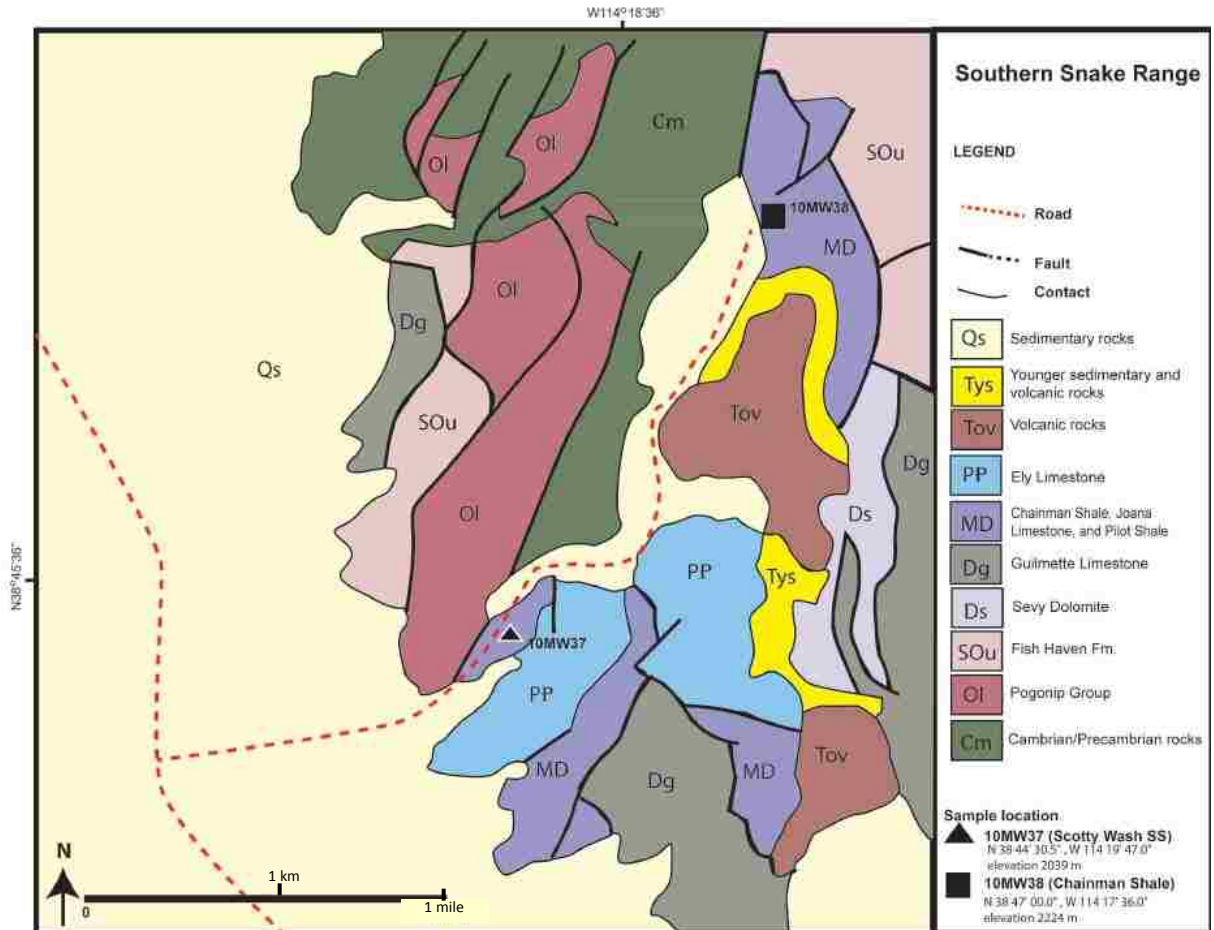


Figure 12.M. Geologic map showing the sample locations in the southern Snake Range (modified from Hose and Blake, 1976).

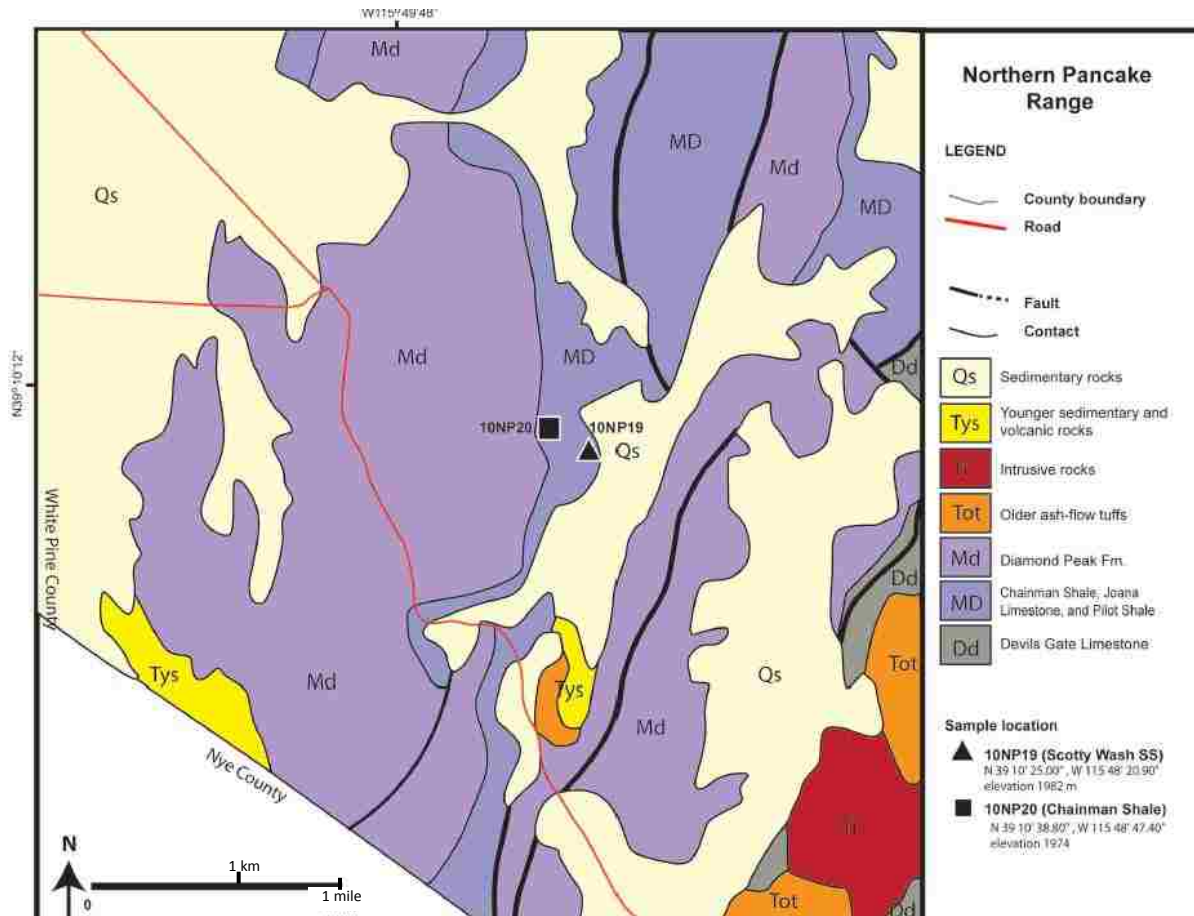


Figure 12.N. Geologic map showing the sample locations in the northern Pancake Range (modified from Hose and Blake, 1976).

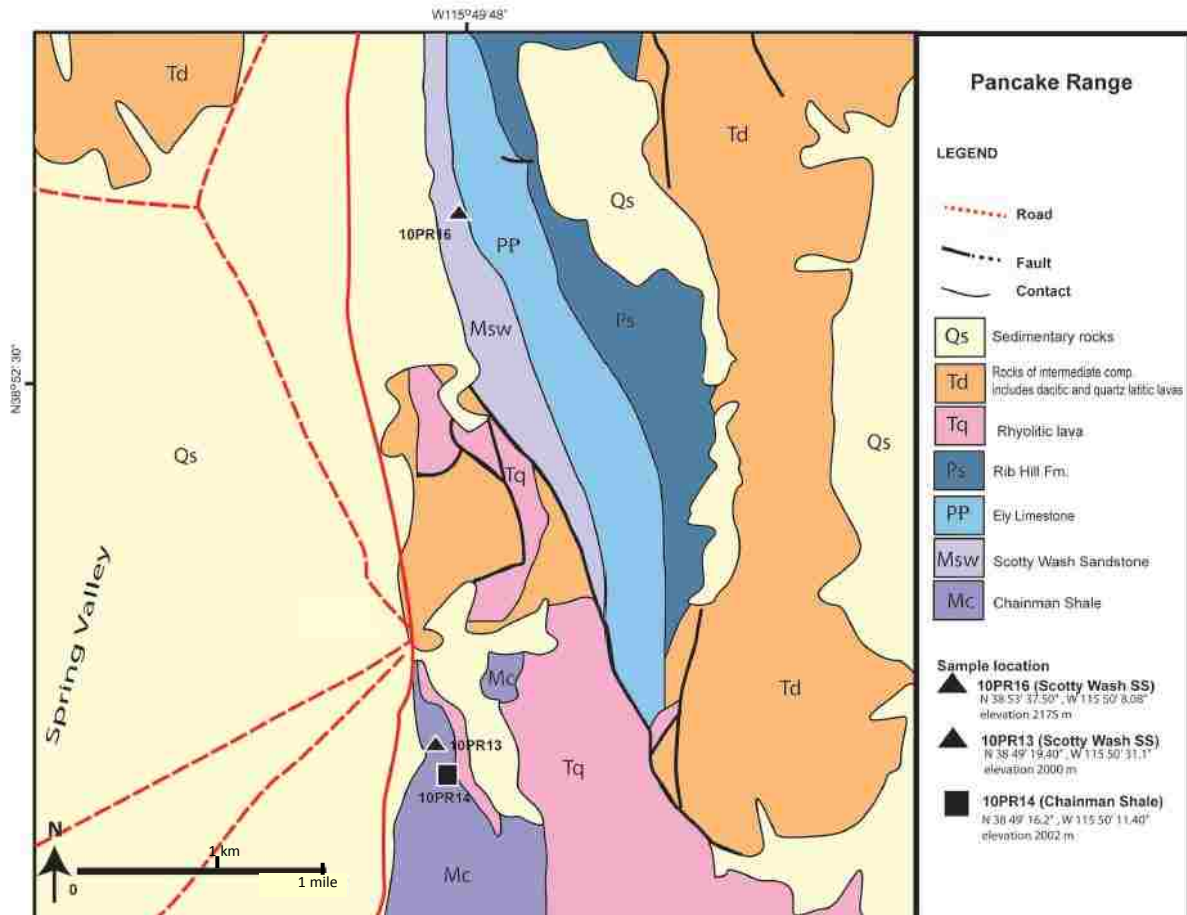


Figure 12.O. Geologic map showing the sample locations in the Pancake Range (modified from Kleinhampl and Ziony, 1985).

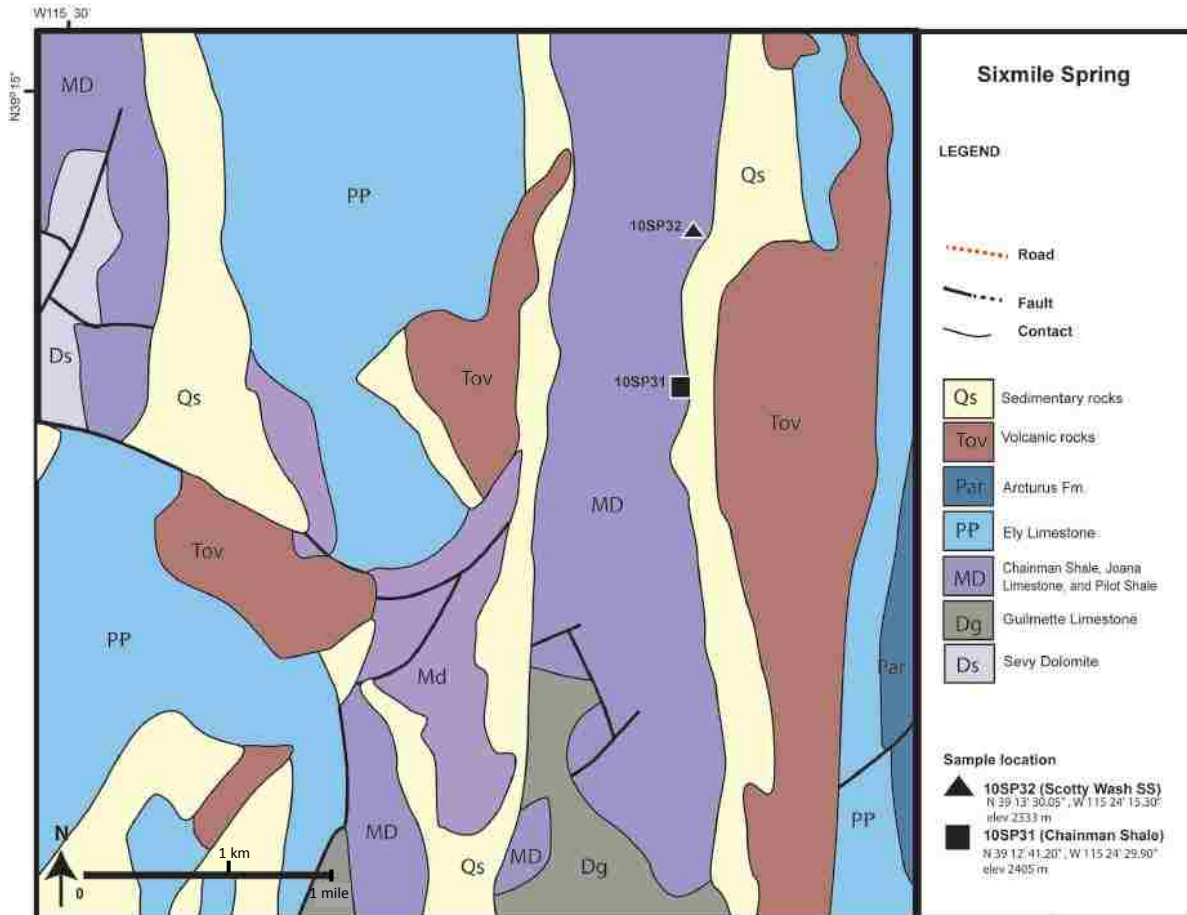


Figure 12.P. Geologic map showing the sample location at Sixmile Spring (modified from Hose and Blake, 1976).

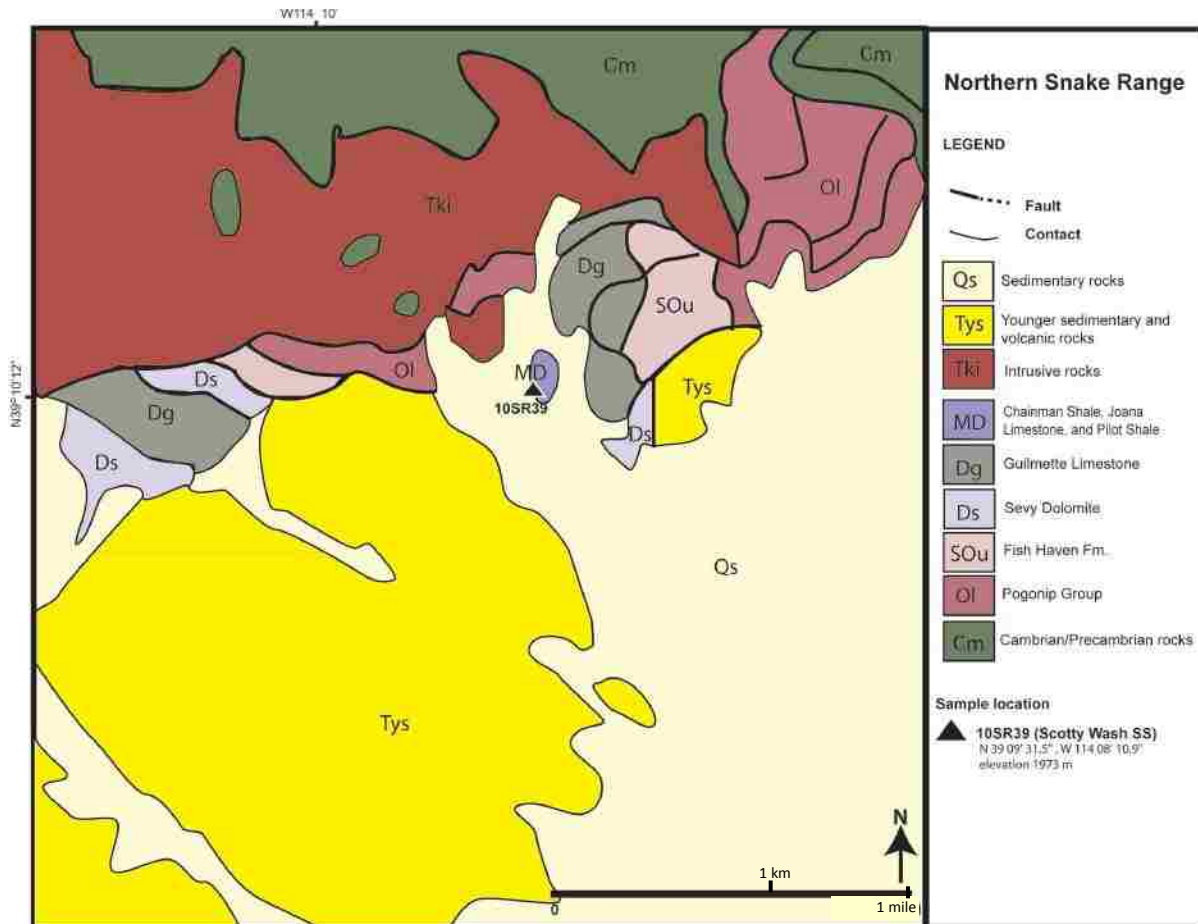


Figure 12.Q. Geologic map showing the sample location in the northern Snake Range (modified from Hose and Blake, 1976).

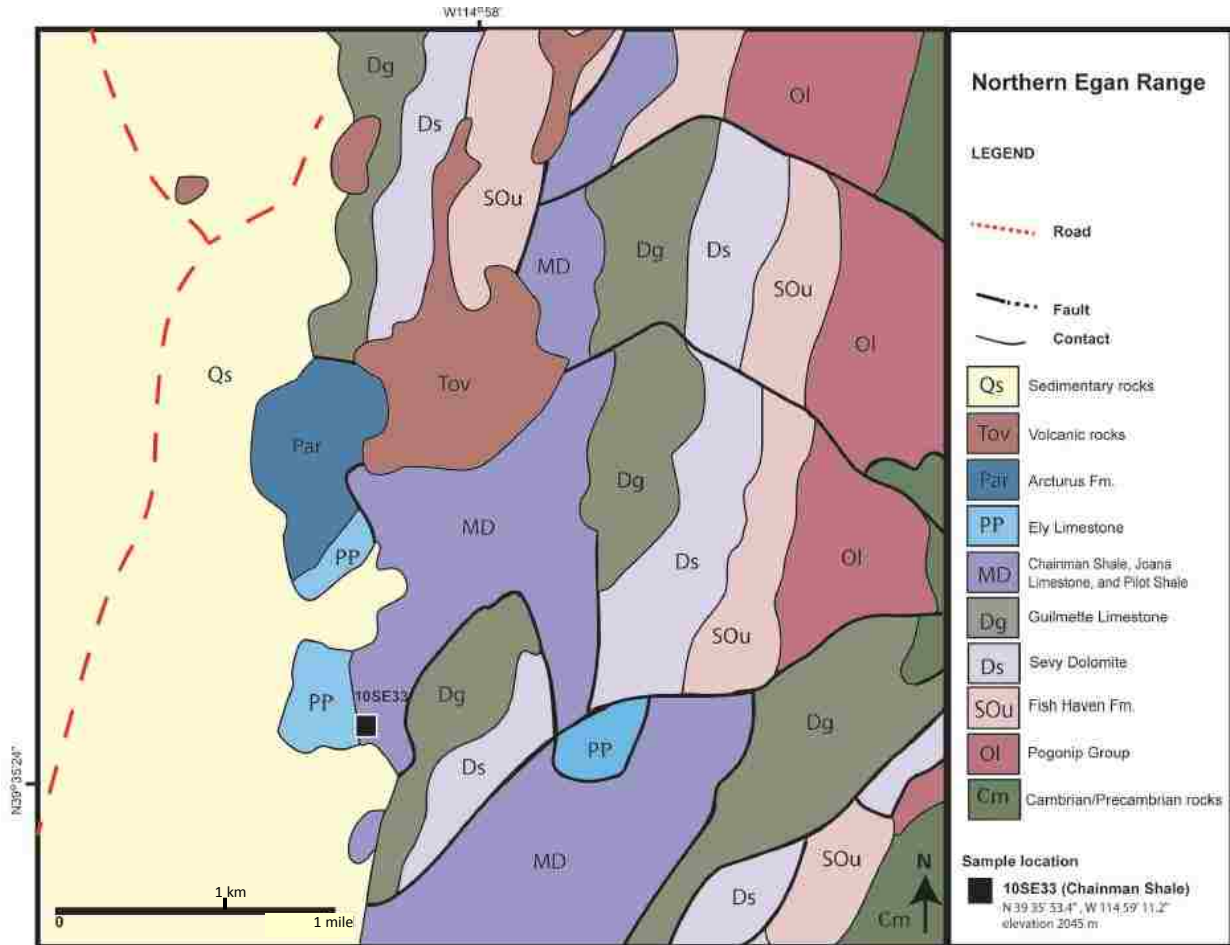


Figure 12.R. Geologic map showing the sample location in the northern Egan Range (modified from Hose and Blake, 1976).

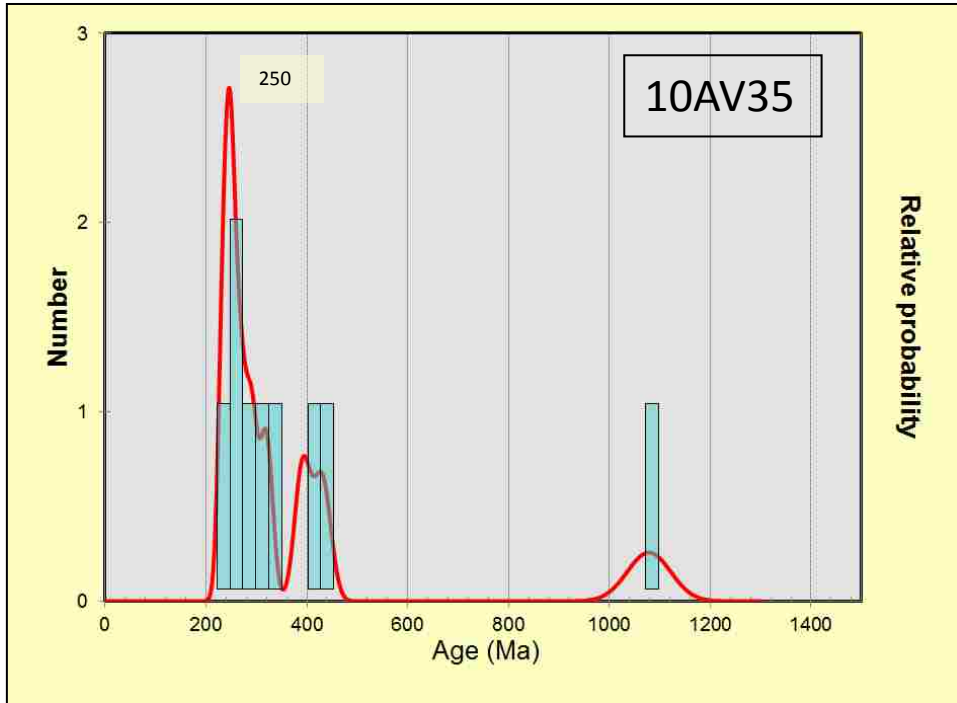


Figure 13.A. Relative probability diagram for zircons collected from Antelope Valley. The Age Peak program (Gehrels, 2009) calculated one age peak at 250 Ma.

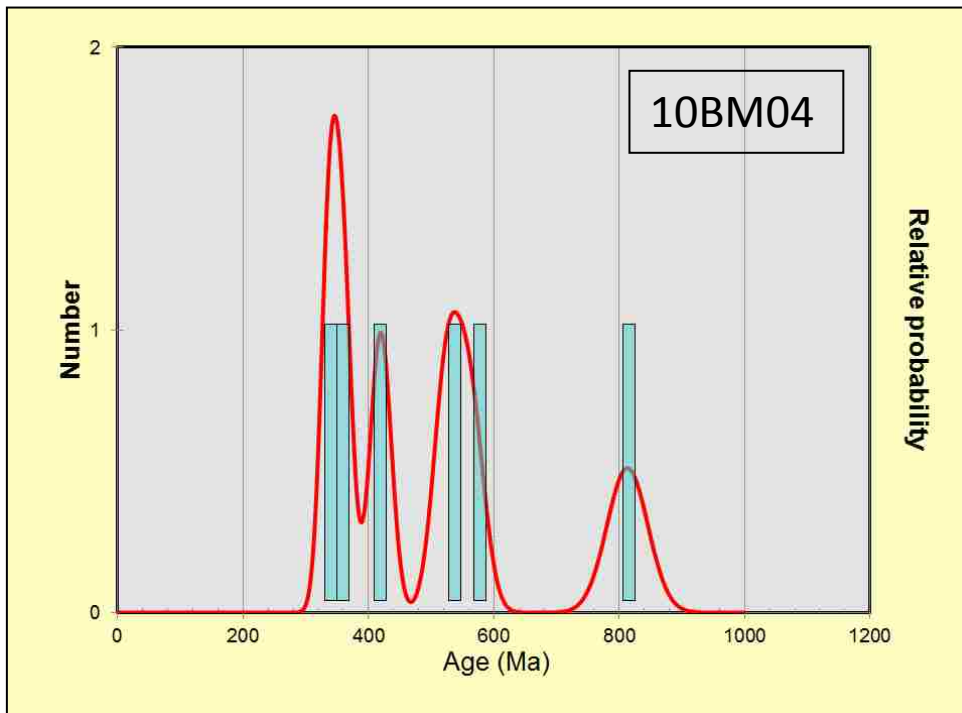


Figure 13.B. Relative probability diagram for zircons collected from Burnt Mtn. The sample did not produce any peak age because the zircon ages are highly distributed.

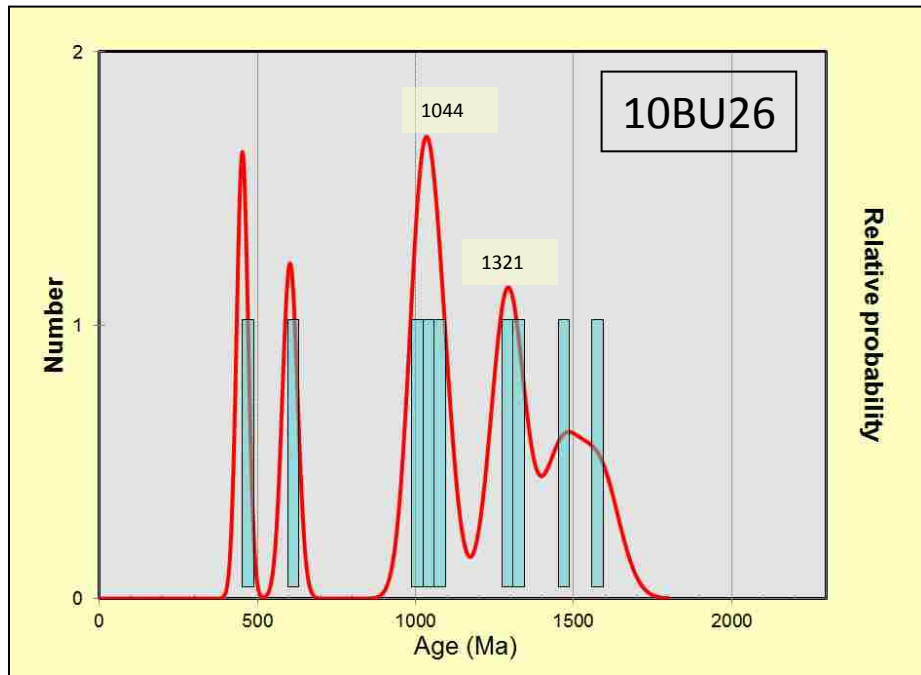


Figure 13.C. Relative probability diagram for zircons collected from Buck Mtn. The Age Peak program (Gehrels, 2009) calculated two age peaks; one at 1044 Ma and another at 1321 Ma.

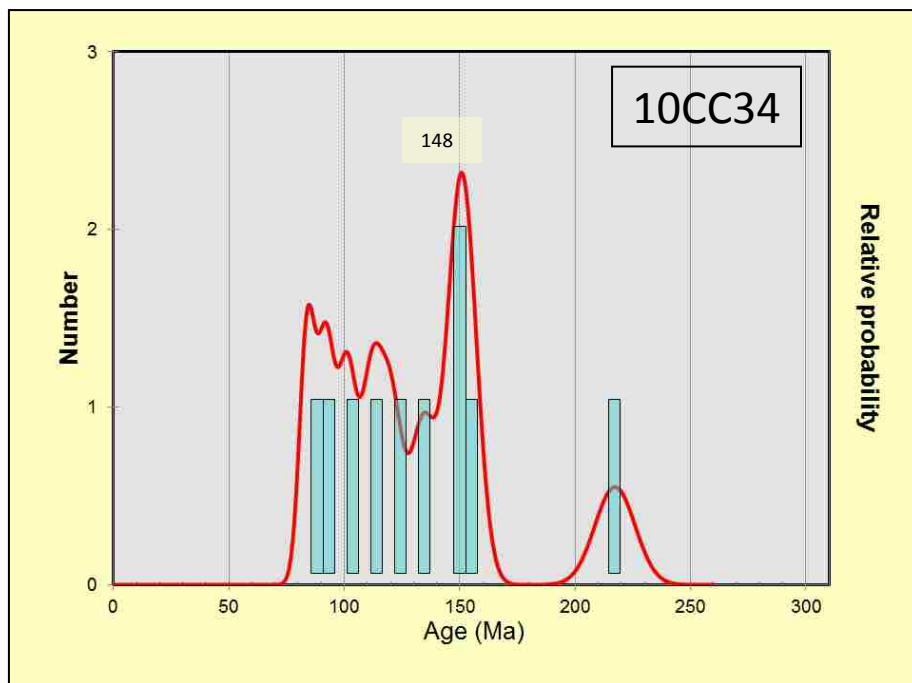


Figure 13.D. Relative probability diagram for zircons collected from Cherry Creek. The Age Peak program (Gehrels, 2009) calculated one age peak at 148 Ma.

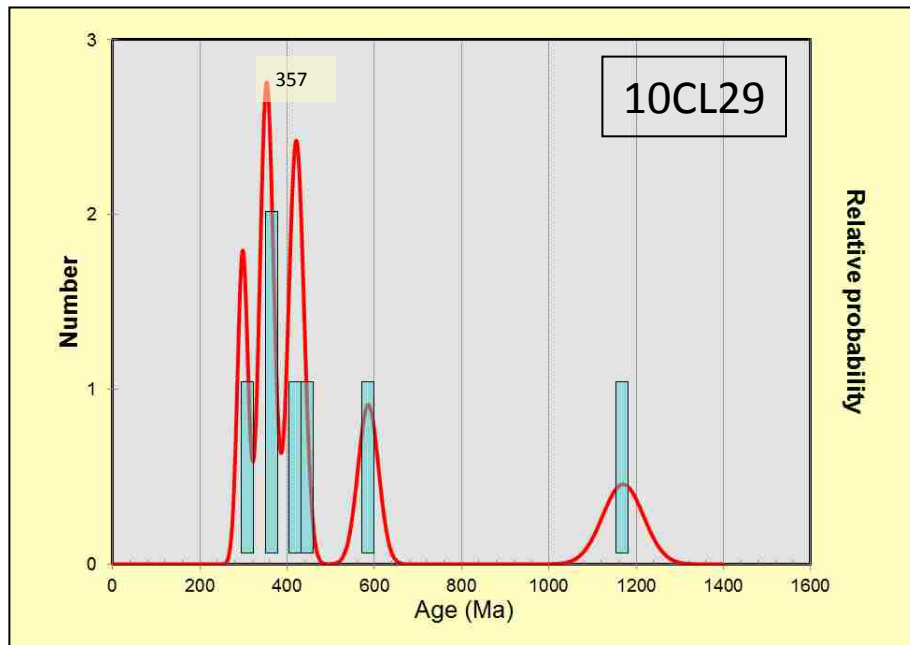


Figure 13.E. Relative probability diagram for zircons collected from Cave Lake. The Age Peak program (Gehrels, 2009) calculated one age peak at 357 Ma.

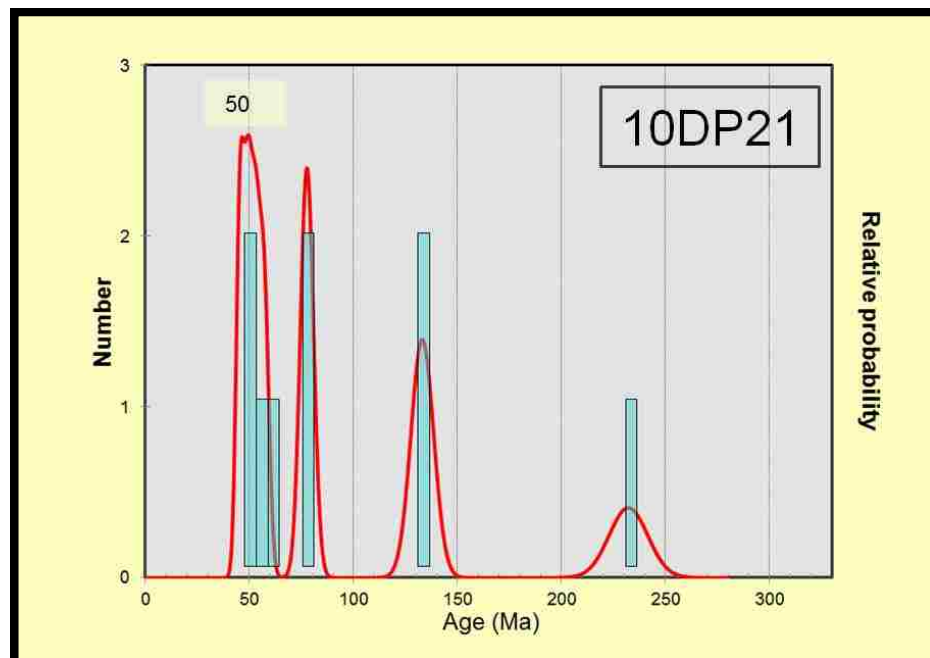


Figure 13.F. Relative probability diagram for zircons collected from Diamond Peak. The Age Peak program (Gehrels, 2009) calculated one age peak at 50 Ma.

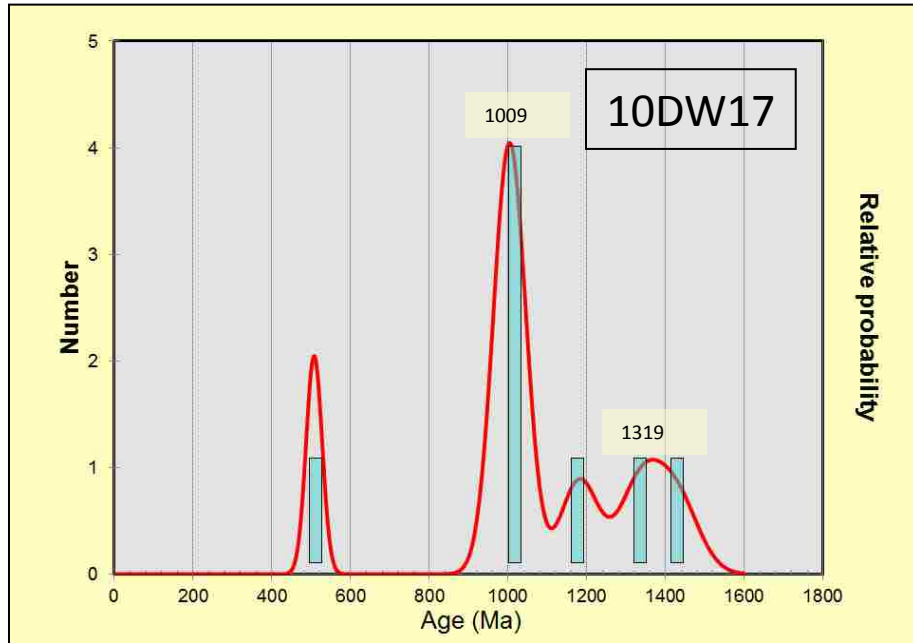


Figure 13.G. Relative probability diagram for zircons collected from Duckwater. The Age Peak program (Gehrels, 2009) calculated two age peaks; one at 1009 Ma and another at 1319 Ma.

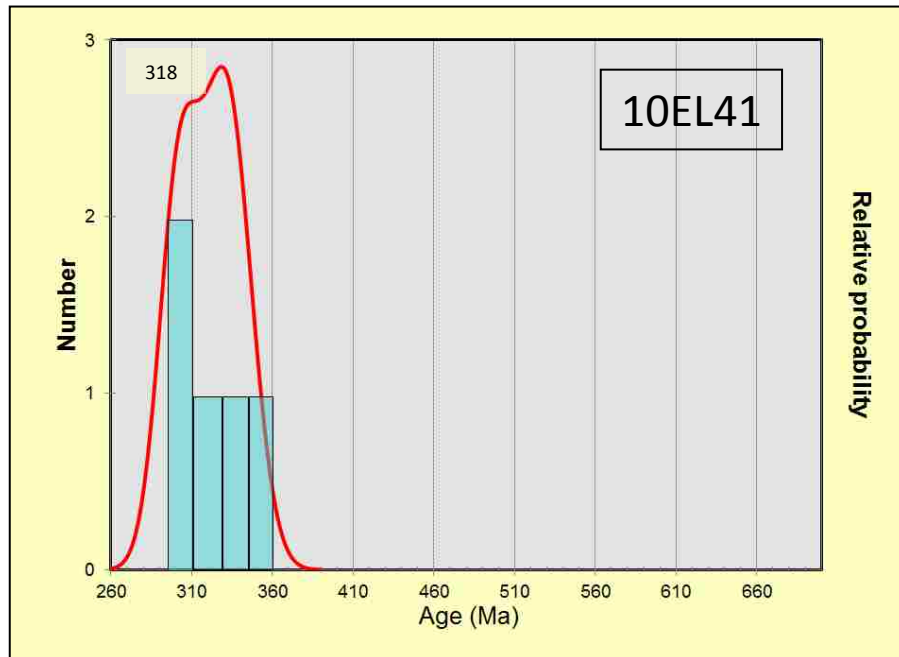


Figure 13.H. Relative probability diagram for zircons collected from Ely. The Age Peak program (Gehrels, 2009) calculated one age peak at 318 Ma.

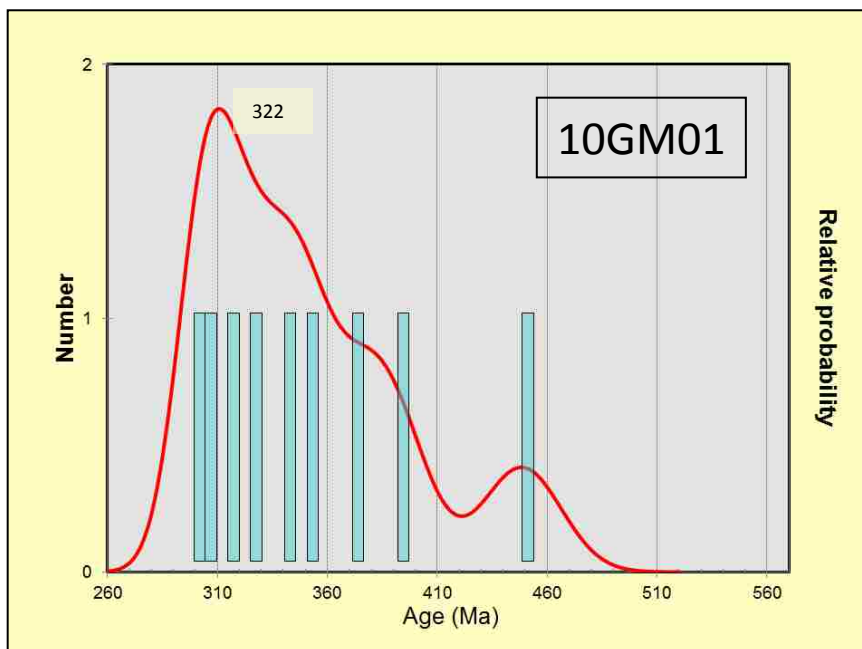


Figure 13.I. Relative probability diagram for zircons collected from Gap Mountain. The Age Peak program (Gehrels, 2009) calculated one age peak at 322 Ma.

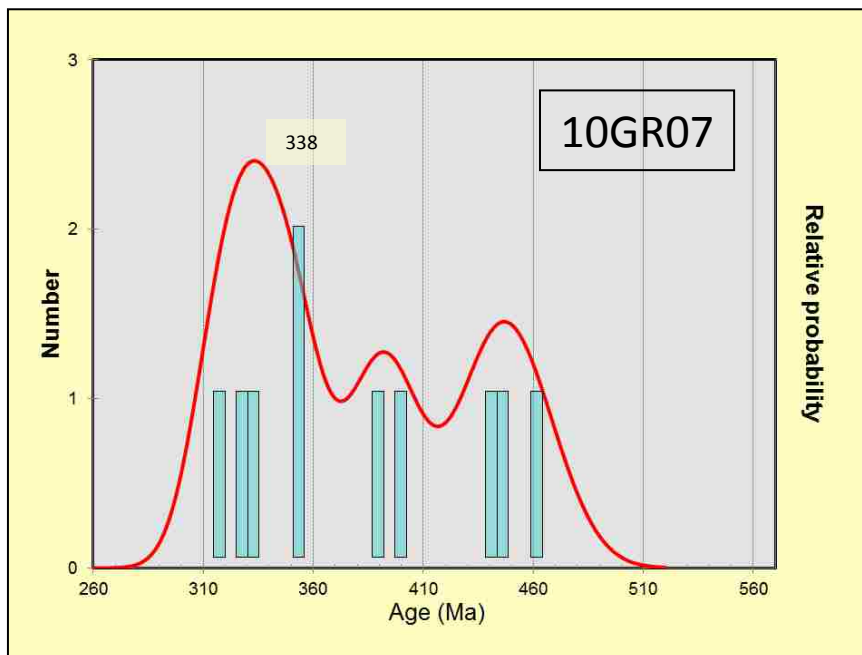


Figure 13.J. Relative probability diagram for zircons collected from Grant Range. The Age Peak program (Gehrels, 2009) calculated one age peak at 338 Ma.

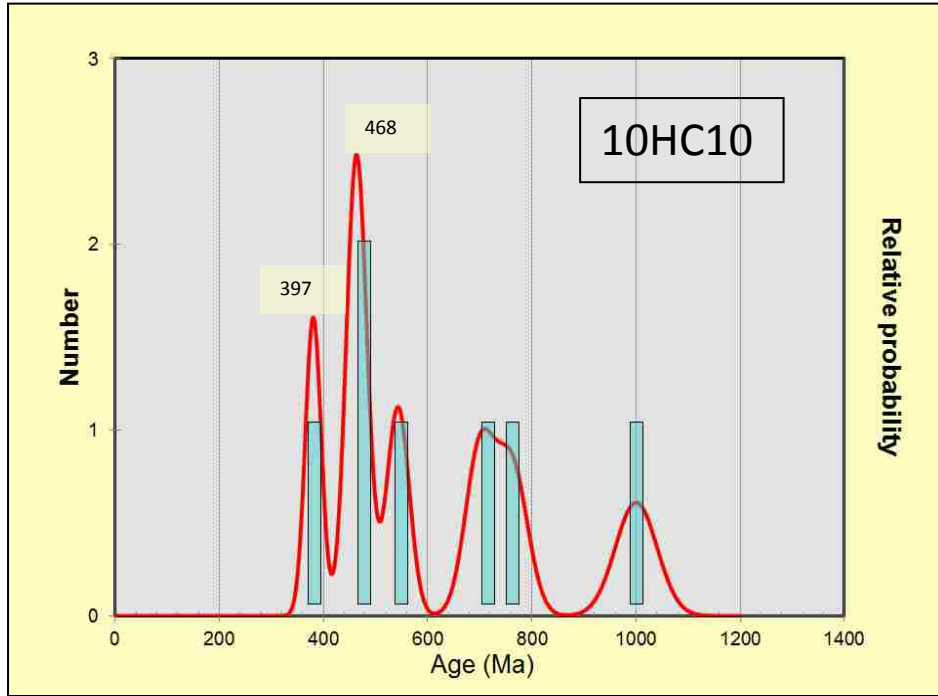


Figure 13.K. Relative probability diagram for zircons collected from Hot Creek. The Age Peak program (Gehrels, 2009) calculated two peaks; one at 397 Ma and a second one at 468 Ma.

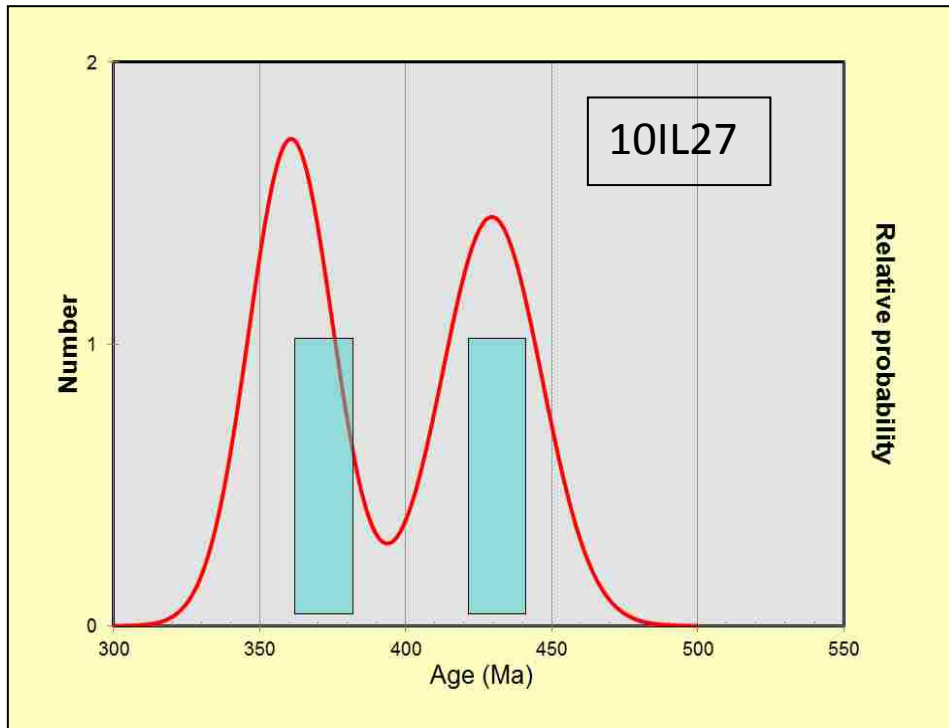


Figure 13.L. Relative probability diagram for zircons collected from Illipah. This sample did not produce any peak ages because only two zircon ages were calculated.

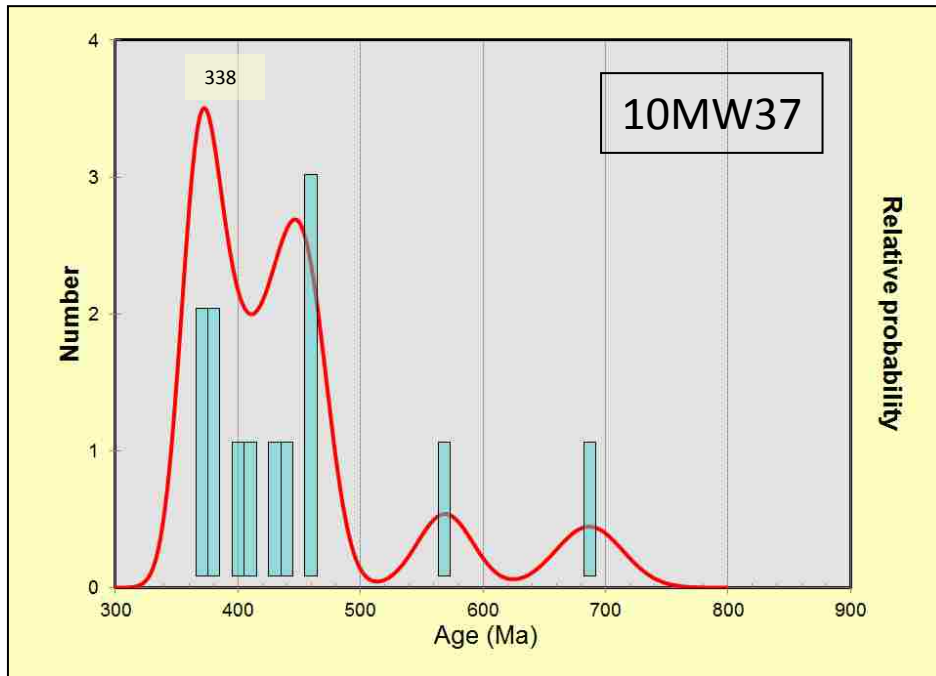


Figure 13.M. Relative probability diagram for zircons collected from the southern Snake Range. The Age Peak program (Gehrels, 2009) calculated one age peak at 338 Ma.

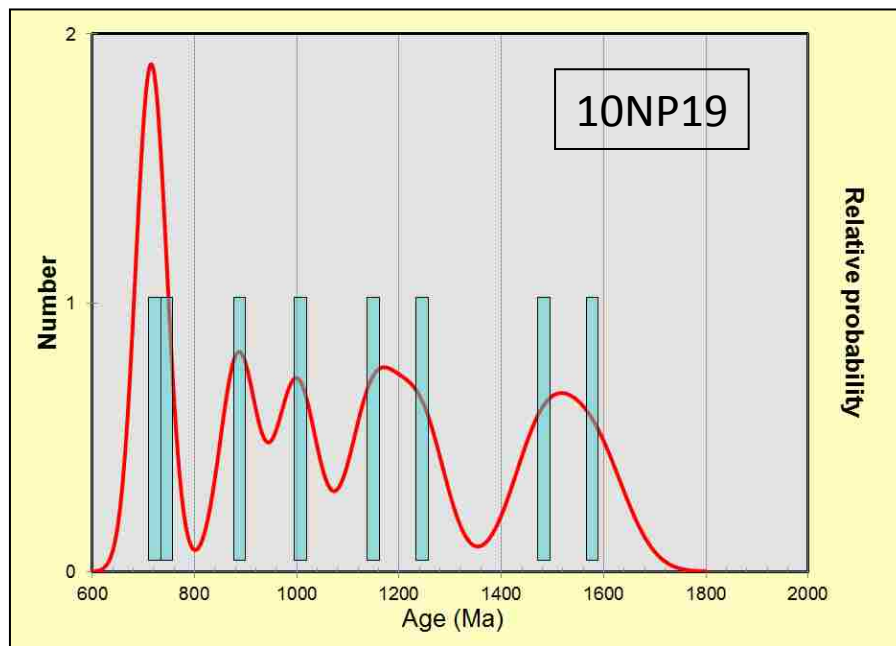


Figure 13.N. Relative probability diagram for zircons collected from the northern Pancake Range. The Age Peak program (Gehrels, 2009) did not calculate any peak ages because the zircon ages are widely scattered.

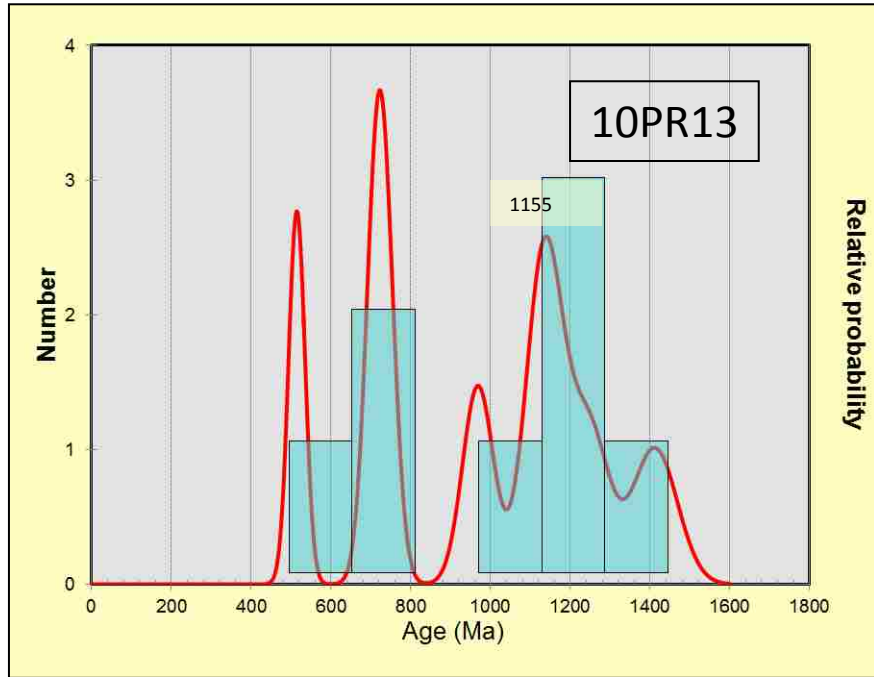


Figure 13.O. Relative probability diagram for zircons collected from Pancake Range (10PR13). The Age Peak program (Gehrels, 2009) calculated one age peak at 1155 Ma.

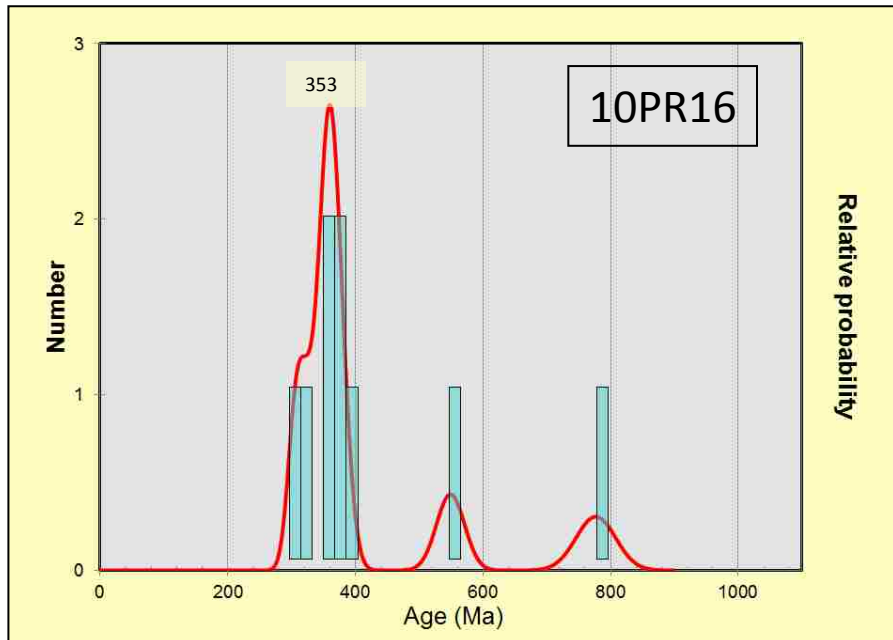


Figure 13.P. Relative probability diagram for zircons collected from Pancake Range (10PR16). The Age Peak program (Gehrels, 2009) calculated one age peak at 353 Ma.

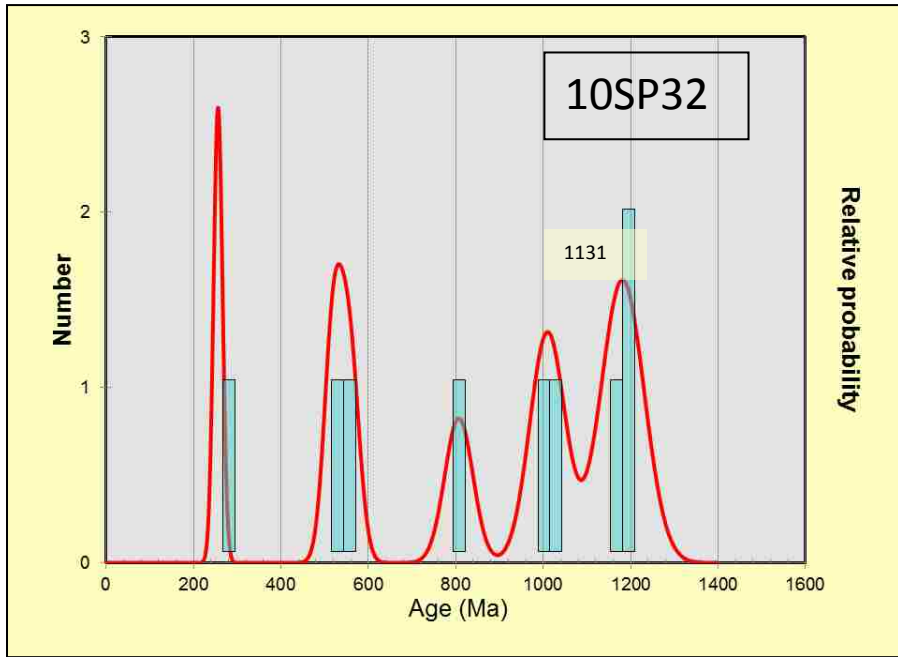


Figure 13.Q. Relative probability diagram for zircons collected from Sixmile Spring. The Age Peak program (Gehrels, 2009) calculated one age peak at 1131 Ma.

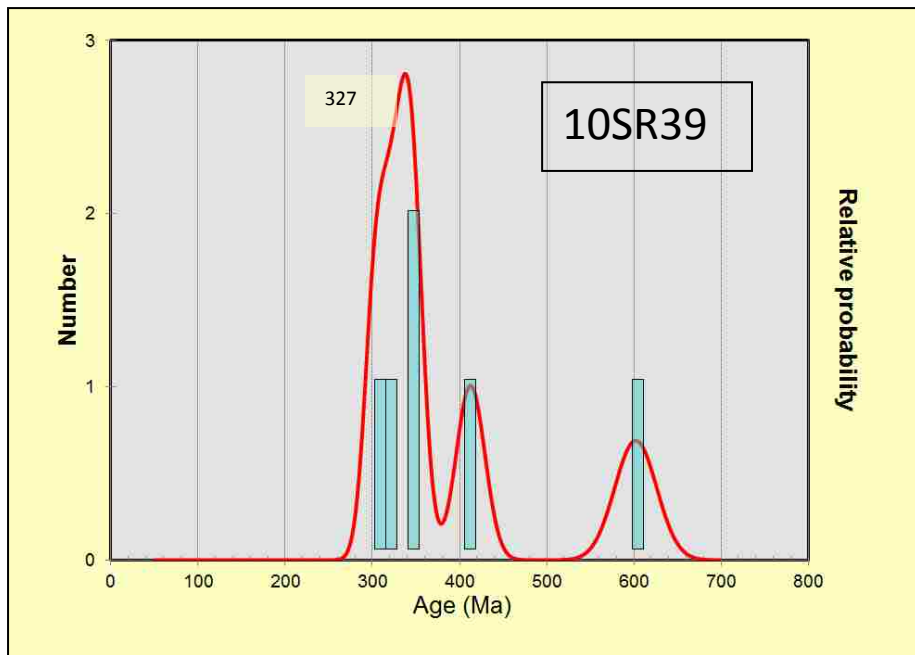


Figure 13.R. Relative probability diagram for zircons collected from the northern Snake Range. The Age Peak program (Gehrels, 2009) calculated one age peak at 327 Ma.

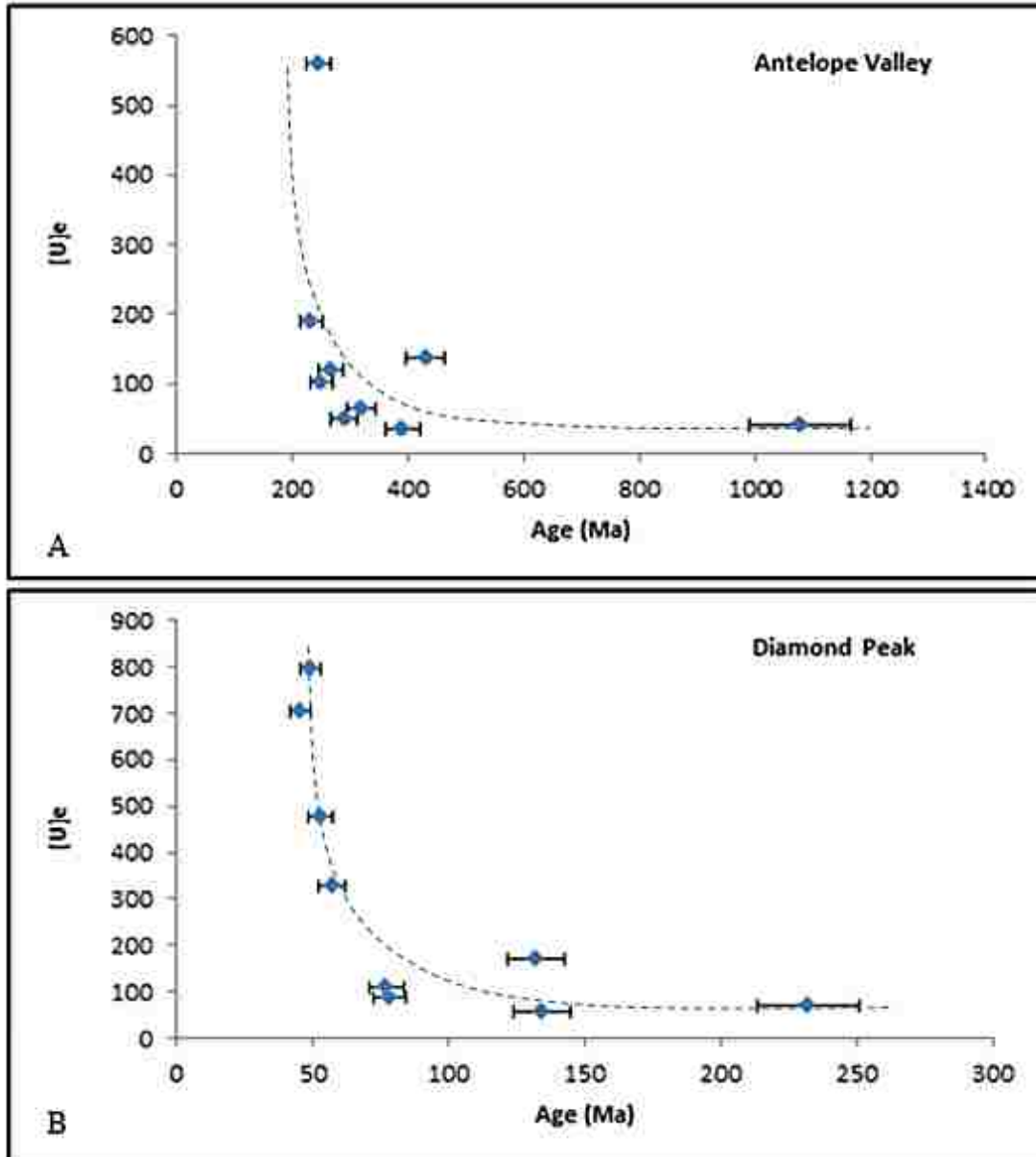


Figure 15. Negative correlation between effective uranium concentration [U]e and helium ages of zircons collected at A) Antelope Valley and B) Diamond Peak that indicate residence within the (U-Th)/He partial retention zone (HePRZ). Effective uranium concentration, a proxy for radiation damage was calculated by $[U]e = [U] + [Th]0.235 + [Sm]0.005$ (e.g. Shuster et al., 2006). The increased value of radiation damage corresponds to decreased helium retentivity within zircon grains (Reiners, 2005; Stockli et al., 2010).



Figure 16. Vitrinite reflectance (Ro) analysis results plotted for each sample location. Red color indicates post mature Ro values. Green colors represent samples in the mature stage. Blue color represents samples in the early mature stage. Letters within each sample number correspond to the name of the locality (HC: Hot Creek, PR: Pancake Range, DP: Diamond Peak, IL: Illipah, EL: Ely, SP: Sixmile Spring, CL: Cave Lake, MW: southern Snake Range, GM: Gap Mtn., GR: Grant Range, DW: Duckwater, AV: Antelope Valley, SE: northern Egan Range, BU: Buck Mtn., BM: Burnt Mtn.).

Hydrocarbon Generation Stage	<u>Maturation</u>		<u>Generation</u>
	Ro (%)	Tmax (°C)	Rock-Eval PI
Immature	<0.60	<430	<0.10
Beginning	0.60	430-435	0.10-0.15
Peak	0.90	445-450	0.15-0.25
Post	>1.20	>460	>0.25

Figure 17. Hydrocarbon generation stage relative to vitrinite reflectance (taken from Peters and Cassa, 1994); vitrinite reflectance (Ro) of <0.60% corresponds to the immature stage, Ro values of 0.60% – 0.90% correspond to the mature stage, and Ro value of >1.20% indicate post-mature stage.

Maturation rank		Mac. paleo Temp. C	Microscopic parameters
Kero- gen	Coal		Vitrin- refl. %Ro
Diagenesis	Peat	50	0.2
	Lignite		0.3
	Sub-bitumin		0.4
Catagenesis	High volatile bituminous	80	0.5
			0.6
			0.7
	0.8		
	0.9		
	1.0		
Metagenesis	Medium volatile bitumin	120	1.3
	Low volatile bitumin	170	1.5
	Sem-anthrac.	200	2.0
	Anthracite	250	2.5
	Meta-anthrac.		3.0
			4.0
			5.0

Figure 18. Modified table (taken from Hunt, 1996) that shows the relationship between maturity rank, temperature, and vitrinite reflectance values.

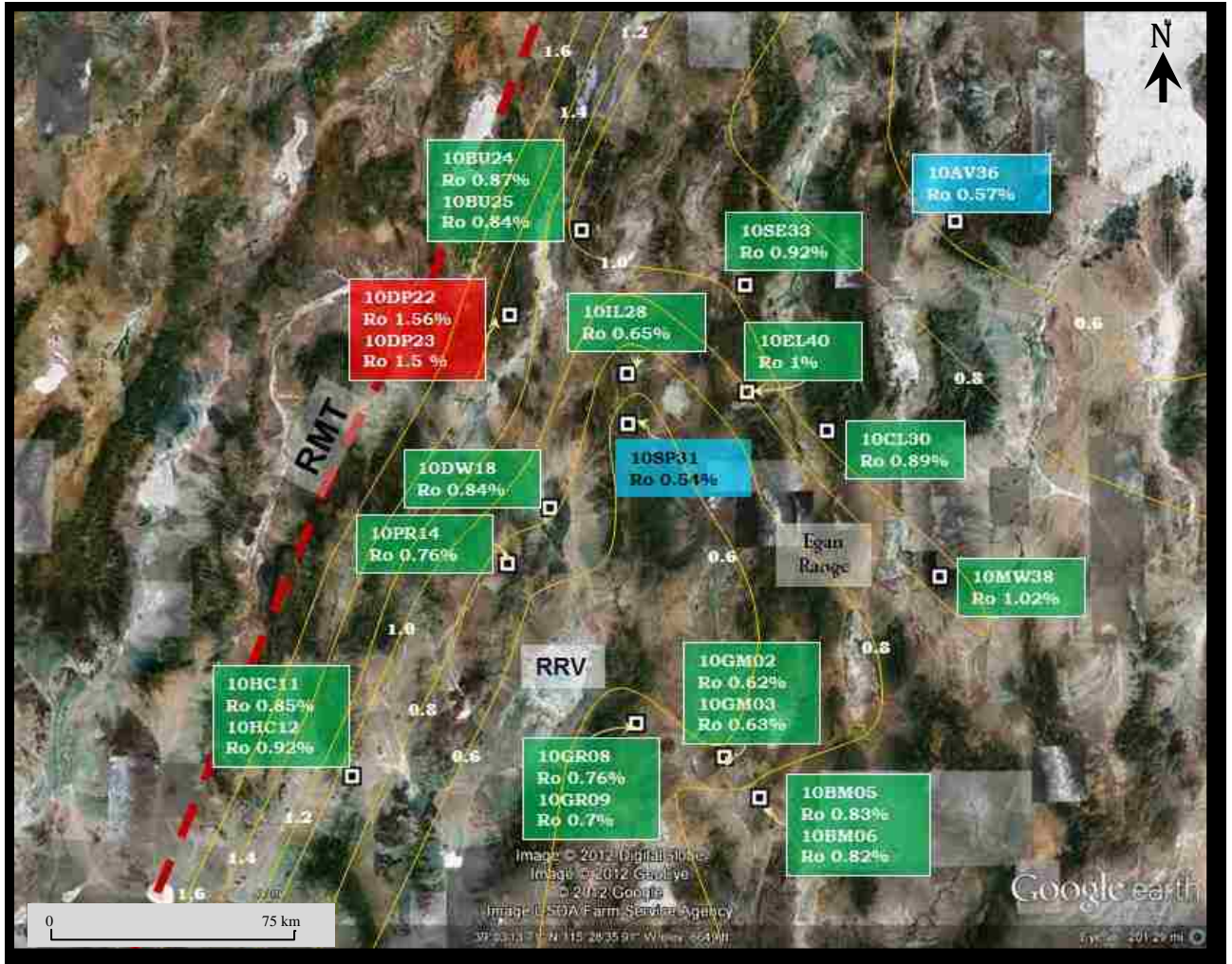


Figure 19. Google Earth image showing Ro values with hand drawn contour lines. The red dashed line represents the approximate location of the Roberts Mountain Thrust (e.g. Trexler et al., 1995; DeCelles, 2004). This figure shows that the highest Ro value occur along the western side of study area, are generally lower in the middle, and slowly higher to the east. The north-eastern area recorded the coolest temperature.

APPENDIX B

TABLES

Table 1. Sandstone samples for (U-He)/Th analyses

STA	Samples	Location	GPS
1	10GM01	Gap Mountain	N 38 17' 10.6" , W 115 3' 53" elev 1854 m
2	10BM04	west of Burnt Mountain	N 38 10' 13.1" , W 114 56' 18.4" elev 1880 m
3	10GR07	Grant Range	N 38 22' 29" , W 115 22' 40.6" elev 1913 m
4	10HC10	Hot Creek	N 38 13' 20.3" , W 116 23' 3.10" elev 1878 m
5	10PR13	Pancake Range	N 38 49' 16.20" , W 115 50' 11.40" elev 2002 m
6	10PR16	Pancake Range	N 38 53' 37.50" , W 115 50' 8.08" elev 2175 m
7	10DW17	Duckwater	N 38 58' 39.10" , W 115 40' 48.20" elev 1796 m
8	10NP19	northern Pancake Range	N 39 10' 25" , W 115' 48' 20.9" elev 1982 m
9	10DP21	Diamond Peak	N 39 30' 47.30" , W 115 50' 14.2" elev 2240 m
10	10BU26	Buck Mountain	N 39 45' 13.20" , W 115 34' 45.40" elev 2137 m
11	10IL27	Illipah	N 39 21' 13" , W 115 24' 5.70" elev 2070 m
12	10CL29	Cave Lake	N 39 11" 11.90" ,W 114 41' 10.90" elev 2234 m
13	10SP32	Sixmile Spring	N 39 13' 30.5" , W 115 24' 15.30" elev 2333 m
14	10CC34	Cherry Creek	N 40 07' 49.7" , W 114 47' 04.3" elev 1980 m
15	10AV35	Antelope Valley	N 39 46' 31.38" , W 114 13' 23.13" elev 2030 m
16	10MW37	southern Snake Range	N 38 44' 30.5" , W 114 19' 47.0" elev 2039 m
17	10SR39	northern Snake Range	N 39 09' 31.5" , W 114 08' 10.9" elev 1973 m
18	10EL41	Ely	N 39 18' 2.07" , W 114 58' 50.01" elev 2071 m

Table 2. Chainman Shale samples for Ro analyses

STA	Location	GPS	Elevation (m)	Samples	Ro (%)
1	Gap Mountain	N 38 17' 03.0" , W 115 3' 47.7"	1824	10GM02	0.62
2	Gap Mountain	N 38 17' 04" , W 115 3' 46.4"	1817	10GM03	0.63
3	Burnt Mountain	N 38 10' 08.50.1" , W 114 56' 18.50"	1861	10BM05	0.83
4	Burnt Mountain	N 38 10' 9.60" , W 114 56' 14.50"	1869	10BM06	0.82
5	Grant Range	N 38 22' 38.10" , W 115 22' 32.80"	1887	10GR08	0.76
6	Grant Range	N 38 22' 37.60" , W 115 22' 34.10"	1891	10GR09	0.7
7	Hot Creek	N 38 13' 23.30" , W 116 23' 1.5"	1838	10HC11	0.85
8	Hot Creek	N 38 12' 23.20" , W 116 23' 9.96"	1842	10HC12	0.92
9	Pancake Range	N 38 49' 16.20" , W 115 50' 11.40"	2002	10PR14	0.76
10	Duckwater	N 38 58' 37.40" , W 115 41' 9.80"	1765	10DW18	0.84
11	northern Pancake Range	N 39 10' 38.80" , W 115 48' 47.40"	1974	10NP20	0
12	Diamond Peak	N 39 30' 47.60" , W 115 50' 7.30"	2189	10DP22	1.56
13	Diamond Peak	N 39 30' 39.30" , W 115 50' 8.30"	2176	10DP23	1.5
14	Buck Mountain	N 39 45' 1.70" , W 115 34' 38.80"	2109	10BU24	0.86
15	Buck Mountain	N 39 44' 58" , W 115 34" 33.90"	2125	10BU25	0.87
16	Illipah	N 39 21' 7.00" , W 115 24' 41.50"	2091	10IL28	0.65
17	Cave Lake	N 39 11' 30.1" , W 114 41" 43.20"	2224	10CL30	0.89
18	Sixmile Spring	N 39 12" 41.20" , W 115 24' 29.90"	2405	10SP31	0.54
19	northern Egan Range	N 39 35' 53.4" , W 114 59' 11.2"	2045	10SE33	0.92
20	Antelope Valley	N 39 46' 25.7" , W 114 13' 21.2"	2020	10AV36	0.57
21	southern Snake Range	N 38 47' 00.0" , W 114 17' 36.0"	2417	10MW38	1.02
22	Ely	N 39 18' 2.07" , W 114 58' 50.01"	2071	10EL40	1

Table 3. Detrital zircon (U-Th)/He laboratory data

No.	Sample	mineral	Age, Ma	err., Ma	U (ppm)	Th (ppm)	Sm (ppm)	[U]e	Th/U	He (nmol/g)	mass (ug)	Ft
1	z10AV35-1	zircon	0.0	0.0	89.5	43.2	0.4	99.6	0.48	0.0	4.60	0.75
2	z10AV35-2	zircon	0.0	0.0	172.2	126.9	0.8	202.0	0.74	0.0	3.55	0.74
3	z10AV35-3	zircon	0.0	0.0	71.9	54.0	0.3	84.6	0.75	0.0	3.56	0.73
4	z10AV35-4	zircon	430.4	34.4	124.0	59.0	0.8	137.9	0.48	244.6	3.49	0.74
5	z10AV35-5	zircon	250.5	20.0	94.2	26.9	0.2	100.6	0.29	106.0	5.31	0.77
6	z10AV35-6	zircon	245.6	19.6	528.8	128.6	1.9	559.1	0.24	548.2	2.87	0.73
7	z10AV35-7	zircon	391.4	31.3	32.6	12.6	0.2	35.6	0.39	54.8	2.55	0.71
8	z10AV35-8	zircon	289.7	23.2	42.0	34.7	0.7	50.2	0.83	57.7	3.37	0.72
9	z10AV35-9	zircon	319.4	25.5	54.7	33.7	0.5	62.7	0.62	81.6	3.76	0.74
10	z10AV35-10	zircon	267.5	21.4	110.0	45.3	0.5	120.6	0.41	127.7	2.88	0.72
11	z10AV35-11	zircon	1078.4	86.3	34.4	30.6	1.3	41.6	0.89	195.3	3.76	0.74
12	z10AV35-12	zircon	232.9	18.6	172.2	74.3	2.8	189.7	0.43	181.1	3.90	0.75
13	z10BM04-1	zircon	0.0	0.0	58.6	32.2	-0.3	66.2	0.55	0.0	3.05	0.72
14	z10BM04-2	zircon	337.0	27.0	47.1	11.9	-0.3	49.9	0.25	67.8	3.19	0.73
15	z10BM04-3	zircon	419.5	33.6	130.1	43.3	0.7	140.3	0.33	236.2	2.83	0.72
16	z10BM04-4	zircon	523.8	41.9	36.5	27.4	1.9	42.9	0.75	89.0	2.66	0.71
17	z10BM04-5	zircon	561.3	44.9	68.1	21.2	1.5	73.1	0.31	167.8	3.17	0.73
18	z10BM04-6	zircon	358.9	28.7	64.5	24.3	1.0	70.3	0.38	103.2	3.64	0.74
19	z10BM04-7	zircon	812.9	65.0	41.0	29.2	0.8	47.9	0.71	166.9	4.04	0.75
20	z10BM04-8	zircon	132.2	10.6	88.4	22.7	0.3	93.8	0.26	51.8	4.91	0.77
21	z10BU26-1	zircon	452.1	36.2	53.1	27.8	0.2	59.6	0.52	112.7	4.43	0.75
22	z10BU26-2	zircon	1300.0	104.0	48.3	24.6	1.5	54.0	0.51	348.0	10.51	0.81
23	z10BU26-3	zircon	1284.2	102.7	31.0	22.6	0.0	36.3	0.73	215.5	4.99	0.77
24	z10BU26-4	zircon	602.6	48.2	178.1	85.7	8.8	198.3	0.48	530.1	6.45	0.79
25	z10BU26-5	zircon	1079.4	86.4	44.1	32.4	0.8	51.7	0.73	268.5	10.38	0.81
26	z10BU26-6	zircon	1035.2	82.8	38.4	24.9	0.5	44.3	0.65	204.4	4.78	0.76
27	z10BU26-7	zircon	1580.0	126.4	51.0	34.5	1.3	59.2	0.68	435.1	3.77	0.75
28	z10BU26-8	zircon	1458.7	116.7	40.2	16.0	0.6	43.9	0.40	292.3	3.54	0.74
29	z10BU26-9	zircon	1006.7	80.5	109.1	48.7	1.8	120.5	0.45	524.3	3.60	0.74
30	z10CC34-1	zircon	150.3	12.0	69.4	40.7	0.0	78.9	0.59	46.7	2.89	0.72
31	z10CC34-2	zircon	91.9	7.4	45.6	30.4	0.3	52.7	0.67	19.6	3.77	0.75
32	z10CC34-3	zircon	149.6	12.0	61.2	20.8	2.2	66.1	0.34	41.8	6.06	0.78
33	z10CC34-4	zircon	83.9	6.7	109.0	67.3	0.7	124.8	0.62	40.9	2.84	0.72
34	z10CC34-5	zircon	217.2	17.4	188.2	44.8	1.5	198.7	0.24	172.4	3.48	0.73

Table 3. Detrital zircon (U-Th)/He laboratory data - (continued)

No.	Sample	mineral	Age, Ma	err., Ma	U (ppm)	Th (ppm)	Sm (ppm)	[U]e	Th/U	He (nmol/g)	mass (ug)	Ft
35	z10CC34-6	zircon	152.9	12.2	135.3	63.3	0.8	150.2	0.47	91.4	3.02	0.73
36	z10CC34-7	zircon	101.0	8.1	88.4	46.0	0.4	99.2	0.52	43.0	7.02	0.79
37	z10CC34-8	zircon	111.5	8.9	89.8	43.0	4.7	100.0	0.48	46.1	4.51	0.76
38	z10CC34-9	zircon	120.2	9.6	209.1	50.6	1.4	221.0	0.24	105.6	3.33	0.73
39	z10CC34-10	zircon	134.1	10.7	41.7	36.8	0.9	50.4	0.88	27.8	4.65	0.76
40	z10CL29-1	zircon	1170.0	93.6	144.5	18.2	0.0	148.7	0.13	750.9	2.77	0.72
41	z10CL29-2	zircon	426.2	34.1	155.3	34.5	1.2	163.4	0.22	281.4	3.06	0.73
42	z10CL29-3	zircon	298.2	23.9	274.3	217.3	4.6	325.4	0.79	399.1	5.39	0.75
43	z10CL29-4	zircon	250.8	20.1	26.9	12.2	2.0	29.7	0.45	30.9	4.31	0.76
44	z10CL29-5	zircon	255.4	20.4	206.0	77.0	3.1	224.1	0.37	239.2	5.43	0.76
45	z10CL29-6	zircon	347.3	27.8	310.0	82.0	1.4	329.3	0.26	488.7	5.69	0.77
46	z10CL29-7	zircon	415.9	33.3	152.5	44.2	1.3	162.9	0.29	299.7	8.35	0.80
47	z10CL29-8	zircon	359.5	28.8	140.9	79.4	2.5	159.6	0.56	226.1	2.62	0.71
48	z10CL29-9	zircon	585.8	46.9	45.7	27.5	1.1	52.2	0.60	134.1	7.05	0.78
49	z10DP21-1	zircon	52.8	4.2	403.1	318.5	16.2	478.1	0.79	101.7	4.35	0.74
50	z10DP21-2	zircon	49.1	3.9	635.3	688.4	20.7	797.2	1.08	157.3	4.58	0.74
51	z10DP21-3	zircon	134.2	10.7	49.7	21.4	0.3	54.7	0.43	29.4	3.23	0.74
52	z10DP21-4	zircon	132.0	10.6	144.4	109.8	7.2	170.3	0.76	89.5	4.08	0.73
53	z10DP21-5	zircon	45.4	3.6	538.4	709.7	14.0	705.3	1.32	130.1	4.72	0.75
54	z10DP21-6	zircon	77.0	6.2	94.2	57.0	1.2	107.6	0.60	36.2	9.32	0.80
55	z10DP21-7	zircon	78.3	6.3	74.6	44.8	0.9	85.1	0.60	29.0	8.49	0.80
56	z10DP21-8	zircon	232.2	18.6	58.2	50.6	1.0	70.1	0.87	68.9	6.68	0.77
57	z10DP21-9	zircon	57.0	4.6	281.7	192.1	9.8	326.9	0.68	75.9	4.50	0.75
58	z10DP21-10	zircon	15.5	1.2	403.5	105.8	0.7	428.4	0.26	30.5	22.98	0.85
59	z10DW17-1	zircon	1181.2	94.5	29.8	26.2	-0.5	35.9	0.88	188.2	4.15	0.75
60	z10DW17-2	zircon	507.4	40.6	39.5	20.0	-0.8	44.2	0.51	88.8	2.48	0.71
61	z10DW17-3	zircon	176.5	14.1	485.3	343.2	43.3	566.2	0.71	398.5	3.30	0.73
62	z10DW17-4	zircon	999.0	79.9	100.6	64.9	2.0	115.8	0.64	473.5	2.33	0.71
63	z10DW17-5	zircon	1332.7	106.6	77.0	42.0	2.5	86.8	0.55	521.7	3.57	0.74
64	z10DW17-6	zircon	1008.2	80.7	78.9	56.7	1.6	92.2	0.72	421.4	6.06	0.78
65	z10DW17-7	zircon	1015.8	81.3	95.0	46.9	2.6	106.1	0.49	444.3	2.49	0.71
66	z10DW17-8	zircon	186.3	14.9	441.7	190.3	19.2	486.5	0.43	357.9	2.78	0.72
67	z10DW17-9	zircon	993.0	79.4	44.9	33.3	1.2	52.7	0.74	236.6	6.44	0.77

Table 3. Detrital zircon (U-Th)/He laboratory data - (continued)

No.	Sample	mineral	Age, Ma	err., Ma	U (ppm)	Th (ppm)	Sm (ppm)	[U]e	Th/U	He (nmol/g)	mass (ug)	Ft
68	z10DW17-10	zircon	1424.4	114.0	24.1	21.4	0.6	29.1	0.89	176.5	2.50	0.71
69	z10EL41-1	zircon	339.6	27.2	59.9	26.0	-0.3	66.0	0.43	89.0	2.82	0.72
70	z10EL41-2	zircon	324.0	25.9	42.8	23.2	-0.4	48.2	0.54	60.9	2.50	0.71
71	z10EL41-3	zircon	305.0	24.4	72.1	37.0	0.0	80.8	0.51	98.3	2.86	0.73
72	z10EL41-4	zircon	299.3	23.9	44.7	51.1	1.1	56.7	1.14	70.9	4.71	0.76
73	z10EL41-5	zircon	283.5	22.7	89.7	24.1	1.5	95.4	0.27	106.6	2.50	0.72
74	z10EL41-6	zircon	332.5	26.6	126.3	43.9	1.3	136.6	0.35	175.3	2.09	0.70
75	z10GM01-1	zircon	327.2	26.2	41.5	46.1	0.0	52.4	1.11	72.5	5.51	0.77
76	z10GM01-2	zircon	299.8	24.0	66.1	40.6	0.0	75.7	0.61	90.0	3.17	0.72
77	z10GM01-3	zircon	374.0	29.9	42.7	29.2	0.2	49.6	0.68	76.6	4.85	0.75
78	z10GM01-4	zircon	350.8	28.1	46.4	13.9	0.9	49.6	0.30	73.1	4.86	0.76
79	z10GM01-5	zircon	306.3	24.5	115.8	26.9	0.7	122.1	0.23	153.2	3.39	0.74
80	z10GM01-6	zircon	283.9	22.7	137.2	54.2	1.2	149.9	0.40	176.4	4.17	0.75
81	z10GM01-7	zircon	448.4	35.9	119.8	63.5	0.9	134.8	0.53	242.8	2.82	0.72
82	z10GM01-8	zircon	392.4	31.4	64.7	35.5	0.6	73.0	0.55	122.7	5.57	0.77
83	z10GM01-9	zircon	342.5	27.4	334.8	28.3	1.0	341.4	0.08	477.0	3.40	0.74
84	z10GM01-10	zircon	315.1	25.2	51.2	26.6	0.5	57.5	0.52	76.3	5.12	0.76
85	z10GR07-1	zircon	313.9	25.1	88.9	25.3	1.1	94.8	0.28	126.6	5.24	0.77
86	z10GR07-2	zircon	388.0	31.0	109.9	42.6	0.2	119.9	0.39	197.0	5.23	0.76
87	z10GR07-3	zircon	327.4	26.2	105.3	73.2	0.2	122.5	0.70	164.7	4.17	0.75
88	z10GR07-4	zircon	395.7	31.7	235.6	123.3	1.4	264.6	0.52	429.9	3.95	0.74
89	z10GR07-5	zircon	348.7	27.9	165.9	57.2	2.4	179.4	0.35	257.2	3.98	0.74
90	z10GR07-6	zircon	331.5	26.5	82.2	25.2	1.0	88.2	0.31	123.1	4.80	0.76
91	z10GR07-7	zircon	446.5	35.7	156.5	51.2	2.5	168.5	0.33	312.2	3.76	0.75
92	z10GR07-8	zircon	437.1	35.0	98.8	70.2	1.2	115.3	0.71	211.2	4.41	0.75
93	z10GR07-9	zircon	460.9	36.9	29.7	10.6	0.3	32.2	0.36	60.9	3.29	0.74
94	z10GR07-10	zircon	350.4	28.0	49.3	32.3	0.4	56.9	0.66	82.4	4.15	0.75
95	z10HC10-2	zircon	217.2	17.4	150.2	80.0	3.4	169.0	0.53	146.3	3.38	0.73
96	z10HC10-3	zircon	457.2	36.6	58.2	30.8	-0.3	65.4	0.53	121.9	3.32	0.73
97	z10HC10-4	zircon	699.5	56.0	27.1	19.1	0.4	31.6	0.70	103.7	12.39	0.82
98	z10HC10-5	zircon	470.0	37.6	71.5	30.2	0.6	78.6	0.42	149.6	2.92	0.73
99	z10HC10-6	zircon	542.8	43.4	47.8	30.0	2.8	54.9	0.63	132.5	8.13	0.79
100	z10HC10-7	zircon	1000.2	80.0	62.0	42.6	1.1	72.1	0.69	325.3	5.66	0.77

Table 3. Detrital zircon (U-Th)/He laboratory data - (continued)

No.	Sample	mineral	Age, Ma	err., Ma	U (ppm)	Th (ppm)	Sm (ppm)	[U]e	Th/U	He (nmol/g)	mass (ug)	Ft
101	z10HC10-8	zircon	761.3	60.9	70.7	39.8	7.5	80.1	0.56	281.3	9.23	0.80
102	z10HC10-9	zircon	380.1	30.4	116.3	112.7	1.3	142.8	0.97	227.3	4.66	0.76
103	z10IL27-1	zircon	429.5	34.4	111.6	35.5	-0.3	119.9	0.32	209.6	3.53	0.73
104	z10IL27-2	zircon	360.7	28.9	24.2	33.4	-0.5	32.0	1.38	46.4	3.66	0.73
105	z10IL27-3	zircon	288.0	23.0	61.9	26.0	0.5	68.0	0.42	79.3	3.92	0.74
106	z10MW37-1	zircon	377.8	30.2	144.7	37.2	1.1	153.4	0.26	247.2	5.28	0.77
107	z10MW37-2	zircon	362.3	29.0	94.5	33.7	0.2	102.4	0.36	157.6	5.44	0.77
108	z10MW37-3	zircon	370.0	29.6	177.7	62.6	0.4	192.5	0.35	296.6	4.47	0.75
109	z10MW37-4	zircon	406.0	32.5	43.1	19.8	0.0	47.8	0.46	82.6	5.39	0.77
110	z10MW37-5	zircon	460.0	36.8	70.7	21.6	0.0	75.8	0.31	149.1	5.69	0.77
111	z10MW37-6	zircon	454.2	36.3	62.5	17.3	0.0	66.6	0.28	134.0	7.73	0.79
112	z10MW37-7	zircon	391.4	31.3	143.1	88.1	1.4	163.8	0.62	263.6	4.45	0.74
113	z10MW37-8	zircon	569.1	45.5	95.4	40.2	0.5	104.9	0.42	254.2	4.56	0.76
114	z10MW37-9	zircon	435.4	34.8	177.8	38.6	1.2	186.8	0.22	351.4	5.59	0.78
115	z10MW37-10	zircon	427.1	34.2	47.2	8.5	0.3	49.2	0.18	86.2	3.90	0.74
116	z10MW37-11	zircon	686.7	54.9	74.2	52.1	0.3	86.4	0.70	255.4	5.51	0.76
117	z10MW37-12	zircon	367.5	29.4	197.7	78.3	1.4	216.1	0.40	322.7	3.30	0.74
118	z10MW37-13	zircon	456.5	36.5	40.8	29.1	0.9	47.7	0.71	91.8	4.89	0.76
119	z10NP19-1	zircon	706.0	56.5	62.7	64.6	2.5	77.9	1.03	230.7	4.38	0.74
120	z10NP19-2	zircon	1478.4	118.3	72.9	45.6	0.8	83.6	0.63	581.5	4.59	0.76
121	z10NP19-3	zircon	885.5	70.8	189.1	106.9	0.0	214.2	0.57	805.8	3.35	0.74
122	z10NP19-4	zircon	1147.0	91.8	34.0	16.5	0.6	37.9	0.48	187.6	2.94	0.73
123	z10NP19-5	zircon	307.6	24.6	482.5	136.1	6.7	514.5	0.28	651.4	3.79	0.75
124	z10NP19-6	zircon	171.5	13.7	943.3	80.7	51.4	962.5	0.09	647.5	2.53	0.72
125	z10NP19-7	zircon	1239.9	99.2	83.6	35.1	1.2	91.8	0.42	473.6	2.12	0.70
126	z10NP19-8	zircon	724.8	58.0	53.2	27.8	0.4	59.8	0.52	192.0	5.73	0.78
127	z10NP19-9	zircon	999.1	79.9	81.3	30.8	0.8	88.6	0.38	390.0	4.38	0.75
128	z10NP19-10	zircon	1579.7	126.4	49.5	28.5	1.1	56.2	0.58	431.8	5.53	0.77
129	z10PR13-1	zircon	712.1	57.0	177.5	116.8	10.6	205.0	0.66	575.2	2.14	0.70
130	z10PR13-2	zircon	514.4	41.2	171.8	59.6	5.9	185.8	0.35	377.8	2.30	0.71
131	z10PR13-3	zircon	1246.3	99.7	66.2	29.6	0.3	73.2	0.45	427.1	5.65	0.78
132	z10PR13-4	zircon	1411.8	112.9	43.0	31.7	0.8	50.5	0.74	366.1	13.76	0.83
133	z10PR13-5	zircon	1128.2	90.3	36.8	27.1	0.7	43.2	0.74	232.9	8.48	0.80

Table 3. Detrital zircon (U-Th)/He laboratory data - (continued)

No.	Sample	mineral	Age, Ma	err., Ma	U (ppm)	Th (ppm)	Sm (ppm)	[U]e	Th/U	He (nmol/g)	mass (ug)	Ft
134	z10PR13-6	zircon	1142.7	91.4	50.1	27.5	0.6	56.5	0.55	322.6	13.59	0.83
135	z10PR13-7	zircon	734.1	58.7	93.1	55.4	0.7	106.1	0.60	348.6	6.35	0.78
136	z10PR13-8	zircon	968.5	77.5	61.4	28.3	0.9	68.0	0.46	316.8	10.67	0.82
137	z10PR13-9	zircon	167.3	13.4	315.1	30.5	18.4	322.4	0.10	245.0	13.24	0.83
138	z10PR16-1	zircon	379.2	30.3	78.5	45.5	0.3	89.2	0.58	134.8	2.89	0.72
139	z10PR16-2	zircon	305.5	24.4	377.4	36.2	2.5	386.0	0.10	494.5	5.41	0.76
140	z10PR16-3	zircon	323.9	25.9	235.1	143.3	3.3	268.7	0.61	347.2	3.05	0.72
141	z10PR16-4	zircon	363.3	29.1	125.7	44.2	1.0	136.1	0.35	210.5	4.90	0.77
142	z10PR16-5	zircon	355.1	28.4	78.1	57.0	0.6	91.5	0.73	135.9	4.43	0.76
143	z10PR16-6	zircon	776.8	62.1	145.8	74.2	4.7	163.3	0.51	541.2	3.92	0.75
144	z10PR16-7	zircon	364.7	29.2	82.9	16.6	0.9	86.8	0.20	136.4	6.33	0.78
145	z10PR16-8	zircon	348.0	27.8	51.4	41.0	1.3	61.1	0.80	88.0	5.07	0.75
146	z10PR16-9	zircon	226.2	18.1	496.8	222.5	7.9	549.1	0.45	504.8	4.17	0.74
147	z10PR16-10	zircon	549.1	43.9	133.3	11.9	2.0	136.1	0.09	319.5	5.08	0.76
148	z10SP32-1	zircon	556.5	44.5	148.3	45.7	2.1	159.1	0.31	356.0	2.64	0.72
149	z10SP32-2	zircon	1187.3	95.0	86.3	37.3	0.6	95.0	0.43	510.3	4.32	0.76
150	z10SP32-3	zircon	519.0	41.5	195.4	70.9	4.9	212.1	0.36	483.1	6.12	0.78
151	z10SP32-4	zircon	1162.1	93.0	44.1	32.9	0.6	51.8	0.75	266.6	3.86	0.75
152	z10SP32-5	zircon	1194.9	95.6	54.7	66.0	3.8	70.2	1.21	343.5	2.26	0.70
153	z10SP32-6	zircon	806.9	64.5	59.9	61.9	2.2	74.4	1.03	243.0	2.75	0.71
154	z10SP32-7	zircon	255.9	20.5	374.4	375.5	11.1	462.7	1.00	461.1	2.59	0.71
155	z10SP32-8	zircon	1006.8	80.5	42.4	32.4	0.6	50.0	0.76	226.2	5.47	0.77
156	z10SP32-9	zircon	18.4	1.5	322.8	136.8	29.7	355.0	0.42	25.6	3.01	0.73
157	z10SP32-10	zircon	1012.6	81.0	93.5	50.5	3.5	105.4	0.54	441.3	2.41	0.71
158	z10SR39-1	zircon	2988.7	239.1	9.9	51.3	13.5	22.0	5.20	308.9	2.69	0.69
159	z10SR39-2	zircon	302.6	24.2	178.8	68.4	0.8	194.9	0.38	245.2	4.67	0.76
160	z10SR39-4	zircon	340.9	27.3	181.3	66.7	0.8	197.0	0.37	286.3	5.69	0.77
161	z10SR39-5	zircon	412.6	33.0	148.3	45.8	0.5	159.1	0.31	261.5	2.84	0.72
162	z10SR39-6	zircon	321.0	25.7	77.0	16.0	0.4	80.8	0.21	105.7	3.87	0.74
163	z10SR39-7	zircon	345.0	27.6	240.4	78.9	1.8	259.0	0.33	366.9	4.12	0.74
164	z10SR39-8	zircon	602.1	48.2	51.5	25.2	0.7	57.4	0.49	146.2	4.64	0.75

REFERENCES

- Ahdyar, L., 2011, Molecular organic geochemistry of the oil and source rocks in Railroad Valley Basin, Eastern Great Basin, Nevada, United States [Ms. thesis]: Las Vegas, University of Nevada Las Vegas, 103 p.
- Anna, L.O., Roberts, L.N., and Potter, C.J., 2007, Geologic assessment of undiscovered oil and gas in the Paleozoic-Tertiary composite total petroleum system of the Eastern Great Basin, Nevada and Utah: U.S. Geological Survey Digital Data Series DDS-69-L, v. 2, 50p.
- Armstrong, R.L., 1972, Low-angle (denudation) faults, hinterland of the Sevier orogenic belt, eastern Nevada and western Utah: Geological Society of America Bulletin, v. 83, p. 1729-1754.
- Cameron, G. J., and Chamberlain, A. K., 1987, Reevaluation of Late Mesozoic thrusting in east-central Nevada: American Association of Petroleum Geologists, Annual Convention, Los Angeles, California, Abstract. Cameron, G., and Chamberlain, A.K., 1987, Reevaluation of late Mesozoic thrusting in east-central Nevada: American Association of Petroleum Geologists Bulletin v. 71, p. 536.
- Carpenter, J.A., Carpenter, D.G., and Dobbs, S.W., 1994, Antler orogeny: paleostructural analysis and constraints on plate tectonic models with a global analogue in southeast Asia, *in* Dobbs, S.W., and Taylor, W.J., eds., Structural and stratigraphic investigations and petroleum potential of Nevada, with special emphasis south of the Railroad Valley producing trend: Nevada Petroleum Society Conference, v. 2, p. 187-240.
- Cashman, P.H. and J.H. Trexler Jr., 1991, The Mississippian Antler foreland and continental margin in southern Nevada: the Eleana Formation reinterpreted: Cooper, J.D. and Stevens, C.H. (eds.), Paleozoic Paleogeography of the Western U.S., II: Pacific Section SEPM, v. 67, p. 271-280.
- Cashman, P.H., and Trexler, J.H., 1994, The case for two, coeval, Mississippian sections at the Nevada Test Site, *in* McGill, S.F., and Ross, T.M., eds., Geological Investigations of an Active Margin: San Bernardino, Calif., Geological Society of America Cordilleran Section Guidebook, 1994, p. 76-81.
- Coney, P.J., and Harms, T.A., 1984, Cordilleran metamorphic core complexes: Cenozoic extensional relics of Mesozoic compression: *Geology*, v. 12, p. 550-554.
- Cook, H.E., 1988, Overview—Geologic history and carbonate petroleum reservoirs of the Basin and Range Province, western United States, *in* Goolsby, S.M., and Longman, M.W., eds., Occurrence and petrophysical properties of carbonate reservoirs in the Rocky Mountain region: Rocky Mountain Association of Geologists Carbonate Symposium, p. 213-227.

- DeCelles, P.G., 2004, Late Jurassic to Eocene evolution of the Cordilleran thrust belt and foreland basin system, western USA: *American Journal of Science*, v. 304, p. 105-168.
- Dickinson, W.R., Harbaugh, D.W., Saller, A.H., Heller, P.L., and Snyder, W.S., 1983, Detrital modes of Paleozoic sandstones derived from Antler Orogen in Nevada: Implications for nature of Antler orogeny: *American Journal of Science*, v. 283, p. 481 - 509.
- Dickinson, W.R., 2002, The Basin and Range Province as a composite extensional domain: *International Geology Review*, v. 44 p. 1-38.
- Druschke, P.A., 2009, The Sheep Pass Formation: A Record of Late Cretaceous and Paleogene Extension within the Sevier Hinterland, East-Central Nevada [Ph.D. thesis]: Las Vegas, University of Nevada Las Vegas, 165 p.
- Eaton, G.P., 1979, Regional geophysics, Cenozoic tectonics and geological resources of the Basin and Range province and adjoining regions, *in* Newman, G.W., and Goode, H.D., eds., *Basin and Range Symposium*: Denver, Colorado, Rocky Mountain Association of Geologists, p. 11-39.
- Faulds, J.E., and Varga R.J., 1998, The role of accommodation zones and transfer zones in the regional segmentation of extended terranes, *in* *The Regional Segmentation of the Basin and Range Province*: Geological Society of America, *Geology of North America*, v. 323, p. 1 – 45.
- Farley, K., Wolf, R., and Silver, L., 1996, The effects of long alpha-stopping distances on (U-Th)/He ages: *Geochimica et Cosmochimica Acta*, v. 60, p. 4223-4229.
- Farley, K.A., 2000, Helium diffusion from apatite: General behavior as illustrated by Durango fluorapatite: *Journal of Geophysical Research*, v. 105, no. B2.
- Farley, K.A., 2002, (U-Th)/He Dating: Techniques, Calibrations, and Applications: *Reviews in Mineralogy and Geochemistry*, v. 47, p. 819-844.
- Forrester, S., 2009, Provenance of the Miocene-Pliocene Muddy Creek Formation near Mesquite, Nevada [M.S. thesis]: Las Vegas, University of Nevada Las Vegas, 165 p.
- French, D.E., 1983, Origins of oil in Railroad Valley, Nye County, Nevada: *American Association of Petroleum Geologists Bulletin*, v. 67, p. 9-21.
- Gabrielse, H., Snyder, W.S., and Stewart, J.H., 1983, Sonoma orogeny and Permian to Triassic tectonism in western North America: *Geology*, v. 11, p. 484–486.
- Gehrels, G., 2009, Age Pick (computer software).

- Giles, K.A., and Dickinson, W.R., 1995, The interplay of eustasy and lithospheric flexure in forming stratigraphic sequences in foreland settings: An example from the Antler foreland, Nevada and Utah, *in* Dorobek, S.L., and Ross, G.M., eds., *Stratigraphic Evolution of Foreland Basins: SEPM (Society for Sedimentary Geology) Special Publication 52*, p. 187–211.
- Giles, K.A., 1996, Tectonically forced retrogradation of the Lower Mississippian Joana Limestone, Nevada and Utah, *in* Longman, M.W., and Sonnenfeld, M.D., eds., *Paleozoic Systems of the Rocky Mountain Region: Denver, Rocky Mountain Section, SEPM (Society for Sedimentary Geology)*, p. 145–164.
- Goebel, K.A., 1991, Paleogeographic setting of Late Devonian to early Mississippian transition from passive to collisional margin, Antler foreland, eastern Nevada and western Utah, *in* Cooper, J.D., and Stevens, C.H., eds., *Paleozoic Paleogeography of the Western United States, Volume II: Los Angeles, Pacific Section, SEPM (Society for Sedimentary Geology), Book 67*, p. 401–418.
- Grabb, R.F., 1994, Extensional tectonics and petroleum accumulations in the Great Basin, *in* R.A. Schalla and E.H. Johnson, eds., *Oil fields in the Great Basin: Nevada Petroleum Society*, p. 41-55.
- Hamilton, W.B., 1978, Mesozoic tectonics of the western United States, *in* Howell, D.G., and McCougall, K.A., eds., *Society of Economic Paleontology and Mineralogy, Pacific Section: Pacific Coast Paleogeography Symposium, v. 2*, p. 33-70.
- Hannah, J.L., and Moores, E.M., 1986, Age relationships and depositional environments of Paleozoic strata, northern Sierra Nevada, California: *Geological Society of America Bulletin*, v. 97, p. 787-797.
- Harbaugh, D.W. and Dickinson, W. R., 1981, Depositional facies of Mississippian clastics, Antler foreland basin, central Diamond Mountains, Nevada: *Journal of Sedimentary Petrology*, p. 1223 – 1234.
- Harris, A.G., Wardlaw, B.R., Rust, C.C., and Merrill, G.K., 1980, Maps for assessing thermal maturity (conodont color alteration index maps) in Ordovician through Triassic rocks in Nevada and Utah and adjacent parts of Idaho and California: U.S. Geological Survey Miscellaneous Investigations Map I-1249, scale 1:2,500,000.
- Hose, R.K., Blake, M.C., and Smith, R.M, 1976, Geology and mineral resources of White Pine County, Nevada: Nevada Bureau of Mines and Geology, Mackay School of Mines, University of Nevada, Bulletin 85, 99 p.
- Hourigan, J.K., Reiners, P.W., and Brandon, M.T., 2005, U-Th zonation-dependent alpha ejection in (U-Th)/He chronometry: *Geochimica et Cosmochimica Acta*, v. 69, p. 3349-3365.

- Hughes, L.J., and Carlson, N.R., 1987, Structure mapping at Trap Spring oilfield, Nevada, using controlled-source magnetotellurics: *First Break*, v. 5, no. 11.
- Hunt, J.M., 1979, *Petroleum Geochemistry and Geology*: New York, W. H. Freeman and Company, 617 p.
- Hunt, J.M., 1996, *Petroleum geochemistry and geology*, 2nd ed.: New York, W.H. Freeman and Company, 743 p.
- Kleinhampl, F.J., and Ziony, J.I., 1985, *Geology of Northern Nye County, Nevada*: Nevada Bureau of Mines and Geology Bulletin 99A, 172 p., 2.
- Ludwig, K., 2008, *Isoplot3.7* (computer program): California, Berkeley.
- Meissner, F., 1995, Pattern of maturity in source rocks of the Chainman Formation, central Railroad Valley, Nye County Nevada and its relation to oil migration and accumulation, *in* Hansen, M.W., Walker, J.P., Trexler Jr., J.H., eds., *Mississippian Source Rocks in the Antler Basin of Nevada and Associated Structural and Stratigraphic Traps*: Reno, Nevada, Petroleum Society, p. 65-74.
- Moller, A., O'Brien, P.J., Kennedy, A., and Kroner, A., 2003, Linking growth episodes of zircon and metamorphic textures to zircon chemistry: an example from the ultrahigh-temperature granulites of Rogaland (SW Norway): *The Geological Society of London*, p. 65-81.
- Montgomery, S.L., Schaftenaar, C.H., Hansen, J.B., and Holm, S., 1999, Ghost Ranch field, Nevada - New discovery from combined 3-D seismic and well log data: *American Association of Petroleum Geologists Bulletin*, v. 83, no. 9, p. 1377-1391.
- Nasdala, L., Reiners, P., Garver, J., Kennedy, A., Stern, R., Balan, E., and Wirth, R., 2004, Incomplete retention of radiation damage in zircon from Sri Lanka: *American Mineralogist*, v. 89, p. 219-231.
- Nevada Bureau of Mines and Geology, 1999, *Generalized geologic map of Nevada*, Nevada Bureau of mines and geology map 57: Mackay School of Mines, University of Nevada, Reno, Nevada.
- North, F.K., 1985, *Petroleum Geology*: Boston, Allen & Unwin, 607 p.
- Pekarek, A.H., 2005, Structure, stratigraphy, and hydrocarbon potential of Butte Valley, White Pine County, Nevada: *The Mountain Geologist*, v. 42, p. 187-201.

- Peters, K.E., and Cassa, M.R., 1994, Applied source rock geochemistry, *in* Magoon, L.B., and Dow, W.G., ed., The petroleum system from source to trap: American Association of Petroleum Geologists, p. 93–120.
- Poole, F.G., and Claypool, G.E., 1984, Petroleum source-rock potential and crude-oil correlation in the Great Basin, *in* Woodward, J., Meissner, F.F., and Clayton, J.L., eds., Hydrocarbon source rocks of the greater Rocky Mountain region: Denver, Colorado, Rocky Mountain Association of Geologists, p. 179-229.
- Poole, F.G., and Sandberg, C.A., 1991, Mississippian paleogeography and conodont biostratigraphy of the western United States, *in* Cooper, J. D., and Stevens, C. H., eds., Paleozoic paleogeography of the Western United States II: SEPM, Pacific Section, v. 67, p. 107-136.
- Reiners, P., Farley, K., and Hickes, H., 2002, He diffusion and (U-Th)/He thermochronometry of zircon: initial results from Fish Canyon Tuff and Gold Butte: Tectonophysics, v. 349, p. 297-308.
- Reiners, P.W., 2005, Zircon (U-Th)/He thermochronometry (in low-temperature thermochronology: techniques, interpretations, and applications): Connecticut, Reviews in Mineralogy and Geochemistry, p. 151–179.
- Roberts, R.J., Montgomery, K.M., and Lehner, R.E, 1967, Geology and mineral resources of Eureka County, Nevada: Reno, Nevada Bureau of Mines and Geology (and Mackay School of Mines press), Bulletin 64, p. 152.
- Rowan, L.C., Pawlewicz, M.J., and Jones, O.D., 1992, Mapping thermal maturity in the Chainman Shale, near Eureka, Nevada, with Landsat thematic mapper images: American Association of Petroleum Geologists Bulletin, v. 76, p. 1008–1023.
- Rowan, E.L., 2006, Burial and thermal history of the central Appalachian Basin, based on three 2-D models of Ohio, Pennsylvania, and West Virginia: U. S. Geological Survey, Reston, 35 p.
- Sadlick, W., 1965, Biostratigraphy of the Chainman Formation (Carboniferous), eastern Nevada and western Utah [Ph.D. thesis]: Salt Lake City, University of Utah, 228 p.
- Salyards, S.L., and Shoemaker, 1987, Landslide and Debris Flow Deposits in Miocene Horse Spring Formation, Nevada: A Measure of Basin and Range Extension: Geology Society of America, Centennial Field Guide.
- Schmauder, Gretchen C., Arehart, Greg B., and Donelick, Raymond A., 2005, Thermal and chemical profiling of the Bald Mountain district, White Pine County, Nevada, *in* Rhoden, H.N., Steininger, R.C., and Vikre, P.G., eds., Geological Society of

- Nevada Symposium 2005: Window to the World, Reno, Nevada, May 2005, p. 531–542.
- Shuster, D.L., Flowers, R.M., and Farley, K.A., 2006, The influence of natural radiation damage on helium diffusion kinetics in apatite: *Earth and Planetary Science Letters*, v. 249, p. 148-161.
- Speed, R.C., and Sleep, N.H., 1982, Antler orogeny: a model: *Geological Society of America Bulletin*, v. 93, p. 815-828.
- Spencer, J.E. 1984. Role of tectonic denudation in warping and uplift of low-angle normal faults: *Geology*, 12, p. 95-98.
- Snyder, W.S., and Trexler, J.H., Jr, 2000, Collapsed borderland model for the Antler orogeny (abst.): *Geological Society of America Abstracts with Programs*, v. 32, no. 7, p. A-382.
- Snyder, W.S., Trexler, J.H., Jr., Cashman, P.H., and Davydov, V.I., 2000, Tectonostratigraphic framework of the upper Paleozoic continental margin of Nevada and southeastern California: Reno, Geological Society of Nevada Program with Abstracts, p. 76–77.
- Stockli, D.F., 2005, Application of low-temperature thermochronometry to extensional tectonic settings, *in* Reiners, P.W. and Ehlers, T.A. (eds), *Low-Temperature Thermochronology: Techniques, Interpretations, and Applications*, v. 58, p. 411-448.
- Stockli, D.F., Wolfe, M.R., Pujols, E.J., Goldsmith, A., Ghorbal, B., 2010, The good, the bad, and the metamict – Bulk He diffusion and radiation damage in zircon and impact on zircon (U-Th)/He thermochronometry: *Thermo2010 Conference Abstract*, v. 2, p.51.
- Tagami, T., Farley, K., and Stockli, D., 2003, (U-Th)/He geochronology of single zircon grains of known Tertiary eruption age: *Earth and Planetary Science Letters*, v. 207, p. 57-67.
- Taylor, W.J., 2001, Mesozoic thrusting in the hinterland of the Sevier orogenic belt-The central Nevada thrust belt [abs.]: *Geological Society of Nevada, 2001 annual meeting abstract*.
- Trexler, J.H., Jr. and Cashman P.H., 1991, Mississippian stratigraphy and tectonics of east-central Nevada: Post-Antler orogenesis: Cooper, J.D. and Stevens, C.H. (eds.), *Paleozoic Paleogeography of the Western U.S., II: Pacific Section SEPM*, v. 67, p. 331-342.

- Trexler, J.H., Jr., and Cashman, P.H., 1991, Mississippian stratigraphy and tectonics of east-central Nevada: Post-Antler orogenesis, *in* Cooper, J.D., and Stevens, C.H., eds., Paleozoic paleogeography of the western United States, Volume II: Tulsa, Society of Economic Paleontologists and Mineralogists, Pacific Section, p. 331–342.
- Trexler, J.H., Snyder, W., Schwarz, D., Kurka, M.T., Crosbie, R., 1995, An overview of the Mississippian Chainman Shale, *in* Hansen, M.W., Walker, J.P., Trexler Jr., J.H., eds., Mississippian source rocks in the Antler Basin of Nevada and associated structural and stratigraphic trap: Reno, Nevada Petroleum Society, p. 45 - 60.
- Trexler, J.H., Jr., Cashman, P.H., Cole, J.C., Snyder, W.S., Tosdal, R.M., and Davydov, V.I., 2003, Widespread Effects of Mid-Mississippian Deformation in the Great Basin of western North America: Geological Society of America Bulletin, v. 115, no. 10, p. 1278-1288.
- Trexler, J.H., Jr., Snyder, W.S., and Cashman, P.H., and Davydov, V.I., 2004, Upper Paleozoic tectonism in Nevada: timing, kinematics, and tectonic significance: Geological Society of America Bulletin (in press).
- Tschanz, C.M., and Pampeyan, E.H., 1970, Geology and mineral resources of Lincoln County, Nevada: Nevada Bureau of Mines and Geology, Mackay School of Mines, University of Nevada, Bulletin, 188 p.
- Walker, C.T., Francis, J.G., and Lumsden, W.W., 1992, Cenozoic attenuation detachment faulting: a possible control on oil and gas accumulation in east-central Nevada: American Association of Petroleum Geologists Bulletin, v. 76, p. 1665–1686.
- Wernicke, B.P., Snow, J.K., and Walker, J.D., 1988, Correlation of Early Mesozoic thrusts in the southern Great Basin and their possible indication of 250-300 km of Neogene crustal extension, *in* Weide, D.L., and Faber, M.L., eds., This Extended Land, Geological Journeys in the Southern Basin and Range, Geological Society of America Cordilleran Section Field Trip Guidebook, p. 255-268.
- Wernicke, B.P., 1981, Low-angle normal faults in the Basin and Range province: nappe tectonics in an extending orogen: Nature, v. 291, p. 645-648.
- Williams, I.S., Buick, I.S. & Cartwright, I., 1996, An extended episode of early Mesoproterozoic metamorphic fluid flow in the Reynolds Range, Central Australia: Journal of Metamorphic Geology, v. 14, p. 29–47.
- Wilson, B.R., and Laule, S.W., 1979, Tectonic and sedimentation along the Antler orogenic belt of central Nevada, *in* Newman, G.W. and Goode, H.D., eds., 1979, Basin and Range symposium and Great Basin field conference: Rocky Mountain Association, p. 81-92.

Wolfe, M.R., and Stockli, D.F., 2010, Zircon (U-Th)/He thermochronometry in the KTB drillhole, Germany, and its implications for bulk He diffusion kinetics in zircon: *Earth and Planetary Science Letters*, v. 295, p. 69-82.

VITA

Graduate College
University of Nevada, Las Vegas

Yuki Yunika Agulia

Degrees:

Bachelor of Science, Geology, 2007
Gadjah mada University, Yogyakarta, Indonesia

Special Honors and Awards:

Member of University of Nevada Las Vegas Imperial Barrel Award Team 2011,
Third Place Rocky Mountain Section of American Association of Petroleum
Geologists.

Best Graduate Poster Presentation, Geosymposium 2011, University of Nevada
Las Vegas.

Thesis title: Burial and Exhumation History of Mississippian Strata in East-Central
Nevada.

Thesis Examination Committee:

Chairperson, Andrew D. Hanson, Ph.D.
Committee Member, Rodney V. Metcalf, Ph.D.
Committee Member, Terry L. Spell, Ph.D.
Graduate Faculty Representative, Vernon F. Hodge, Ph.D.